

**Studies Toward the Biosynthesis of  
Chimonanthine in *Chimonanthus praecox***

by

**Soo Hur**

B.Sc. (Spec.), University of Alberta, 2012

Thesis Submitted in Partial Fulfillment of the  
Requirements for the Degree of  
Master of Science

in the  
Department of Chemistry  
Faculty of Science

© **Soo Hur**

**SIMON FRASER UNIVERSITY**

**Spring 2016**

All rights reserved.

However, in accordance with the *Copyright Act of Canada*, this work may be reproduced, without authorization, under the conditions for "Fair Dealing." Therefore, limited reproduction of this work for the purposes of private study, research, criticism, review and news reporting is likely to be in accordance with the law, particularly if cited appropriately.

# Approval

**Name:** Soo Hur  
**Degree:** Master of Science (Chemistry)  
**Title:** *Studies Toward the Biosynthesis of Chimonanthine in Chimonanthus praecox*  
**Examining Committee:** Chair: Dr. Michael H. Eikerling  
Professor

**Dr. Robert A. Britton**  
Senior Supervisor  
Professor

---

**Dr. David Vocadlo**  
Co-Supervisor  
Professor

---

**Dr. Erika Plettner**  
Supervisor  
Professor

---

**Dr. Roger Linington**  
Internal Examiner  
Associate Professor

---

**Date Defended/Approved:** January 18, 2016

## Abstract

Chimonanthine is the building block of a series of natural products found in terrestrial plants including members of *Psychotria* in the family of *Rubiaceae*. Studies have shown that alkaloids containing the chimonanthine core display interesting analgesic, inhibition of melanogenesis, and anti-cancer activities. The goal of this study is to explore the precursor directed biosynthesis of chimonanthine and the enzymes involved in the biosynthesis of chimoanthine as well as to identify these enzymes for potential use as biocatalysts that can generate libraries of modified natural products. Herein we report the identification of a suitable plant containing these enzymes and demonstrate the feasibility of new assays by showing that feeding of plants with synthetic precursors leads to the production of labelled chimonanthine.

**Keywords:** chimonanthine; precursor-directed biosynthesis; calycantheaceous alkaloid, pyrrolidinoindoline alkaloids;

## Acknowledgements

First of all, I would like to thank Prof. Robert Britton, and Prof. David Vocadlo for allowing me to work in their labs in the last two and half years. The project they gave me was very interesting because I was able to explore various science including chemistry, biochemistry, and some biology, all at the same time. Their thoughtful ideas, and detailed instructions led me to develop initial steps to start research, and their patience and attitude shown to me have made my time at Simon Fraser University enjoyable.

I am also thankful for having Prof. Erika Plettner as my supervisory committee member. Her knowledge in biosynthesis of natural products gave me a lot of great idea to try new experiments, which eventually led me to obtain the data I wanted. Thank you for giving me time to discuss the research progress, and providing me various ideas to initiate new experiments.

Also, the time I spent with all of the members of the Britton group, and the Vocadlo group was enjoyable, and it was good time to discuss science with them. I would like to say special thank you to Dr. Stanley Chang for giving me opportunities to work on synthetic organic chemistry for total synthesis of ascospiroketal A. I learned a lot of interesting chemistry under your supervision. Another special thanks to Dr. Milan Bergeron-Brelek and Michael Holmes for giving me various ideas on my research, and sacrificing their time to help with my scientific writing. Also, Dr. Milan Bergeron-Brelek provided me with a neat, warm and nice bed, and lots of great food on one of the weekends during Basic Military Officer Qualification training. The food you provided I will never forget. I'd like to thank Dr. Robby Zhai, Dr. Ajay Naidu, Dr. Matt Nodwell, Dr. Jake Goodwin-Tindall, Dr. Shira Halperin, Jason Draper, Hope Fan, Vijay Dhand, Matt Taron, Abhi Bagai, Chris Adamson, Daniel Kwon, Micahel Meanwell and Venugopal Rao Challa for making the working lab environment fun and productive.

Lastly, I appreciate the unlimited support and love from my family. They always motivated me whenever I feel discouraged. I do not think that I would make it without their support and love.

# Table of Contents

Approval.....	ii
Abstract.....	iii
Acknowledgements.....	iv
Table of Contents.....	v
List of Tables.....	vii
List of Figures.....	viii
List of Schemes.....	x
List of Acronyms.....	xi

<b>Chapter 1. Introduction .....</b>	<b>1</b>
1.1. Enzymes in Nature and in Chemistry.....	1
1.2. Calycanthaceous Alkaloids.....	6
1.3. Chimonanthine .....	9
1.3.1. Background Information.....	9
1.3.2. Early Syntheses of Chimonanthine.....	11
1.3.3. First Enantioselective Syntheses of Chimonanthine .....	13
1.3.4. Additional Total Syntheses of Chimonanthine. ....	16
1.3.5. Biosynthetic Studies of Chimonanthine.....	17
1.4. Proposed Biosynthesis of Chimonanthine.....	18
1.5. Main Goals of This Study.....	19

<b>Chapter 2. Studies towards the Biosynthesis of (-)- and meso-Chimonanthine .....</b>	<b>21</b>
2.1. Background Information.....	21
2.2. Preparation of Precursor Analogues.....	25
2.3. <i>In Planta</i> Experiment (Feeding Experiment) .....	26
2.3.1. Screening Precursor Analogues .....	26
2.3.2. Isolation of Unnatural Products, (-)-5,5'-Difluoro-chimonanthine and meso-5,5'-Difluoro-chimonanthine .....	31
2.4. In Vitro Assay .....	35
2.4.1. Background Information.....	35
2.4.2. Cytoplasmic Protein Extraction from Leaf .....	36
2.4.3. Cytoplasmic Protein Extraction from Root.....	39
2.4.4. <i>In vitro</i> Assay with Protoplast.....	42
2.4.5. Proteins from Cell Walls .....	43
2.5. Summary.....	49
2.6. Future Direction.....	50
2.7. Experimental .....	52
2.7.1. General Considerations.....	52
2.7.2. Experimental Information for Tryptamine Analogues .....	54
2.7.3. Experimental Information for <i>N<sub>b</sub></i> -methyltryptamine analogues.....	59
2.7.4. Synthetic Standards of D <sub>6</sub> -chimonanthines.....	63
2.7.5. Feeding Precursors <i>in planta</i> and Screening Precursors by LC-MS.....	65
2.7.6. Isolation of Fluorinated Unnatural Products .....	65

2.7.7.	Plant Protein Extraction with P-PER™ Plant Protein Extraction Kit and <i>in vitro</i> Assay .....	67
2.7.8.	Plant Protein Extraction from Leaves Using Blender and <i>in vitro</i> Assay .....	68
2.7.9.	Plant Protein Extraction From Roots Using Blender and <i>in vitro</i> Assay <sup>[83]</sup> .....	69
2.7.10.	Root protein separation by Ammonium Sulfate Precipitation.....	69
2.7.11.	Preparation of Protoplasts <sup>[84]</sup> .....	70
2.7.12.	<i>In Vitro</i> Assay with Protoplasts .....	70
2.7.13.	Preparation of Cell Wall <sup>[88]</sup> .....	70
2.7.14.	Preparation of Cell Wall proteins <sup>[89]</sup> .....	71
<b>References</b>	.....	<b>72</b>
Appendix A.	Total Synthesis of Ascospiroketal A Through a Ag <sup>I</sup> -Promoted Cyclization Cascade .....	79

## List of Tables

Table 2.1.	Results after feeding experiment.....	28
Table 2.2.	Isolation of chimonanthines and unnatural chimonanthines by HPLC .....	32
Table 2.3	Localization of Biosynthesis of Chimonanthine.....	36
Table 2.4	In vitro assay with protein extracts by P-PER™ Plant Protein Extraction Kit.....	37
Table 2.5.	In vitro assay with protein extracts from homogenized plant leaf samples after blending .....	38
Table 2.7.	In vitro assay with 113 and protein extracts from homogenized plant root samples after blending and ammonium sulfate precipitation.....	41
Table 2.8.	LC methods on LC-MS analysis .....	65
Table 2.9.	HPLC eluent system to isolate difluorochimonanthines .....	66
Table 2.10.	Extraction buffers and reaction buffers used in <i>in vitro</i> assay .....	68

## List of Figures

Figure 1.1.	Examples of well-known alkaloids; morphine (6), cocaine (7), and nicotine (8) .....	3
Figure 1.2	Examples of (bis)indoline calycanthaceous alkaloids. ....	7
Figure 1.3.	Chimonanthine homologues: hodgkinsine (55) and quadrigemine C (56).....	9
Figure 1.4.	Structure of (-)-chimonanthine (29), (+)-chimonanthine (30), and meso-chimonanthine (31).....	9
Figure 1.5.	Illustration of tail-flick model with mouse.....	10
Figure 1.6.	Kirby's Radiolabelled Precursors and Radiolabelled Chimonanthine products from <i>Chimonanthus praecox</i> .....	17
Figure 2.1.	Illustration of unnatural product synthesis by PDB <sup>[70,71]</sup> .....	21
Figure 2.2.	Precursor directed biosynthesis of nostocarboline analogues .....	23
Figure 2.3.	Illustration of experimental scheme. (a) <i>in planta</i> assay (b) <i>in vitro</i> assay. ....	24
Figure 2.4.	Precursor analogues to study PDB of chimonanthine.....	26
Figure 2.5.	Feeding precursor analogues into leaves of <i>chimonanthus praecox</i> .....	27
Figure 2.6.	Target unnatural chimonanthine analogues after feeding <i>Chimonanthus praecox</i> with 108: (-)-5,5'-fluorochimonanthine (128), and meso-5,5'-fluorochimonanthine (129) .....	31
Figure 2.7.	HPLC separation of alkaloid extracts after 5-fluorotryptamine (108) was fed to <i>Chimonanthus praecox</i> . ....	32
Figure 2.8.	NMR spectra of various temperature NMR experiments on <sup>1</sup> H and <sup>19</sup> F NMR of isolated meso-5,5'-difluoro-chimonanthine (129) .....	34
Figure 2.9.	Feeding D <sub>3</sub> -N <sub>b</sub> -methyltryptamine into different plant parts. Order from left to right. A) One whole leaf. B) Small pieces of a leaf. C) Stem. D) Branch. E) Root. F) Control. ....	35
Figure 2.10.	Image of roots of <i>Chimonanthus praecox</i> washed with distilled water. ....	40
Figure 2.11.	Fluorescent microscopy images of plant cells. Native plant cells (left) and a protoplast after enzymatic digestion (Right). ....	42
Figure 2.12.	Images of ground leaves in liquid nitrogen in a mortar (a), cell wall powders after removing cellular components (b) and cell wall proteins on SDS-PAGE (c).....	45
Figure 2.13.	Extracted ion chromatograms of <i>m/z</i> of 383.2042 ± 0.002 in the time interval of 4.4 min to 5.2 min after incubation of precursor with different amount of cell walls .....	46



Figure 2.14.	LC-MS EIC chromatograms. ....	48
Figure 2.15.	O'Connor's mutasynthesis in <i>Catharanthus roseus</i> . ....	51

## List of Schemes

Scheme 1.1.	Chemoenzymatic synthesis of 10-deoxymethynolide (3) and acetyl-narbonolide (5) .....	2
Scheme 1.2.	Biosynthetic route of morphine (42).....	5
Scheme 1.3.	Woodward's proposed biosynthesis of calycanthine (28) .....	8
Scheme 1.4.	Melanin biosynthetic route.....	11
Scheme 1.5.	Hendrickson's total synthesis of chimonanthine .....	12
Scheme 1.6.	Scott's total synthesis of chimonanthine and proposed mechanism .....	13
Scheme 1.7.	Overman's total synthesis of <i>meso</i> -chimonanthine.....	14
Scheme 1.8.	Overman's total synthesis of (-)-chimonanthine.....	15
Scheme 1.9.	Overman's total synthesis of (+)-chimonanthine.....	16
Scheme 1.10.	Proposed biosynthetic pathway of chimonanthine from tryptophan. ....	18
Scheme 1.11.	Proposed mechanism of biosynthesis from <i>N<sub>b</sub></i> -methyltryptamine (37) to chimonanthine.....	19
Scheme 2.1.	Synthesis of fluorinated unnatural precursor derivatives.....	25
Scheme 2.2.	Expected incorporation of 113 to 118 <i>in vitro</i> assay with root protein extract .....	40
Scheme 2.3.	Comparison between uncontrolled and controlled oxidative dimerization to afford natural product .....	44
Scheme 2.4.	Possible route of dirigent protein mediated biosynthesis of chimonanthine.....	49

## List of Acronyms

2,2-DMP	2,2-dimethoxypropane
4'OMT	4-O-methyltransferase
6OMT	6-O-methyltransferase
AcOH	Acetic acid
ACP	Acyl carrier protein
AT	Acyl transferase
BCl <sub>3</sub>	Boron trichloride
BSA	Bovine serum albumin
CH <sub>2</sub> Cl <sub>2</sub>	Dichloromethane
CH <sub>2</sub> O	Formaldehyde
CNMT	Coclaurine <i>N</i> -methyltransferase
CODM	Codeine <i>O</i> -demethylase
COR	Codeine reductase
CSA	Camphosulfonic acid monohydrate
DCM	Dichloromethane
DCT	Dopachrome tautomerase
DEAD	Diethyl azocarboxylate
DH	Dehydratase
DIPA	Diisopropylamine
DMF	Dimethylformamide
DMPU	1,3-Dimethyl-3,4,5,6-tetrahydro-2-pyrimidinone
DOPA	Dihydroxyphenylalanine
DRR	1,2-Dehydroreticuline reductase
DRS	1,2-Dehydroreticuline synthase
DTT	Dithiothreitol
EDTA	Ethlyenediaminetetraacetic acid
EIC	Extracted Ion Chromatogram
EMCCD	Electron multiplying charge coupled device
ER	Enoyl reductase
Et <sub>2</sub> O	Diethyl ether
Et <sub>3</sub> N	Triethyl amine

EtOH	Ethanol
FAD	Flavin adenine dinucleotide
FeCl <sub>3</sub>	Iron (III) chloride
G6P	Glucose-6-phosphate
G6PDH	Glucose-6-phosphate dehydrogenase
GC	Gas chromatography
GC-MS	Gas chromatography-mass spectrometry
HMPA	Hexamethylphosphoramide
HN <sub>3</sub>	Hydrazoic acid
HPLC	High performance liquid chromatography
HR	High resolution
I <sub>2</sub>	Iodine
INMT	Indoleethylamine <i>N</i> -methyltransferase
JRES	J-resolved spectroscopy
KR	Ketoreductase
KS	Ketosynthase
LC	Liquid chromatography
LC-MS	Liquid chromatography-mass spectrometry
LDA	Lithium diisopropylamide
L-DOPA	L-3,4-dihydroxyphenylalanine
LiAlD <sub>4</sub>	Lithium aluminium deuteride
LiAlH <sub>4</sub>	Lithium aluminium hydride
LiCl	Lithium chloride
Me <sub>3</sub> Al	Trimethyl aluminium
MeMgI	Methyl magnesium iodide
MeOH	Methanol
MES	2-( <i>N</i> -Morpholino)ethanesulfonic acid
MM-NAC	Methylmalonyl <i>N</i> -acetylcysteamine
MOPS	3-( <i>N</i> -Morpholino)propanesulfonic acid
MPE	Maximum possible effect
mRNA	Messenger ribonucleic acid
MS	Mass spectrometry
Na	Sodium

NaBH(OAc) <sub>3</sub>	Sodium triacetoxyborohydride
NaBH <sub>4</sub>	Sodium borohydride
NADH	Nicotinamide adenine dinucleotide
NADP	Nicotinamide adenine dinucleotide phosphate
NaH	Sodium hydride
NaHMDS	Sodium bis(trimethylsilyl)amide
NCS	Norcochlorine synthase
NH <sub>3</sub>	Ammonia
NMR	Nuclear magnetic resonance
PAH	Phenylalanine hydroxylase
Pb(OAc) <sub>4</sub>	Lead (IV) acetate
PBS	Phosphate buffered saline
PDB	Precursor-directed biosynthesis
PEG	Polyethyleneglycol
Ph <sub>3</sub> P	Triphenylphosphine
PhH	Benzene
PVPP	Poly(vinylpyrrolidone)
Red-Al	Sodium bis(2-methoxyethoxy)aluminumhydride
RNA	Ribonucleic acid
SalAT	7-O-Acetyltransferase
SalR	Salutaridine reductase
SDS-PAGE	Sodium dodecyl sulfate – polyacrylamide gel electrophoresis
SmI <sub>2</sub>	Samarium (II) iodide
T6ODM	Thebaine 6-O-demethylase
TDC	Tryptophan decarboxylase
TE	Thioesterase
TFA	Trifluoroacetic acid
TH-1	Tryptophan hydroxylase 1
THF	Tetrahydrofuran
TLC	Thin layer chromatography
TRP-1	Tyrosinase related protein 1
TRP-2	Tyrosinase related protein 2
TYDC	Tyrosine decarboxylase

Zn

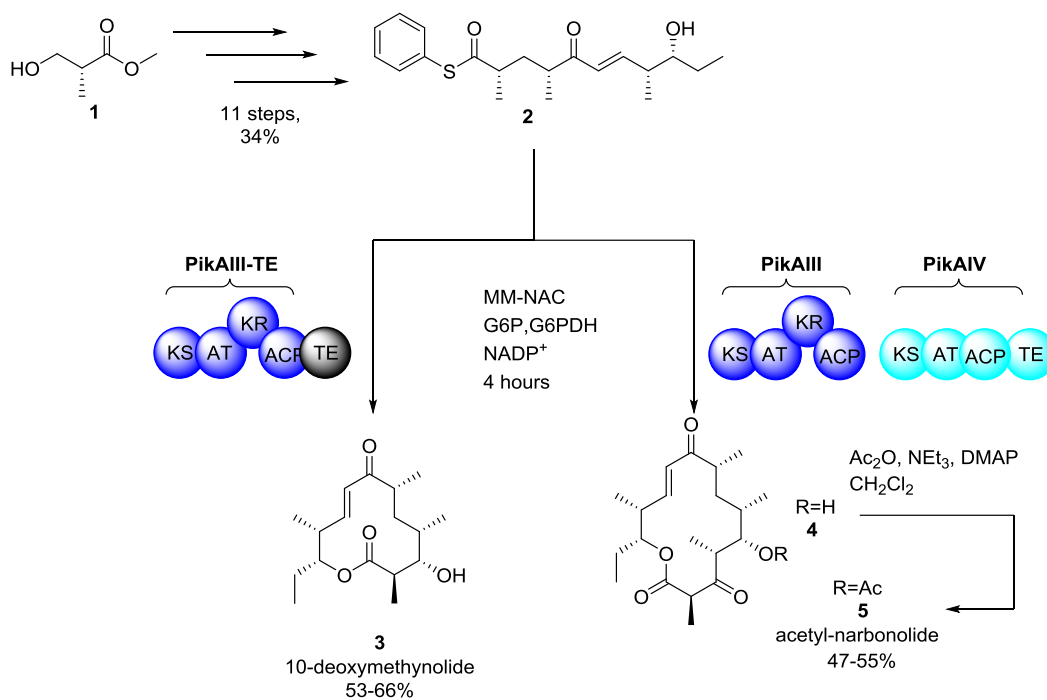
Zinc

# Chapter 1.

## Introduction

### 1.1. Enzymes in Nature and in Chemistry

In Nature, living organisms (e.g. mammals, plants) produce useful natural products via numerous biosynthetic processes that rely on enzymes, which possess several unique characteristics such as high substrate specificity and enantioselectivity.<sup>[1-4]</sup> A large number of these enzymes have now been identified and structurally characterized. For example, polyketide biosynthesis has been the subject of intense research and is now largely understood to rely on collections of enzymes that form “modules” which are responsible for adding one more acetate or propionate unit to a growing polyketide chain and effect subsequent functional group transformations (e.g., reduction or dehydration). The biosynthesis of polyketides starts with a loading module, and ends with a thioesterase which removes the polyketide natural product from the biosynthetic machinery.<sup>[5-7]</sup> Understanding this biosynthetic pathway has allowed scientists to exploit this molecular machinery in the synthesis of many unnatural polyketides. An example of this is shown in Scheme 1.1, where Sherman and co-workers carried out the chemoenzymatic synthesis of 10-deoxymethynolide (**3**) and acetyl-narbonolide (**5**). The substrate **2** was prepared in 11 steps from the Roche ester (**1**) then further elaborated and lactonized by the actions of PikAIII-TE to afford **3** or two modules of PikAIII/PikAIV to afford the related macrolactone **5**.<sup>[8]</sup> This rapid synthesis of these complicated polyketides illustrates the power of using biosynthetic pathways to compliment total syntheses.



**Scheme 1.1. Chemoenzymatic synthesis of 10-deoxymethynolide (3) and acetyl-narbonolide (5)**

Alkaloids are a very large class of natural products that necessarily contain a nitrogen atom and have played an important role historically as a source of natural medicines (e.g. opium poppy from 200 BC).<sup>[9]</sup> However, the biosynthetic pathways for the production of alkaloids have not been well elucidated compared to pathways for other natural products such as polyketides, terpenoids, and carbohydrates. For example, morphine (6), the most well-known alkaloid, was first isolated in 1805 by Friedrich Sertürner,<sup>[10]</sup> but elucidation of the enzymes responsible for morphine biosynthesis was only established in the early 2000s.<sup>[11]</sup>



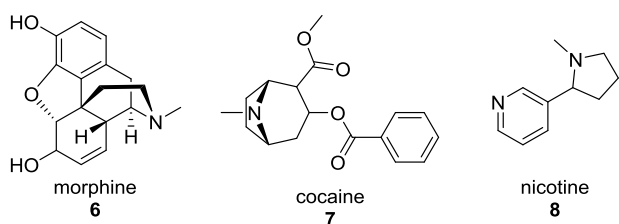
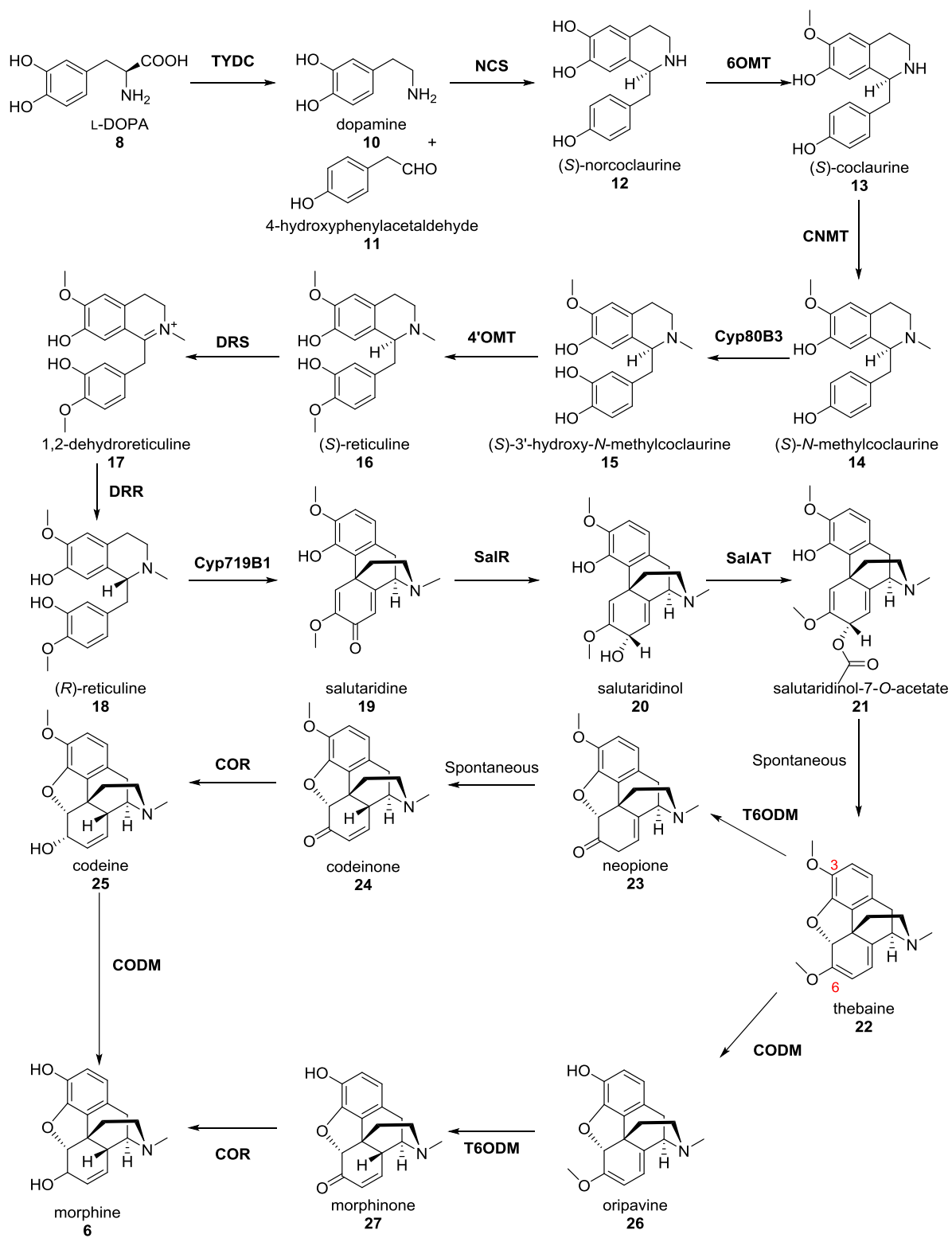


**Figure 1.1. Examples of well-known alkaloids; morphine (6), cocaine (7), and nicotine (8)**

The difficulties in elucidating pathways involved in alkaloid biosynthesis is in part related to the fact that there exist numerous structurally distinct families of alkaloids whose natural production initiates with a unique starting material and consequently each biosynthetic step requires discrete enzymes. For example, the biosynthesis of morphine (**6**) is depicted in Scheme 1.2.<sup>[11–13]</sup> This pathway initiates with decarboxylation of L-DOPA (**9**) by tyrosine decarboxylase (TYDC) to afford dopamine (**10**). Norcoclaurine synthase (NCS) utilizes substrates **10** and 4-hydroxyphenylacetaldehyde (**11**) to yield (*S*)-norcoclaurine (**12**), which is then methylated by norclaurine 6-*O*-methyltransferase (6OMT) to obtain (*S*)-coclaurine (**13**). Subsequent methylation by coclaurine *N*-methyltransferase (CNMT) affords (*S*)-*N*-methylcoclaurine (**14**). Then, a selective oxidation of an aromatic ring by *N*-methylcoclaurine-3-hydroxylase (Cyp80B3) affords (*S*)-3'-hydroxy-*N*-methylcoclaurine (**15**), which undergoes selective methylation on hydroxyl group by 3'-hydroxy-*N*-methylcoclaurine 4-*O*-methyltransferase (4'OMT) to obtain (*S*)-reticuline (**16**). Iminium ion mediated epimerization of substrate **16** to (*R*)-reticuline (**18**) is performed by two enzymes: 1,2-dehydroreticuline synthase (DRS) and 1,2-dehydroreticuline reductase (DRR). Salutaridine synthase (Cyp719B1) cyclizes **18** to yield salutaridine (**19**). Salutaridine reductase (SalR) reduces ketone function in **19** to produce salutaridinol (**20**). Salutaridinol 7-*O*-acetyltransferase (SalAT) specifically acetylates the C7 alcohol function to provide salutaridinol-7-*O*-acetate (**21**), which spontaneously cyclizes to thebaine (**22**).

There are two possible routes from thebaine (**22**) to morphine (**6**). The first pathway is from **22** to neopinone **23** via removal of the methyl group at the 6 position by thebaine 6-*O*-demethylase (T6ODM). Then, **23** spontaneously undergoes rearrangement to codeinone (**24**). The reduction of the enone to an allylic alcohol by codeine reductase (COR) yields codeine (**25**). The last step in the first pathway involves

demethylation by codeine O-demethylase (CODM) to obtain morphine (**6**). The second route from **22** to **6** involves demethylation CODM to afford oripavine (**26**), which undergoes another demethylation by T6ODM to yield mophinone (**27**). Lastly, **27** undergo reduction by COR to obtain morphine (**6**).



**Scheme 1.2. Biosynthetic route of morphine (42)**

(Scheme 1.2 – continued from previous page)

TYDC: tyrosine decarboxylase, NCS: norcoclaurine synthase, 6OMT: 6-O-methyltransferase, CNMT: coclaurine *N*-methyltransferase, Cyp80B3: *N*-methylcoclaurine 3-hydroxylase, 4'OMT: 3'-hydroxy-*N*-methylcoclaurine 4-Omethyltransferase, DRS: 1,2-dehydroreticuline synthase, DRR: 1,2-dehydroreticuline reductase, Cyp719B1: salutaridine synthase, SalR: salutaridine reductase, SalAT: 7-O-acetyltransferase, T6ODM: thebaine 6-O-demethylase, COR: codeine reductase, CODM: codeine O-demethylase

Thus, biosynthetic studies on alkaloids are complicated by their unique and complex structures. However, there is no doubt that further studies towards the identification of biosynthetic pathways are useful as they would support the large scale syntheses of these potentially important natural products as well as analogues. In this thesis, the biosynthesis of one member of the family of calycanthaceous alkaloids, chimonanthine, is studied. In the following section, the history, bioactivity, and synthetic and biosynthetic efforts towards chimonanthine will be discussed.

## 1.2. Calycanthaceous Alkaloids

The study on calycanthaceous alkaloids started with a letter written in November, 1887 by Mr. J. H. H. Boyd. <sup>[14]</sup>

“Hundreds of cattle and sheep have died here in the past five years from ‘bubby’ (the eccentric name of *Calycanthus glaucus*). The seeds only are poisonous. When a brute gets a sufficient dose, from five to ten well-filled pods, it makes for the nearest water and often falls dead while drinking, or it may live three or four weeks and then die. The symptoms are like those of a man extremely drunk, except that any noise frightens it. Stamp the ground hard close to a brute poisoned with ‘bubby,’ and it will jump and jerk and tremble for several minutes. That is our method of telling when they have taken it. The eyes turn white and glassy, and while lying they throw back the head and look as if dead already. ‘Bubby’ does not seem to hurt a brute so much if it cannot get water. Our best remedy is apple brandy, strong coffee and raw eggs poured down as soon as possible after finding. It is certain that ‘bubby’ is the most poisonous of any shrub or weed in existence here, from the fact that when brutes have once eaten it they will take it every time they can get it. It grows on every hillside, along all branches (creeks), in every fence corner and almost everywhere.”

In 1888, Eccles studied the poisonous “bubby” seeds (*Calycanthus glaucus*) in order to elucidate the toxic components from the extracts, and was the first to report a

new compound, calycanthine (**28**) which represents the first entry of a new class of alkaloids which have become known as the calycanthaceous alkaloids (Figure 1.2).<sup>[15]</sup> Interestingly, during this study it was reported that alkaloid **28** was not toxic. The isolated sample of (+)-calycanthine also allowed for the detailed description of several physical properties, including specific bad odour, poor solubility in water and good solubility in diethylether or chloroform. Furthermore, it was noted that the colour of the alkaloids change after coming into contact with several acids. For example, when **28** was treated with concentrated sulphuric acid, the initial mixture turned into a yellow solution. In the presence of concentrated ‘muriatic acid’ (HCl), the solution turned yellow initially and then turned olive green. A combination of concentrated sulphuric acid and sugar made a “lovely” pink red colour. Also, Eccles reported that (+)-calycanthine (**28**) made up 2% of the total mass of the seed. One year after this initial discovery, Wiley determined that the alkaloid has the molecular formula  $C_{18}H_{40}N_2O_{11}$ .<sup>[14]</sup>

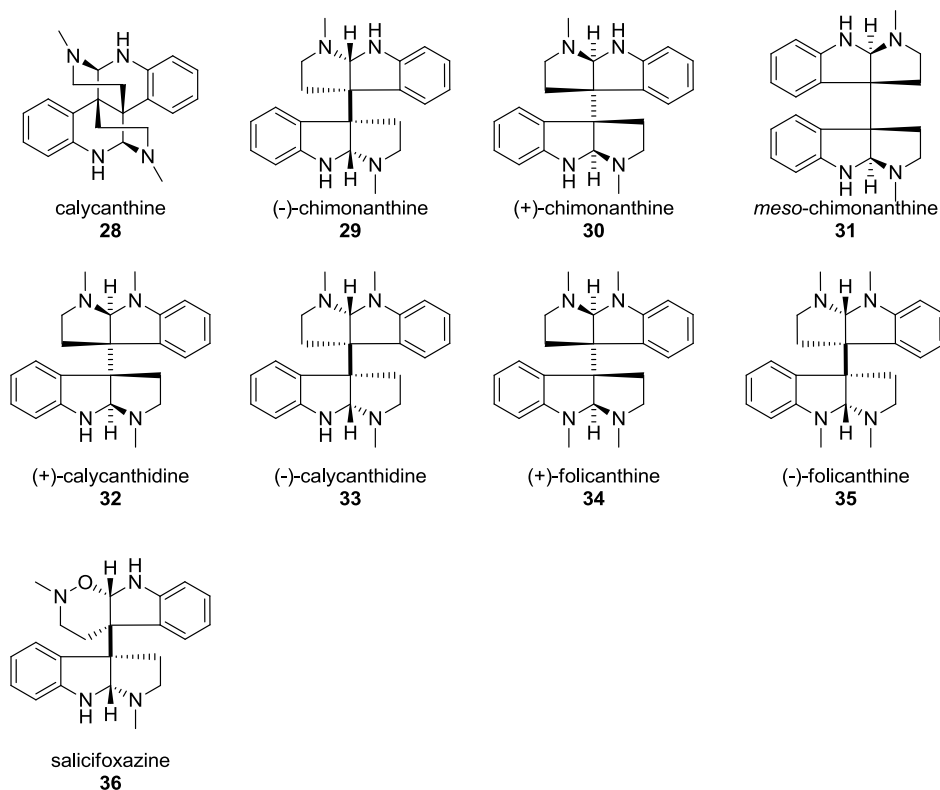
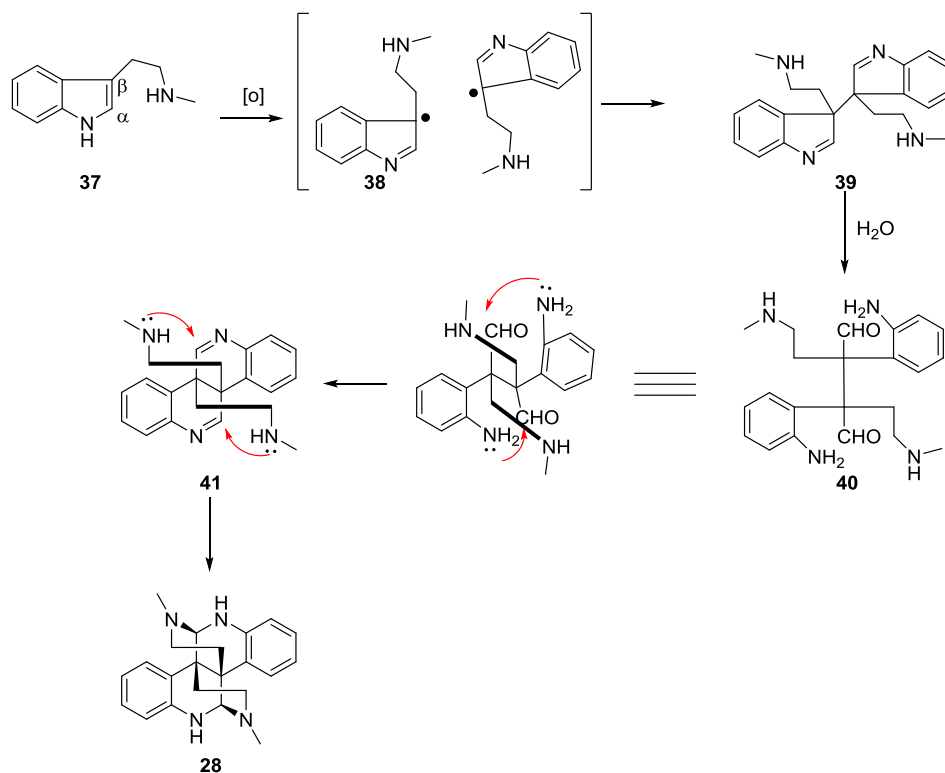


**Figure 1.2** Examples of (bis)indoline calycanthaceous alkaloids.

Nearly twenty years after these initial studies, Gordin reported that there was no oxygen atom in (+)-calycanthine (**28**) and determined that the molecular formula was

$C_{11}H_{14}N_2$  by measuring the amount of  $CO_2$  and volume of  $N_2$  released from calycanthine (**28**).<sup>[16,17]</sup> A further twenty years later, in 1925, the molecular formula was doubled by Späth and Stroh to  $C_{22}H_{28}N_4$ .<sup>[18]</sup> In a subsequent study by Barger, the molecular formula of (+)-calycanthine (**28**) was further revised to  $C_{22}H_{26}N_4$  in 1939.<sup>[19]</sup> However, the molecular structure was not elucidated until 1960 when Woodward, Clark and Katz determined the structure of (+)-calycanthine (**28**) by degradation methods.<sup>[20]</sup> They also proposed a potential biosynthetic pathway (Scheme 1.3) to (+)-calycanthine (**28**) beginning with the  $\beta,\beta'$ -oxidation of *N*<sub>b</sub>-methyltryptamine (**37**). The same year, the structure of (+)-calycanthine (**28**) was confirmed by Hamor via X-ray crystallography of the alkaloid.<sup>[21]</sup>



**Scheme 1.3. Woodward's proposed biosynthesis of calycanthine (28)**

The discovery of a number of new calycanthaceous alkaloids was reported following the isolation of (+)-calycanthine.<sup>[19,22–26]</sup> (Figure 1.2) Additionally, several homologues of (+)-calycanthine (**28**) produced by medicinal terrestrial plants (e.g. *Psychotria* sp.) were identified that contain a central *meso*-chimonanthine unit as part of their structure (highlighted in blue, Figure 1.3).<sup>[27–32]</sup>

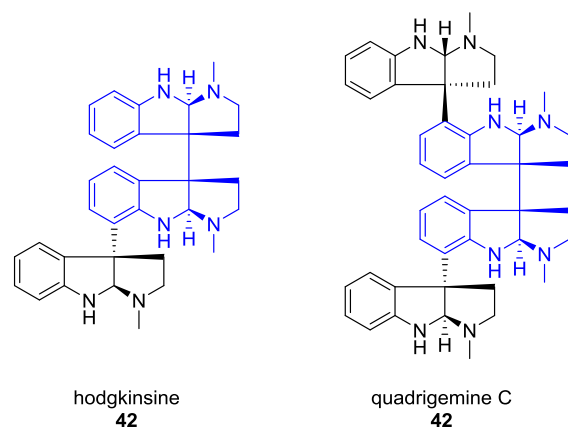


**Figure 1.3. Chimnanthine homologues: hodgkinsine (55) and quadrigemine C (56)**

## 1.3. Chimnanthine

### 1.3.1. Background Information

In 1961, (-)-chimonanthine (**29**), a structural isomer of calycanthine (**28**), was discovered by Hodson from the leaves of *Chimonanthus fragrans*, Lindl.<sup>[33]</sup> The structure of (-)-chimonanthine (**29**) was determined in the following year via x-ray crystallography by Hamor.<sup>[34]</sup> Interestingly, the enantiomeric (+)-chimonanthine (**30**) was later isolated in 1983 by Tokuyama from the skin of colombian poison-dart frog,<sup>[35]</sup> and again in 1999 by Potier from plants of the *Psychotria* species.<sup>[30]</sup> Despite having been synthesized prior to its isolation, *meso*-chimonanthine (**31**) was also isolated from *Psychotria forsteriana* in 1992.<sup>[36]</sup>

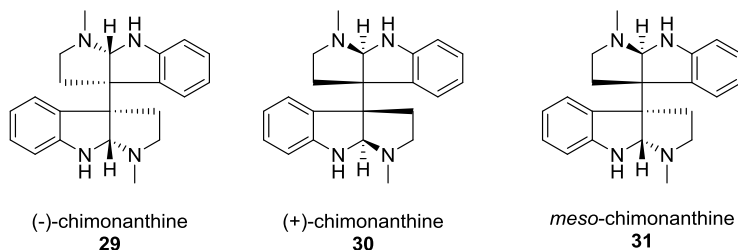


**Figure 1.4. Structure of (-)-chimonanthine (29), (+)-chimonanthine (30), and *meso*-chimonanthine (31).**

In 2002, Verotta performed a comparative study on the analgesic properties of chimonanthines to morphine (**6**), and found that the former family of natural products (**29-31**) exhibit strong binding affinities toward the  $\mu$ -opioid receptor.<sup>[37]</sup> In the tail-flick mouse assay (Figure 1.5), Verotta compared (-)- and (+)-chimonanthines (**29** and **30**) with morphine (**6**) by measuring the change in the response time after causing pain to the mouse.<sup>[38]</sup> While morphine (**6**) displayed 100% maximum possible effect (MPE) at 6 mg/kg, (-)-chimonanthine (**29**) displayed 40% MPE at 10 mg/kg and (+)-chimonanthine (**30**) displayed 66% MPE at 5 mg/kg. In the capsaicin induced pain model, Verotta reported that a dosage of 0.25 mg/kg of (-) and (+)-chimonanthines (**29, 30**), the mice reduced licking at the site where capsaicin was injected, and they observed that inhibition of licking diminished by 47% and 38% when administered with (-)-chimonanthine (**29**) and (+)-chimonanthine (**30**), respectively. Furthermore, (-)-chimonanthine (**29**), (+)-chimonanthine (**30**) and *meso*-chimonanthine (**31**) displayed strong binding affinity ( $K_i$ ) to  $\mu$ -opioid receptor with  $271 \pm 85$  nM,  $652 \pm 159$  nM and  $341 \pm 29$  nM, respectively. As a comparison, morphine (**6**) displayed  $0.76 \pm 0.04$  nM binding affinity towards the same receptor. These results suggested that chimonanthines could be good lead candidates as analgesics.

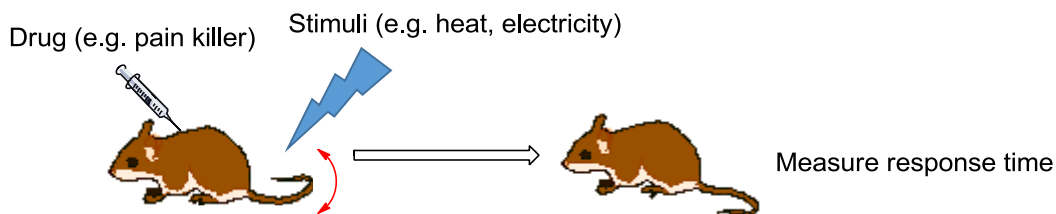
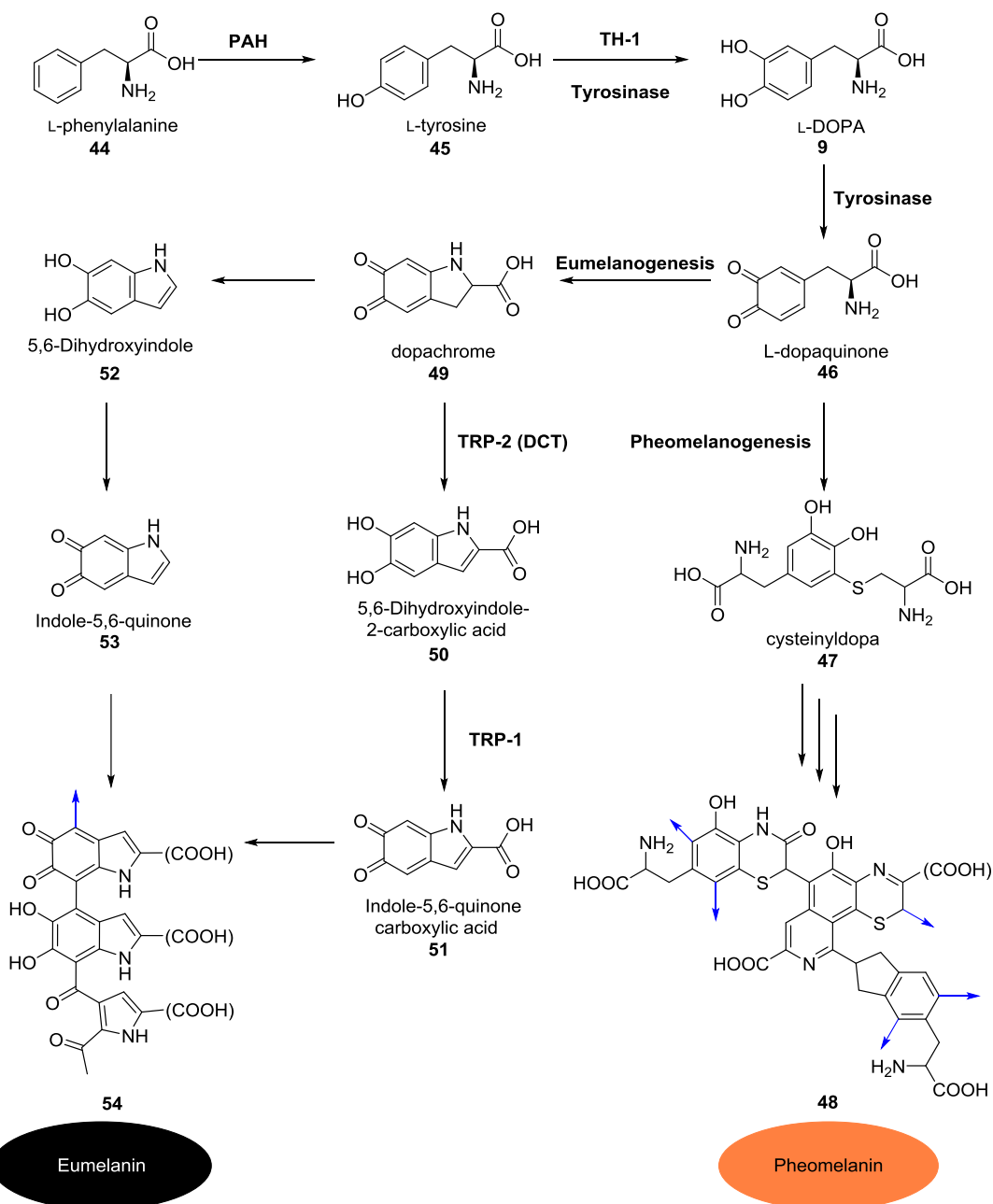


**Figure 1.5. Illustration of tail-flick model with mouse**

Further investigations into the biological activity of the chimonanthines revealed that (-)-chimonanthine (**29**) inhibits melanogenesis, *in vitro* (see Scheme 1.4). This pathway is responsible for the generation of melanin in the body. The study reported that (-)-chimonanthine (**29**) showed inhibition of melanin production in B16 melanoma 4A5 cells ( $IC_{50} = 1.4$   $\mu$ M), and compared favourably to the commercially available tyrosinase inhibitor arbutin ( $IC_{50} = 174$   $\mu$ M). However, the inhibition mechanism associated with chimonanthine has not been reported yet.<sup>[39-41]</sup>





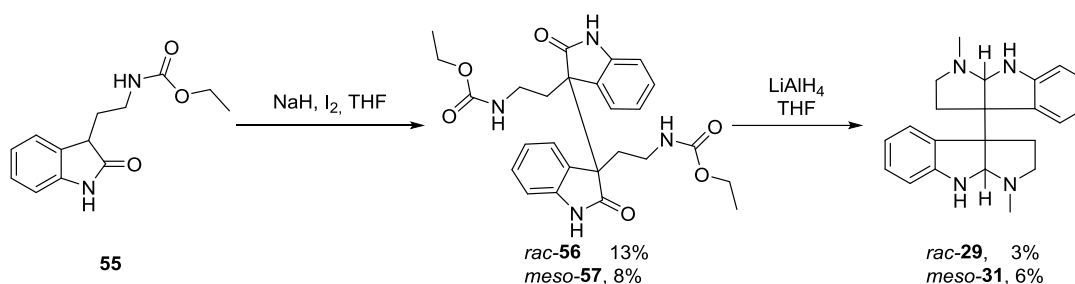
### Scheme 1.4. Melanin biosynthetic route

The blue arrows in chemical structures of eumelanin and pheomelanin indicate where elongation occurs, and the COOH groups in parenthesis can be substituted with H.

### 1.3.2. Early Syntheses of Chimonanthine

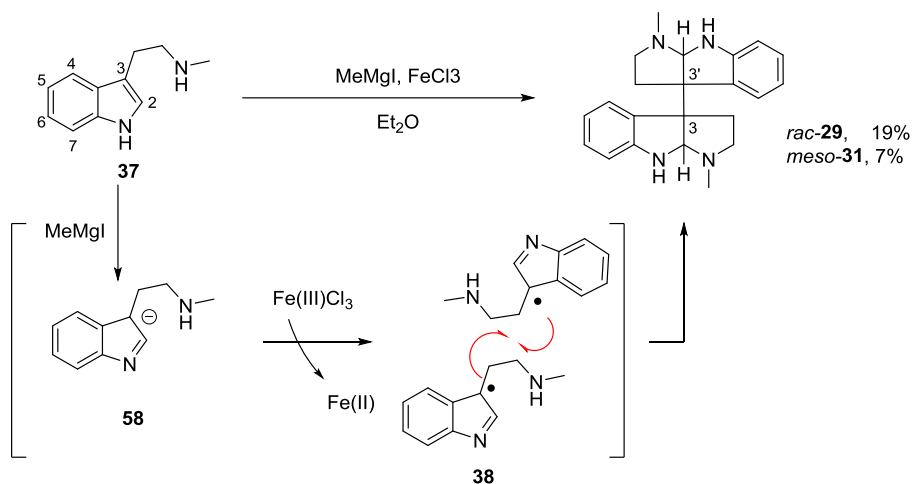
The interesting biological activity and intriguing structural characteristics of chimonanthine has inspired the development of several synthetic routes to these

compounds. The major challenge in these syntheses relates to the controlled introduction of the two adjacent quaternary all-carbon stereocentres, for which several new methods were devised. In 1962, Hendrickson reported the first total synthesis of *rac*-chimonanthine (*rac*-**29**) and *meso*-chimonanthine (**31**) (Scheme 1.5).<sup>[42,43]</sup> This biomimetic total synthesis of chimonanthine relied on an oxidative dimerization of **55** to afford the key C-C bond. This biomimetic sequence supported the previously proposed biosynthesis of calycanthine by Woodward (see Scheme 1.3).



**Scheme 1.5. Hendrickson's total synthesis of chimonanthine**

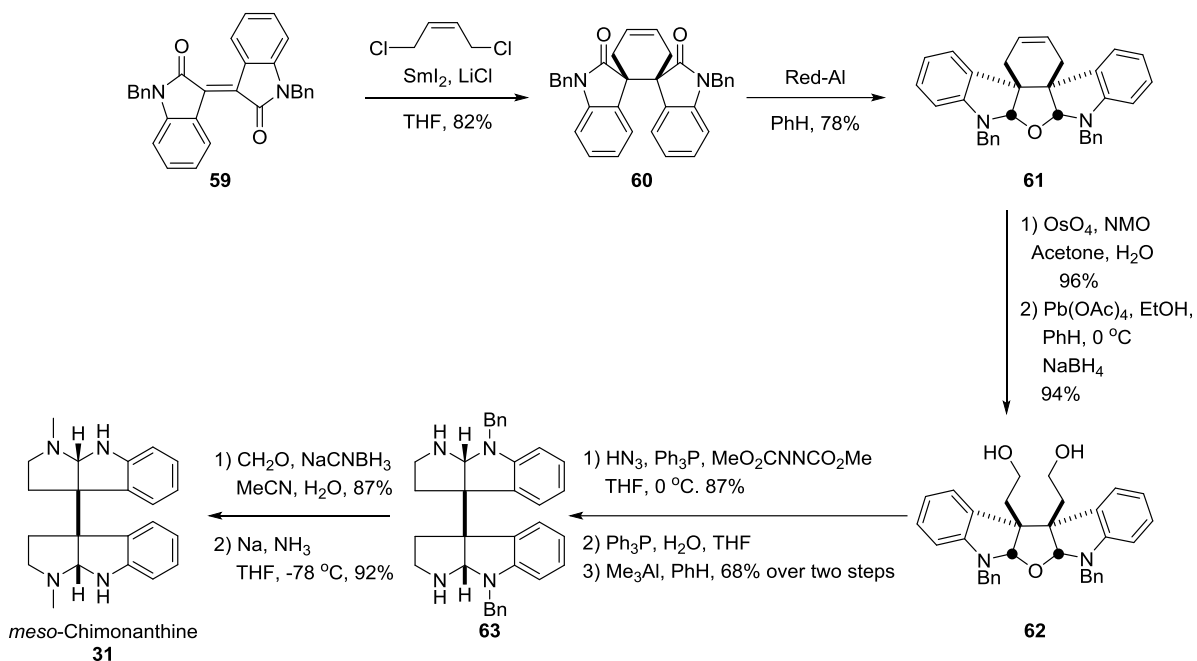
Two years later, Scott reported the second total synthesis of chimonanthine via oxidative dimerization of *N*<sub>6</sub>-methyltryptamine (**37**) (Scheme 1.6).<sup>[44]</sup> This synthesis utilized a common biological building block **37** and was achieved in a single step with an improved yield compared to that reported by Hendrickson. The proposed mechanism for this key transformation is depicted in Scheme 1.6. Thus, deprotonation of the indole nitrogen by methylmagnesium iodide affords the resonance-stabilised anion **58**. The anion then undergoes a single electron oxidation with iron (III) chloride to afford a C3 radical which undergoes radical recombination with an equivalent coupling partner to provide the key C3-C3' bond to yield chimonanthine (*rac*-**29**, *meso*-**31**).



**Scheme 1.6. Scott's total synthesis of chimonanthine and proposed mechanism**

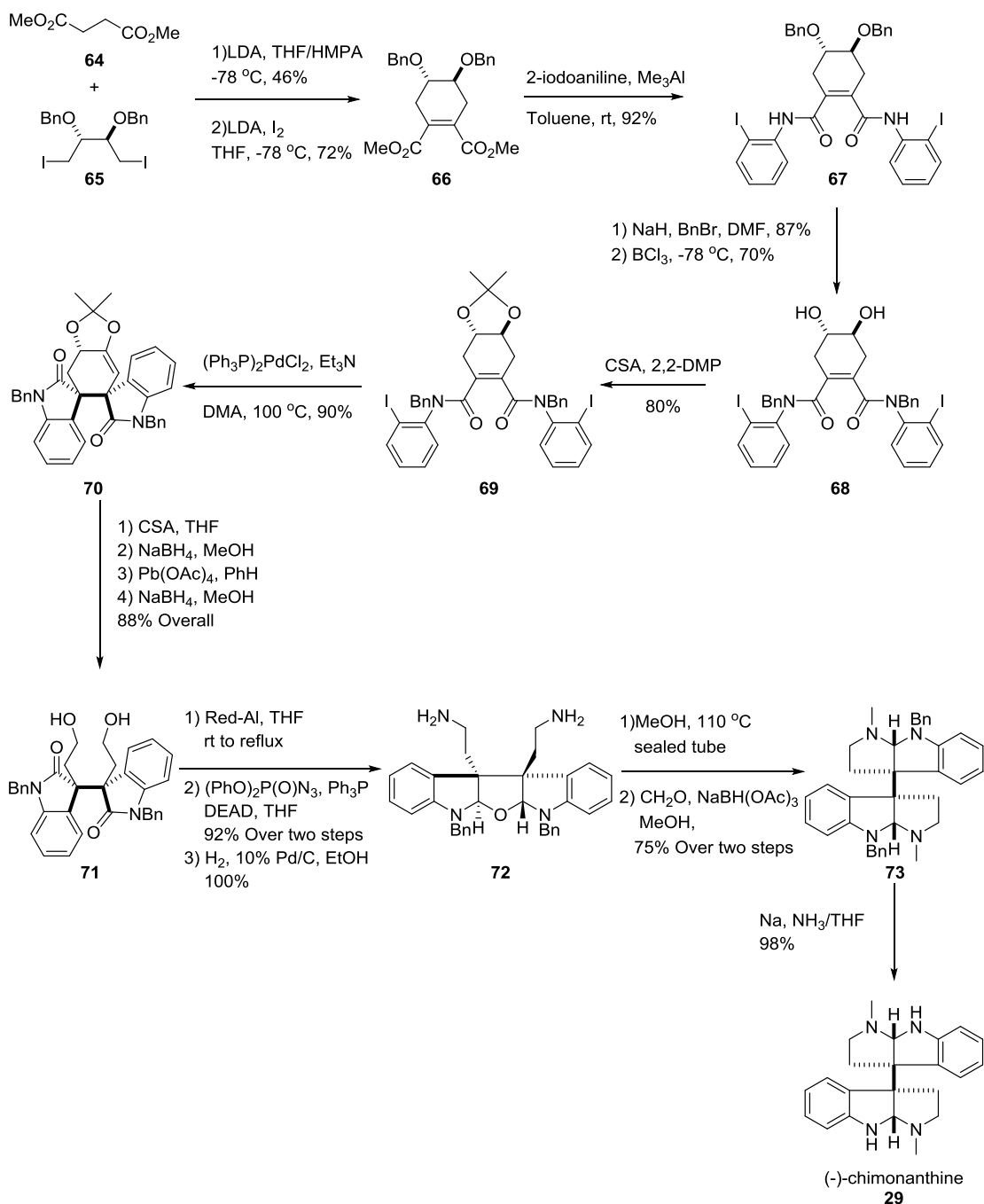
### 1.3.3. First Enantioselective Syntheses of Chimonanthine

While the racemic syntheses of the chimonanthines were achieved with few synthetic steps, their enantioselective synthesis presented a major challenge. Overman and coworkers completed the first total synthesis of *meso*, (+)- and (-)-chimonanthine through a series of enantioselective syntheses that proved to be landmarks in asymmetric synthesis. For *meso*-chimonanthine, the readily available isoindigo **59** was converted to **60** via samarium mediated reductive dialkylation (Scheme 1.7).<sup>[45]</sup> Reduction by Red-Al afforded hexacyclic intermediate **61**, which was dihydroxylated and cleaved to afford diol **62**. Subsequent Mitsunobu reaction, azide reduction and exposure to trimethylaluminum provided bis(pyrroloindoline) **63**. Finally, methylation and deprotection afforded desired product *meso*-**31**.



### Scheme 1.7. Overman's total synthesis of *meso*-chimonanthine

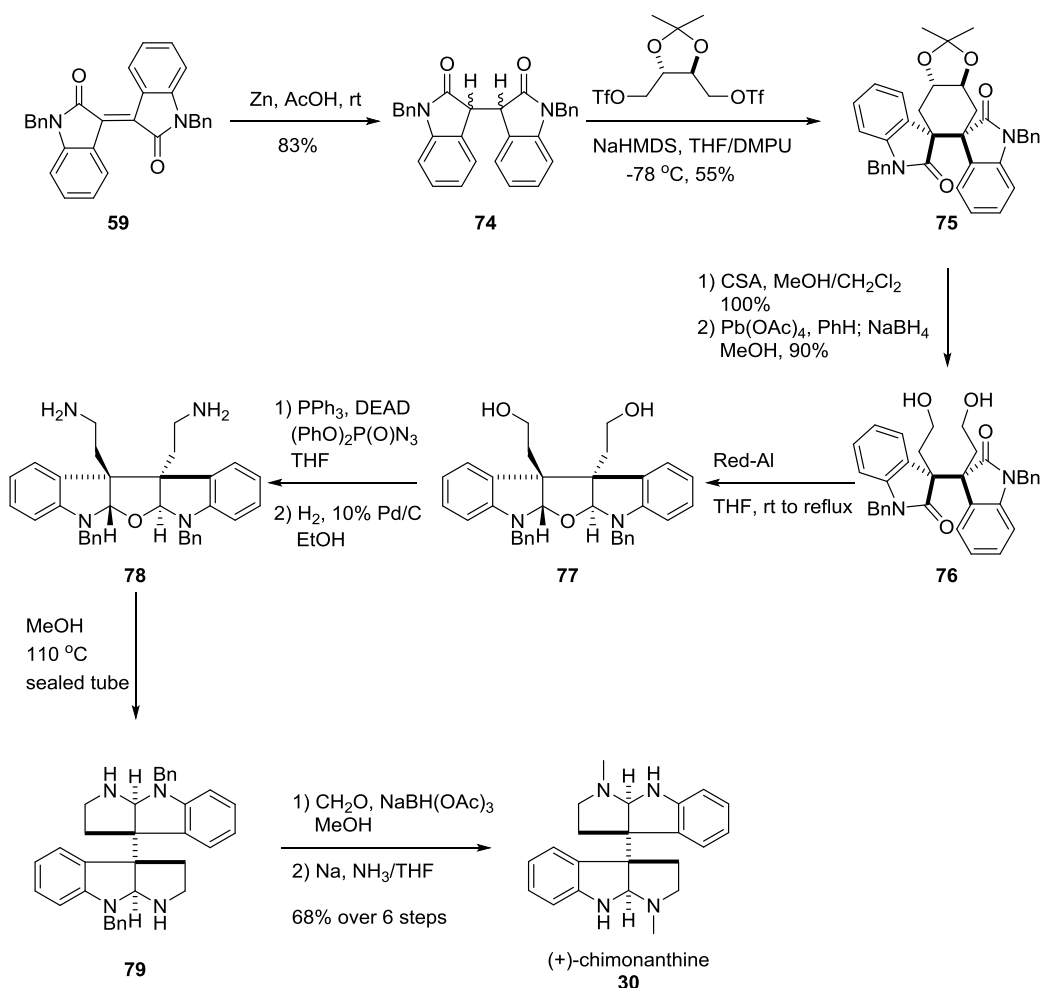
In 1999, Overman reported an enantioselective total synthesis of (-)-chimonanthine (**29**, Scheme 1.8).<sup>[46]</sup> The key reaction in the total synthesis of **29** is an intramolecular double Heck reaction cascade of **69** to **70**. In this single step, the vicinal quaternary all-carbon stereocentres were introduced in high yield. Following synthetic steps that included cleavage of the cyclohexene ring to provide diol **71**. Further reduction and a Mitsunobu reaction afforded **72**, the heating of which in methanol and subsequent bis-methylation yielded bispyrroloindoline **73**. Lastly, removal of benzyl group from **73** provided the desired product (-)-chimonanthine (**29**).



**Scheme 1.8. Overman's total synthesis of (-)-chimonanthine**

Following his successful synthesis of (-)-chimonanthine (**43**), Overman reported a modified synthesis of (+)-chimonanthine (**30**, Scheme 1.9) in 2000.<sup>[47]</sup> An interesting highlight in Overman's synthesis of **30** involves dialkylation of dihydroisoindigo **74** to afford bisoxyindole **75**. In a single step, the desired all-carbon quaternary stereocentres

were introduced in excellent yield. The remaining synthetic steps to (+)-**30** were identical to those employed in the total synthesis of (-)-**30**.



**Scheme 1.9. Overman's total synthesis of (+)-chimonanthine**

### 1.3.4. Additional Total Syntheses of Chimonanthine. .

Following Overman's elegant enantioselective syntheses of *meso*, (-) and (+)-chimonanthines (**31**, **29**, **30**), numerous total syntheses of chimonanthine have been reported. In 2002, Takayama achieved a two-step synthesis of *rac*-chimonanthine (*rac*-**29**) and *meso*-chimonanthine (**31**).<sup>[48]</sup> In 2007, Movassaghi reported the total synthesis of (+)-chimonanthine (**30**) via the Co-mediated homodimerization of tryptophan after benzylic bromination.<sup>[49]</sup> In 2012, Matunaga developed an enantioselective synthesis of (+)-chimonanthine (**30**) in six steps through the use of a Schiff base.<sup>[50]</sup> In 2013, Ma

reported a highly enantioselective synthesis of (-)-chimonanthine (**29**) in three steps via bromocyclization of tryptamine.<sup>[51]</sup> Due in part to these efforts, there have been significant advances in achieving the C3-C3' dimerization of indole derivatives leading to the synthesis of several chimonanthine analogues.<sup>[52-61]</sup>

### 1.3.5. Biosynthetic Studies of Chimonanthine

While there have been multiple syntheses of chimonanthine and related analogues reported, only one study relating to the biosynthesis of this unique alkaloid has been reported.<sup>[62,63]</sup>

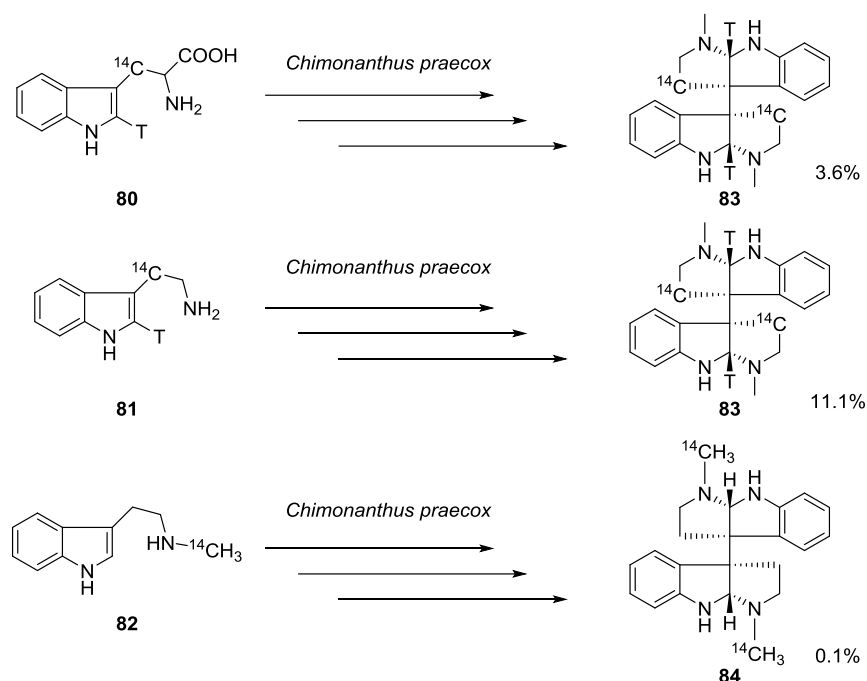


**Figure 1.6. Kirby's Radiolabelled Precursors and Radiolabelled Chimonanthine products from *Chimonanthus praecox***

The radiolabelled precursors were fed to *Chimonanthus praecox*, and the percentage of incorporation rate was determined by the ratio of radioactivity of isolated chimonanthine (counts per minute) over weight of isolated chimonanthine.

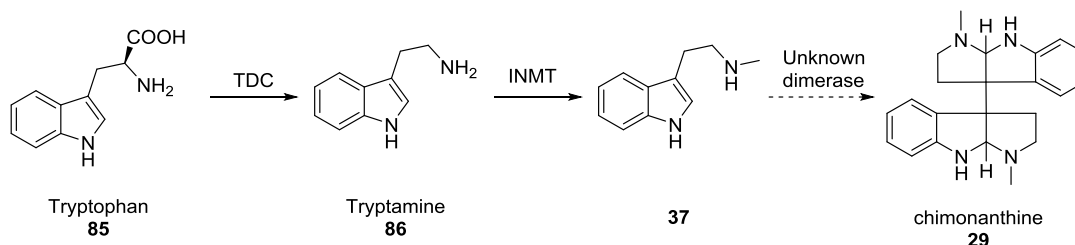
In this single study, Kirby synthesized radiolabelled tryptamine derivatives (**80-82**, Figure 1.6) and then fed solutions of these compounds to the leaves of *Chimonanthus fragrans*, a terrestrial plant from southern China. After seven days, the alkaloids were isolated by extraction, and the incorporation of radiolabelled precursors

into chimonanthine was evaluated. From the radioactivity data, it was determined that the radiolabelled tryptophan (**80**), tryptamine (**81**) and *N*<sub>b</sub>-methyltryptamine (**82**) were incorporated to the isolated sample of chimonanthine at a rate of 3.6%, 11.1% and 0.1%, respectively. These results indicated that tryptamine in particular was a biological starting point for the biosynthesis of chimonanthine. The low incorporation rate for the radiolabelled *N*<sub>b</sub>-methyltryptamine (**82**) compared to that of tryptamine (**81**) was postulated to result from the low solubility of this compound in water.

Unfortunately, since Kirby's study 45 years ago, there have been no further studies on the biosynthesis of chimonanthine.

## 1.4. Proposed Biosynthesis of Chimonanthine

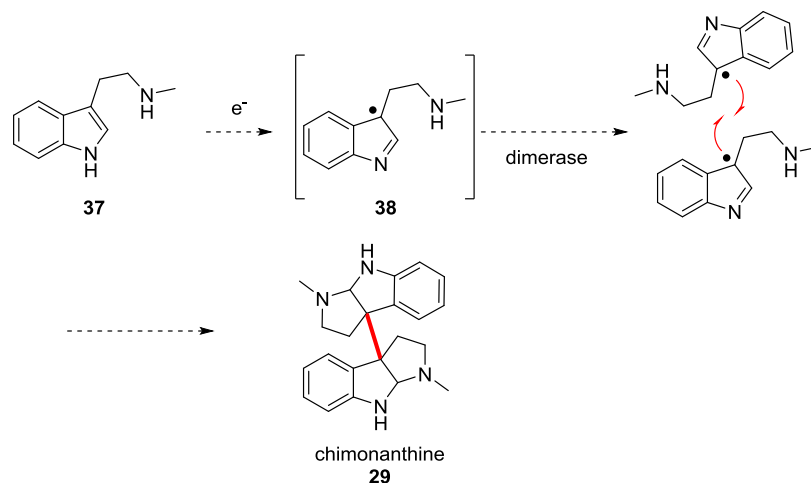
The biosynthetic pathway proposed by Kirby involves the steps tryptophan (**85**) → tryptamine (**86**) → *N*<sub>b</sub>-methyltryptamine (**37**) → chimonanthine. (Scheme 1.10) It is reasonable that tryptophan decarboxylase (TDC) is involved in the removal of carboxylate group from tryptophan (**85**) to yield tryptamine (**86**).<sup>[64–66]</sup> Then, indolethylamine *N*-methyltransferase (INMT),<sup>[67–69]</sup> a well-characterized enzyme, could effect methylation of the primary amine to afford *N*<sub>b</sub>-methyltryptamine (**37**). The final dimerization step of *N*<sub>b</sub>-methyltryptamine (**37**) into chimonanthine involves unidentified enzyme(s).



**Scheme 1.10. Proposed biosynthetic pathway of chimonanthine from tryptophan.**

The unknown dimerase that carries out the conversion of **37** into chimonanthine was proposed to be responsible for the oxidation of **37** required for recombination of the resultant radicals to form the two adjacent quaternary all-carbon stereocentres (Scheme 1.11).





**Scheme 1.11. Proposed mechanism of biosynthesis from *N*<sub>b</sub>-methyltryptamine (37) to chimonanthine.**

## 1.5. Main Goals of This Study

Since the discovery of (-)-chimonanthine (**29**) approximately 55 years ago, the chemical syntheses of chimonanthines and their derivatives have attracted considerable interest from the synthetic community owing to their interesting molecular structures and potentially useful biological activities. However, the biosynthesis of chimonanthine is not well established. More specifically, the key enzyme responsible for the dimerization of *N*<sub>b</sub>-methyltryptamine (**37**) to provide chimonanthine is unknown. Based on Kirby's proposal in 1969, the protein is postulated to have two important functions: i) oxidation of a reactive indole intermediate to form a radical, and ii) promoting an enantioselective carbon-carbon bond formation reaction with an equivalent radical intermediate. Importantly, identification of this dimerase could allow for the chemoenzymatic synthesis of chimonanthines and chimonanthine analogues using cheap and commercially available starting materials.

The goal of the thesis was to develop methods to investigate the unknown enzyme responsible for the oxidative dimerization of *N*<sub>b</sub>-methyltryptamine (**37**). The following chapter of this thesis includes a discussion of *in planta* experiments. Similar to Kirby's study, halogenated or isotope labelled tryptamine derivatives were prepared (e.g.

fluorinated tryptamine derivative, deuterated tryptamine derivative), and these precursors were fed into a chimonanthine-producing plant, *Chimonanthus praecox*. Once suitable biosynthetic precursors were identified, *in vitro* experiments were initiated. Then, the results from protein extractions, cell component preparation (protoplast and cell wall) are presented, and examination reaction buffers with an ultimate goal of producing chimonanthine analogues using cell extracts.

## Chapter 2.

# Studies towards the Biosynthesis of (-)- and *meso*-Chimonanthine

## 2.1. Background Information

Precursor-directed biosynthesis (PDB) is a method used to exploit existing biosynthetic pathways to natural products by feeding unnatural precursors that can be transformed through these pathways into structurally related unnatural products.<sup>[70,71]</sup> As illustrated in Figure 2.1, PDB relies on the administration of unnatural precursor of the natural biosynthetic precursor into a target tissue or organism. In Nature, only natural precursors are used to synthesize a natural product. However, when a synthetic unnatural precursor analogue is administered to a particular organism, this unnatural substrate can, in some cases, be assimilated into the biosynthetic pathways of the natural product, leading to the formation of an unnatural product that is structurally related to the natural product. The biosynthetic machinery (e.g., enzymes) is then exploited to produce analogues of the targeted natural products.<sup>[72–74]</sup>

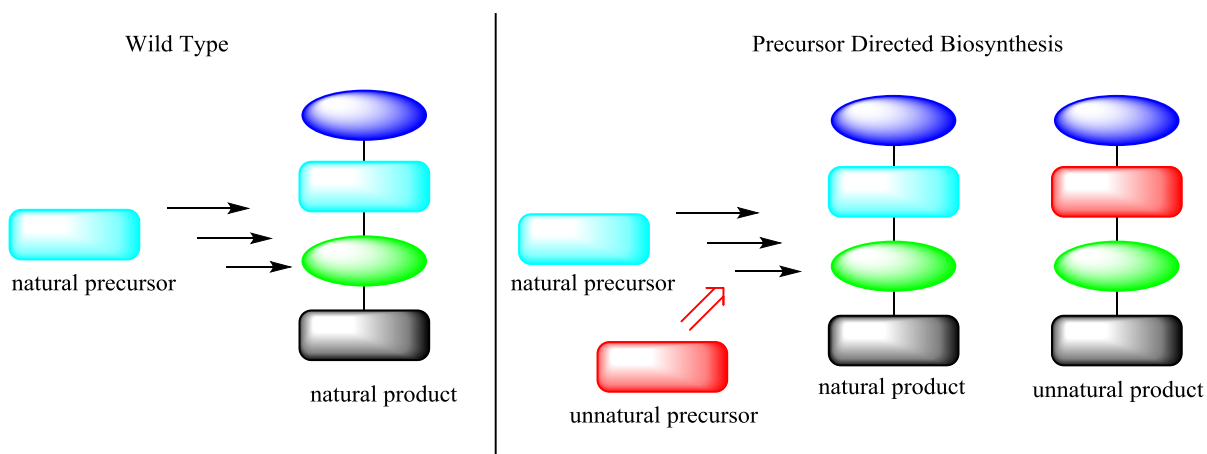
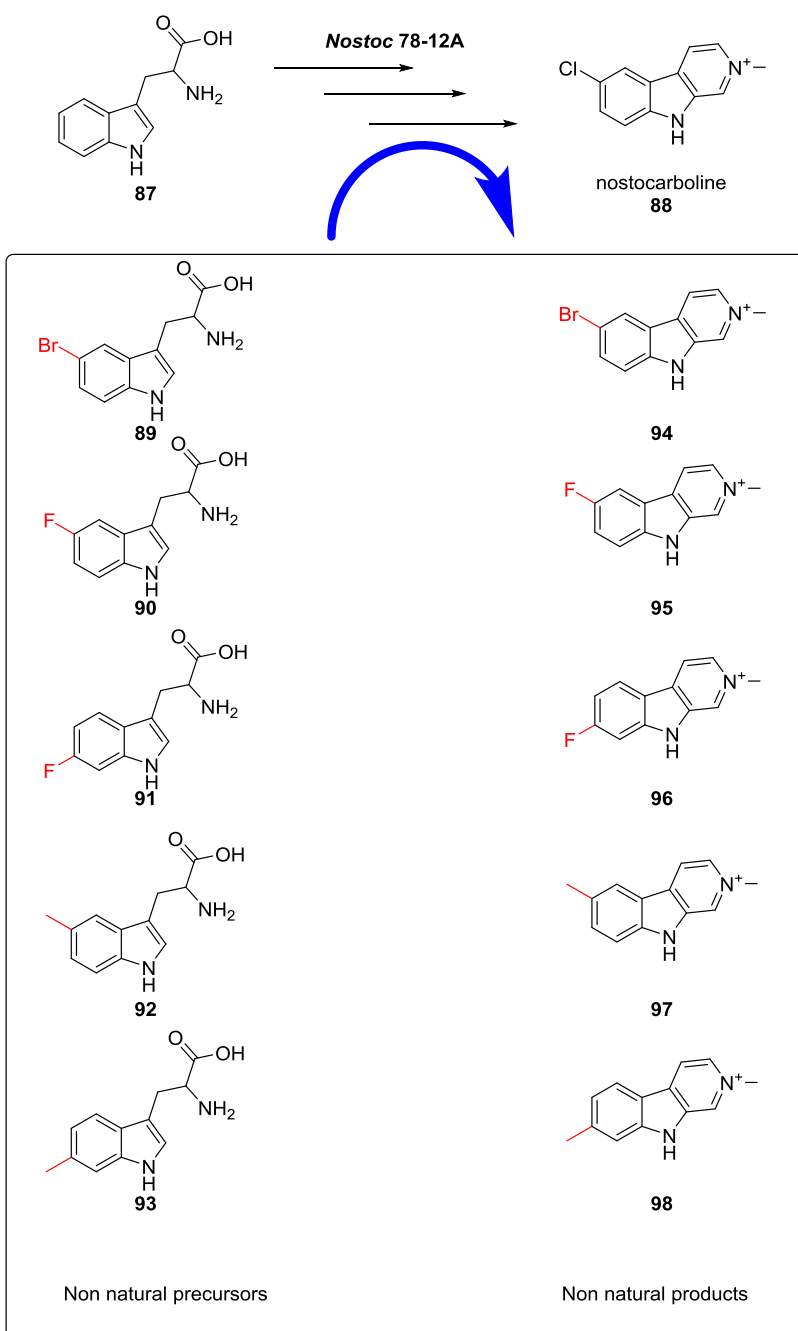


Figure 2.1. Illustration of unnatural product synthesis by PDB<sup>[70,71]</sup>

The application of PDB begins with the careful selection of suitable precursor analogues. Early stages of these experiments focus specifically on understanding how the administered unnatural precursors are tolerated by the biosynthetic machinery of a particular organism. The selected unnatural precursors must be able to reach the sites where the organism maintains the enzymes required to produce the natural product of interest. The production of unnatural products can then be tracked by analytical techniques such as HPLC, TLC, LC-MS, GC-MS or NMR. After confirming their production, anticipated unnatural products are then isolated and their structure characterized using modern spectroscopic methods. In some cases, at the same time, unnatural biosynthetic intermediates can also be isolated from this process such that one can track molecules produced during the biosynthetic cycle en route to the target natural product.<sup>[70,71,75]</sup> For example, in Figure 2.2, nostocarboline (**88**) is biosynthesized from tryptophan (**87**) in a strain of cyanobacterium *Nostoc* 78-12A, and one of the key steps in the biosynthesis of nostocarboline is chlorination of the C5 position. By feeding halogenated or methylated precursor analogues (**89-93**) into this strain, these precursors bypass the halogenation step and enter into the biosynthetic pathway to yield various nostocarboline analogues (**94-98**).<sup>[76]</sup>

Efforts toward the PDB of chimonanthine are discussed in this Chapter. The species *Chimonanthus praecox*, notably the identical one used in Kirby's studies described earlier (Section 1.3.5), was cultivated in the SFU greenhouse facility. We initiated our study with the chemical synthesis of potentially useful unnatural precursors that would be used in subsequent *in planta* feeding experiments (Figure 2.2. (a)). These feeding experiments were performed by delivering the unnatural precursors into *Chimonanthus praecox* plant tissues, including leaves and roots by placing the plant tissues in series of unnatural precursor solutions. Then allowing the plant tissue several days to incorporate the precursors forms chimonanthine analogues. After a sufficient incubation period, the alkaloids were extracted from the leaves and roots, then the crude samples were analyzed by LC-MS to monitor production of specific *m/z* of target chimonanthine analogues (Table 2.1). The main goals of these initial experiments were to screen for precursors that could be incorporated in the biosynthetic pathway of (-)- and *meso*-chimonanthine (**29**, **31**), as well as to then isolate and characterize potential unnatural chimonanthines.



**Figure 2.2. Precursor directed biosynthesis of nostocarboline analogues**

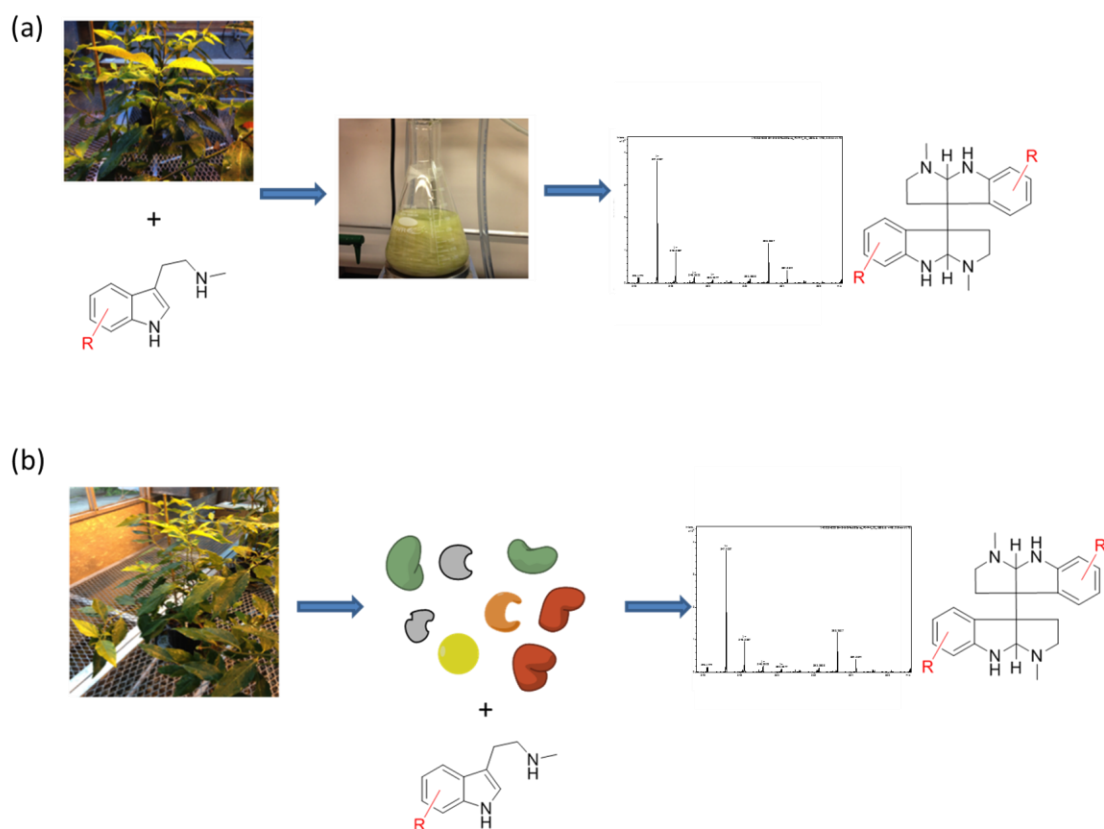


**Figure 2.3. Illustration of experimental scheme. (a) *in planta* assay (b) *in vitro* assay.**

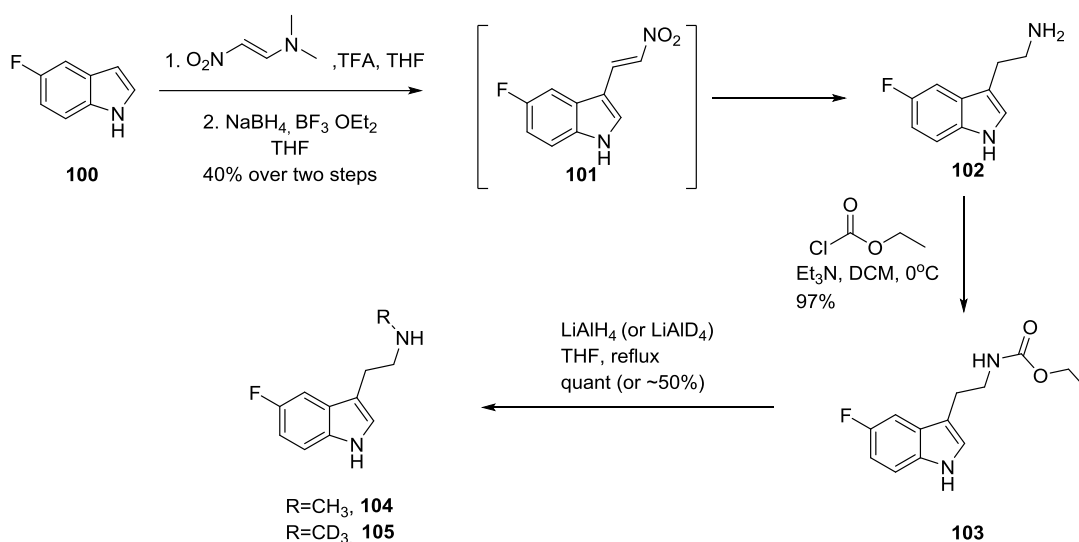
(a) *in planta* experiment: unnatural precursors screening and isolation of unnatural products. (b) *in vitro* experiment: studies toward the identification of a dimerase catalyzing the production of chimonanthine. Analytical tools such as NMR and/or LC-MS allow detection of targeted unnatural product(s)

Following the identification of suitable unnatural precursors, this study focused on the extraction of protein and components of cells from *Chimonanthus praecox* followed by *in vitro* assays on the biosynthesis of chimonanthine (Figure 2.2. (b)). Specifically, the extracted protein or cell components are incubated with unnatural precursors shown to be competent in the PDB studies, then the presence of chimonanthine analogues is assessed using LC-MS analyses. Following these studies, the proteins or cells are further separated by either protein size or cell fractionation, respectively. These different types of fractions can then be analyzed for their ability to produce the unnatural products. The ultimate goal of this study is to isolate the unknown enzyme(s) that is(are)

responsible for the C-C bond formation/dimerization between two *N*<sub>6</sub>-methyl-tryptamines (**37**) that yields chimonanthine.

## 2.2. Preparation of Precursor Analogues

As described in Section 1.3.5., Kirby's study led to the proposal for a biosynthetic pathway involving the conversion of tryptophan (**85**) to tryptamine (**86**), which is then converted to *N*<sub>6</sub>-methyl-tryptamine (**37**) and finally dimerized to provide chimonanthine (e.g. **29**) (Scheme 1.10). In order to select suitable unnatural precursor candidates for our feeding experiments, we began our investigation by evaluating commercially available and synthetically accessible analogues of tryptamine and *N*<sub>6</sub>-methyl-tryptamine.



**Scheme 2.1. Synthesis of fluorinated unnatural precursor derivatives**

In Scheme 2.1, 5-fluoroindole (**100**) undergoes alkylation to afford nitroalkene **101**. Then, without purification of **101**, the nitro group is reduced using NaBH<sub>4</sub> to yield 5-fluorotryptamine (**102**). Addition of chloroethylformate to **102** yields carbamate **103**, which after reduction using LiAlH<sub>4</sub> or LiAlD<sub>4</sub> furnishes the desired unnatural precursors **104** or **105**. The same chemistry was applied to prepare compounds **37**, **110**, **112**, and **115** (Figure 2.4, see experimental for details). The other precursor analogs used in this study were purchased from AK Scientifics and/or Alfa Aesar.

The unnatural precursors have unique molecular weight distinguishable from natural precursor, and also have unique characteristics, for example, the fluorinated precursors **108**, **109**, **113**, and **114** can be tracked by  $^{19}\text{F}$ -NMR, and brominated precursors (**111** and **115**) display specific isotope patterns in MS analysis (Figure 2.4).

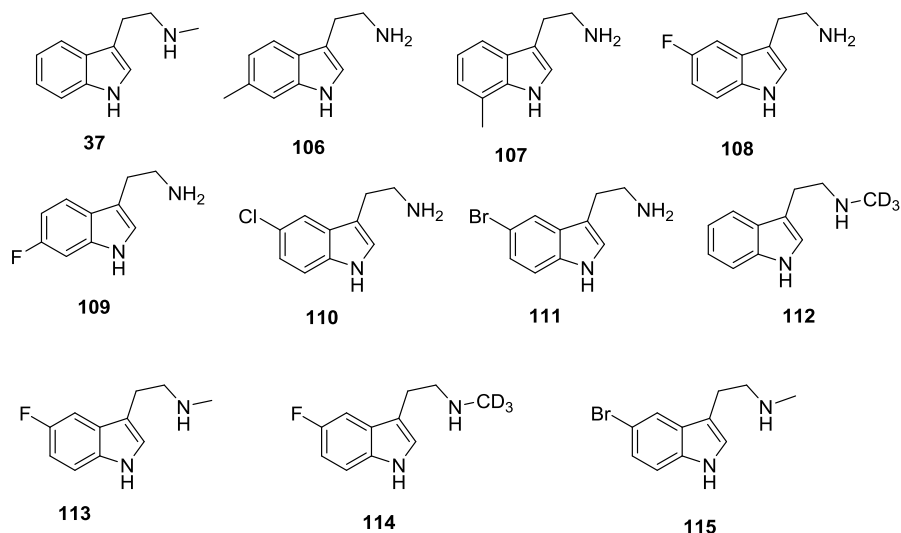


**Figure 2.4.** Precursor analogues to study PDB of chimonanthine

## 2.3. *In Planta* Experiment (Feeding Experiment)

### 2.3.1. Screening Precursor Analogues

The precursor analogues were dissolved independently in weakly acidic water (pH = 4) and fed to the leaves of *Chimonanthus praecox* by standing the stems of leaves in the water solution as described by Kirby.<sup>[63]</sup> This process required a five-day incubation period in a greenhouse and, after this time, the leaves were collected and ground using a mortar and pestle with freezing in liquid nitrogen. The powdered green leaves were suspended in methanol and stirred overnight. The solvent was collected by filtration to remove insoluble plant debris and then concentrated *in vacuo*. The crude alkaloid samples were then obtained by acid/base and chloroform extractions (see Experimental 2.7.6). The resulting crude mixtures were submitted for LC-MS analyses to detect the presence of potential unnatural products.



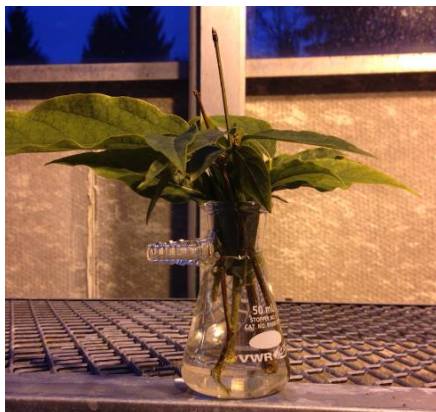


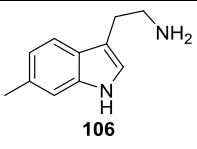
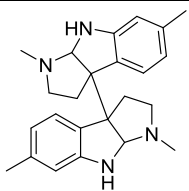
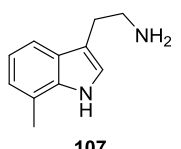
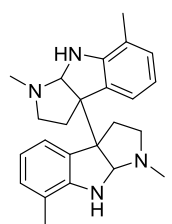
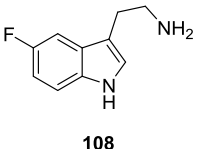
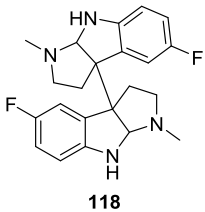
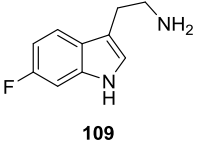
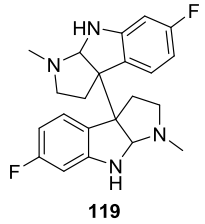
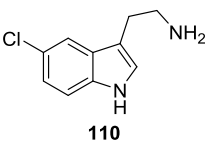
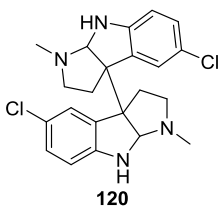
**Figure 2.5. Feeding precursor analogues into leaves of *chimonanthus praecox***

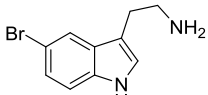
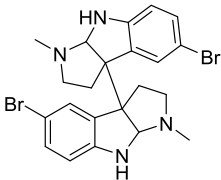
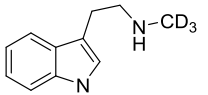
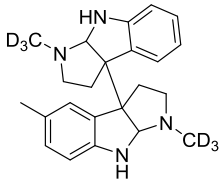
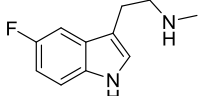
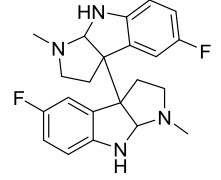
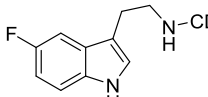
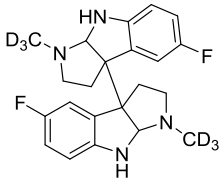
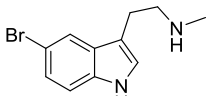
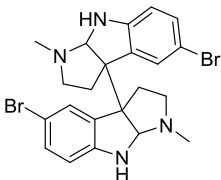
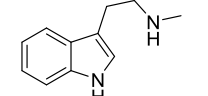
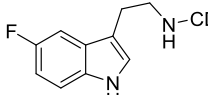
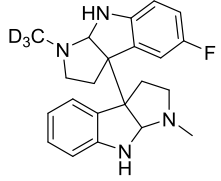
In our studies, we used the extracted ion chromatogram (EIC) function for our high resolution-liquid chromatography-mass spectrometry experiments. Specifically, EIC allows the detection of the specific  $m/z$  of interest from the entire data acquired in chromatographic run. The use of this technique is critical for the detection of small amounts of unnatural products in the presence of larger amounts of the natural products and other small molecules. In Table 2.1, the expected unnatural products from feeding experiments involving either one or two unnatural precursors are presented.

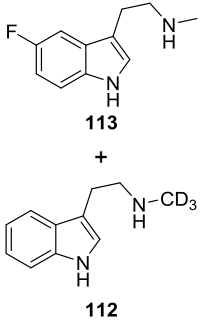
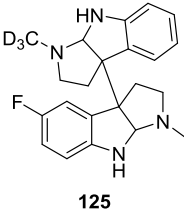
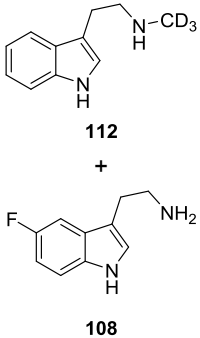
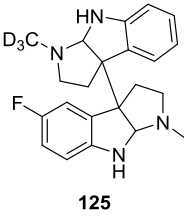
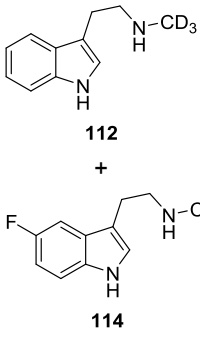
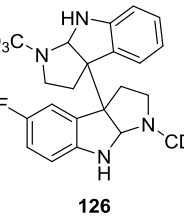
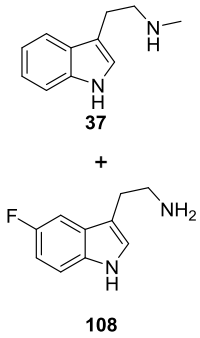
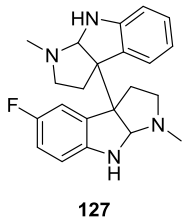
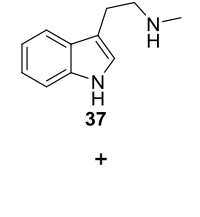
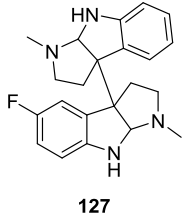
From the results of LC-MS analyses the formation of unnatural products was preliminarily established by monitoring their unique  $m/z$ . Administration of a single precursor or two precursors simultaneously were performed. The relative level of incorporation was estimated by calculating by the ratio of areas of  $m/z$  of unnatural product over areas of  $m/z$  of (-)-chimonanthine (**29**) observed in the LC chromatograms using the MS as a detector in EIC mode. The LC-MS analysis in EIC mode indicated that precursor analogues **107**, **108**, **109**, **112**, **113**, and **114** were incorporated into the expected unnatural chimonanthine analogues (**117**, **118**, **119**, **122**, and **123**). Furthermore, 6-methyltryptamine **106**, 5-chlorotryptamine (**110**), 5-bromotryptamine (**111**), and 5-bromo- $N_b$ -methyltryptamine (**115**) did not provide the  $m/z$  expected for the potential chimonanthine analogues (**116**, **120**, and **121**). Interestingly, after feeding with 7-methyltryptamine (**107**), LC-MS analysis detected the expected  $m/z$  of the corresponding chimonanthine analogue (**117**). As shown in Table 2.1, two other precursor analogues also gave rise to the anticipated  $m/z$  of their corresponding chimonanthine analogues. Based on these preliminary results suggesting that C5 and

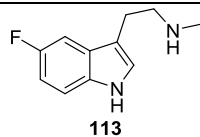
C6 substituted products were not formed, we postulate that somewhat larger substituents, such as Cl, Br. And CH<sub>3</sub>, at these positions may not be tolerated by the enzymes in the biosynthetic pathway leading to chimonanthine.

**Table 2.1. Results after feeding experiment**

Entry	Precursors	Expected chimonanthine analogue	Exact <i>m/z</i> of chimonanthine analogue	Detection of the <i>m/z</i> of chimonanthine analogue	Incorporation (%)
1	 106	 116	375.2543	No	NI
2	 107	 117	375.2543	Yes, 373.2545	1.97
3	 108	 118	383.2042	Yes, 383.2043	9.34
4	 109	 119	383.2042	Yes, 383.2038	17.1
5	 110	 120	415.1451	No	NI

<b>6</b>	 <b>111</b>	 <b>121</b>	503.0440	No	NI
<b>7</b>	 <b>112</b>	 <b>122</b>	353.2607	Yes, 353.2614	0.54
<b>8</b>	 <b>113</b>	 <b>118</b>	383.2042	Yes, 383.2043	1.1
<b>9</b>	 <b>114</b>	 <b>123</b>	389.2418	Yes, 389.2413	2.12
<b>10</b>	 <b>115</b>	 <b>121</b>	503.0441 505.0421 507.0400	No	NI
<b>11</b>	 <b>37</b> +  <b>114</b>	 <b>124</b>	368.2324	Yes, 378.2325	0.79

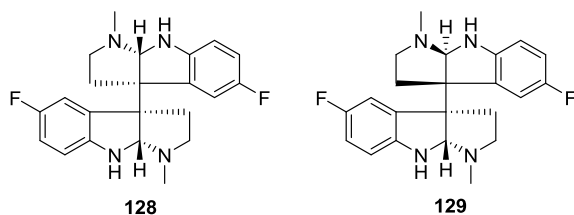
12	 <p>113 +</p> <p>112</p>	 <p>125</p>	368.2324	Yes, 368.2325	1.12
13	 <p>112 +</p> <p>108</p>	 <p>125</p>	368.2324	Yes, 368.2319	1.06
14	 <p>112 +</p> <p>114</p>	 <p>126</p>	371.2512	Yes, 371.2508	0.79
15	 <p>37 +</p> <p>108</p>	 <p>127</p>	365.2136	Yes, 365.2137	1.30
16	 <p>37 +</p> <p>127</p>	 <p>127</p>	365.2136	Yes, 365.2144	1.11



NI: No incorporation

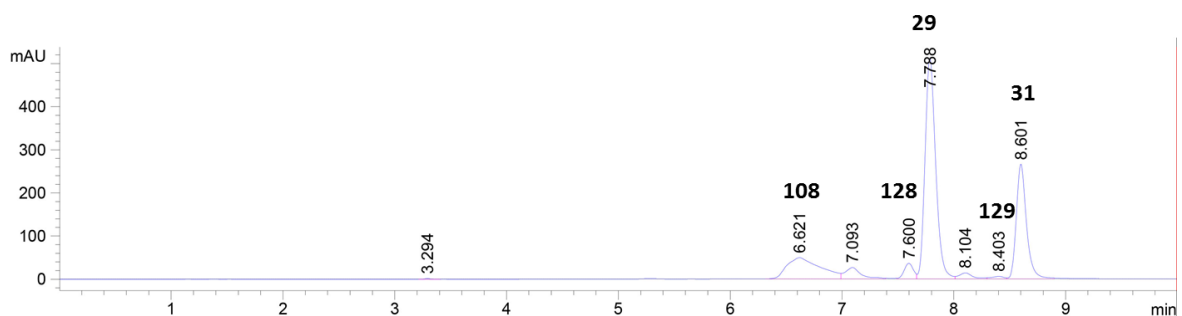
### 2.3.2. Isolation of Unnatural Products, (-)-5,5'-Difluoro-chimonanthine and *meso*-5,5'-Difluoro-chimonanthine

After identifying several putative precursor analogues, we decided to utilize 5-fluorotryptamine (**108**) as our model precursor analogue for our *in planta* experiments. This choice was largely driven by the generation of a strong *m/z* signal associated with that of the target unnatural product by LC-MS analyses (entry **3**, Table 2.1) but also by the ability to monitor formation of this product by  $^{19}\text{F}$  NMR spectroscopy. The feeding experiments were therefore scaled-up in order to isolate sufficient quantities of the unnatural products **128** and **129** (Figure 2.6) that would enable proper characterization to confirm results from LC-MS analyses.



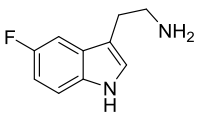
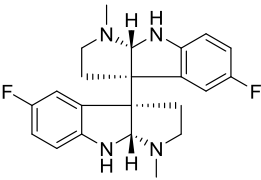
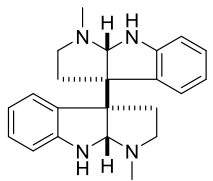
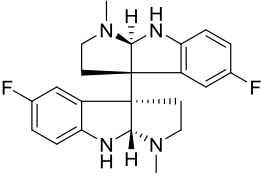
**Figure 2.6. Target unnatural chimonanthine analogues after feeding *Chimonanthus praecox* with 108: (-)-5,5'-fluorochimonanthine (128), and *meso*-5,5'-fluorochimonanthine (129)**

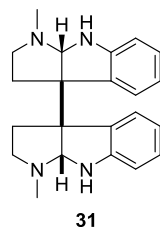
The extracted crude alkaloids (40 mg) obtained from plant tissues after the feeding experiments were solubilized in methanol prior to purification by preparative HPLC (Figure 2.7).



**Figure 2.7.** HPLC separation of alkaloid extracts after 5-fluorotryptamine (108) was fed to *Chimonanthus praecox*.

**Table 2.2.** Isolation of chimonanthines and unnatural chimonanthines by HPLC

Retention time (min)	Isolated product	Amount isolated (mg)
6.62	 <b>108</b> 5-fluorotryptamine	6
7.6	 <b>128</b> (-)-5,5'-difluoro-chimonanthine	~0.7
7.8	 <b>29</b> (-)-chimonanthine	10
8.4	 <b>129</b> <i>meso</i> -5,5'-difluoro-chimonanthine	~0.05

*meso*-chimonanthine

Only the characterized products are reported in the table. The other fractions were not fully characterized.

Table 2.2 summarizes the characterization of the isolated alkaloids. Among the 40 mg of the crude alkaloid preparation, 6 mg (15%) was the administered compound **108**. The amounts of the known natural products, (-)-chimonanthine (**29**) and *meso*-chimonanthine (**31**) were 10 mg (25%), and 6 mg (15%), respectively. The desired chimonanthine analogues, **128**, and **129** were collected, and the amounts were approximately 0.7 mg (1.75%) and 0.05 mg (0.1%), respectively. Some remaining material may be present in the additional peaks observed in the chromatogram but these have not been characterized.

After separation, each fraction was submitted for LC-MS analysis. The fractions with the expected *m/z* were combined and characterized by <sup>1</sup>H-NMR and <sup>19</sup>F-NMR spectroscopy. (-)-5,5'-Difluorochimonanthine (**128**, Figure 2.6) showed the desired *m/z* when analyzed by LC-MS and eluted at a retention time of 1.5 minutes. As expected, the <sup>1</sup>H-NMR spectrum displayed three characteristic aromatic proton resonances ( $\delta$  6.4 to 6.9 ppm) and a single fluorine resonance ( $\delta$  127.1 ppm) in the <sup>19</sup>F-NMR spectrum. This provided good evidence for the incorporation of fluorine into the unnatural product **128**.

While the characterization of (-)-5,5'-difluorochimonanthine (**128**) was not particularly challenging, the characterization of *meso*-5,5'-difluorochimonanthine (**129**) presented several interesting challenges. Based on the LC-MS analyses of *meso*-5,5'-difluorochimonanthine (**129**), we observed the desired *m/z* signal corresponding to the unnatural product at a retention time of 4.2 minutes. As depicted in Figure 2.8, <sup>1</sup>H-NMR and <sup>19</sup>F-NMR analyses performed at room temperature were not enough to allow proper characterization. The resonances from the <sup>1</sup>H-NMR spectra were very broad and *J*-couplings could not be determined. The <sup>19</sup>F-NMR spectrum included two fluorine

resonances at room temperature ( $\delta$  129.2 and 129.4 ppm), which did not match with the expected single fluorine resonance.

We speculated that the broad signals may stem from the presence of slowly interconverting atropisomers. Accordingly, we were able to resolve this issue by increasing the temperature of the sample being analyzed by NMR spectroscopy up to 80 °C. As indicated in Figure 2.6, an increase in temperature during acquisition of  $^1\text{H}$ -NMR spectra resulted in spectra with much sharper resonances, presumably due to the more rapid interconversion of two atropisomers. Additionally, the corresponding  $^{19}\text{F}$ -NMR spectra recorded at higher temperatures also indicated coalescence of two separate fluorine resonances into a single resonance.

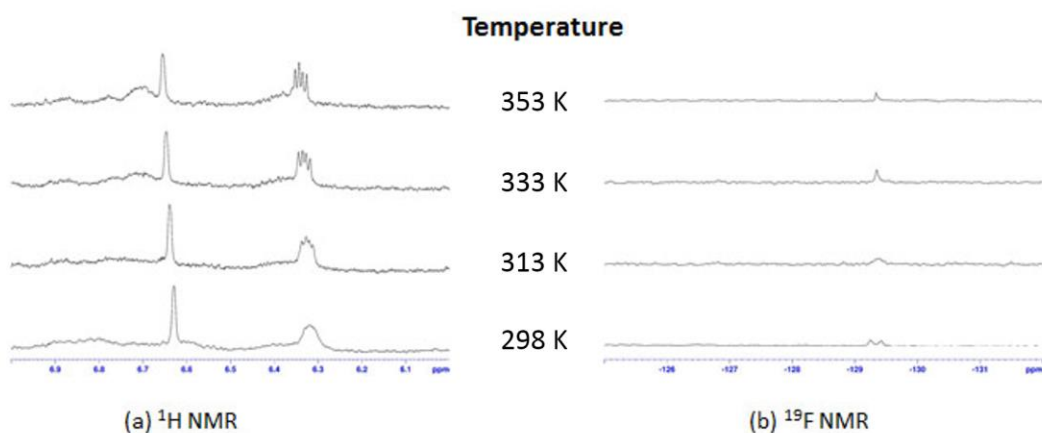


**Figure 2.8.  $^1\text{H}$  and  $^{19}\text{F}$  NMR spectra of isolated *meso*-5,5'-difluorochimonanthine (**129**) acquired at various temperatures**

The NMR experiments were performed at four different temperatures, 25, 40, 60 and 80 °C).

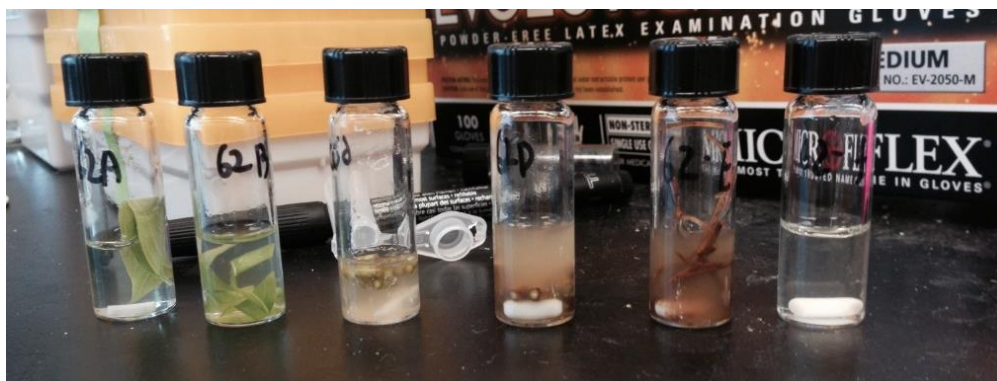
Based on these NMR spectroscopic experiments, we were able to characterize *meso*-5,5'-difluorochimonanthine (**129**). It indicated *meso*-**129** is not formally *meso* at room temperature, but rather is a mixture of two atropisomers. Also, at higher temperature, the atropisomers rapidly interconvert such that the atropisomers display a spectrum characteristic of a *meso* compound.<sup>[77–82]</sup> It is expected that an energy barrier must be overcome in order to rotate the C3-C3' bond; thus, at room temperature there are two possible conformations of *meso*-5,5'-difluorochimonanthine (**129**).



## 2.4. In Vitro Assay

### 2.4.1. Background Information

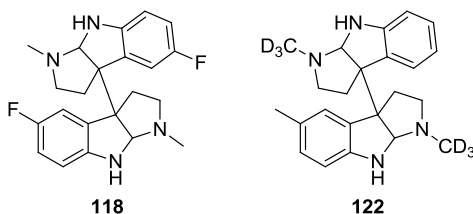
It was previously proposed<sup>[20,62]</sup> that an unknown dimerase is responsible for catalyzing the dimerization of *N*<sub>b</sub>-methyltryptamine (**37**) to provide chimonanthine (**29**, see Scheme 1.10). While our initial work has shown that *Chimonanthus praecox* can incorporate *N*<sub>b</sub>-methyltryptamine (**37**) into the synthesis of chimonanthine, it was necessary to extract proteins from *C. praecox* to further investigate and ultimately isolate the enzyme responsible for the transformation of interest. An important aspect of our study also aimed at addressing the location of this enzyme within the plant.



**Figure 2.9. Feeding D<sub>3</sub>-N<sub>b</sub>-methyltryptamine into different plant parts. Order from left to right. A) One whole leaf. B) Small pieces of a leaf. C) Stem. D) Branch. E) Root. F) Control.**

The different parts of *Chimonanthus praecox* were incubated with precursors at room temperature, and stirred for three days.

In order to pinpoint the location of the enzyme catalyzing the dimerization reaction en route to chimonanthine (**29**), we first selected specific components of *Chimonanthus praecox* including leaves, stems, branches and roots (Figure 2.9). These individual plant parts were placed in an aqueous solution of D<sub>3</sub>-*N*<sub>b</sub>-methyltryptamine (**112**) and 5-fluorotryptamine (**108**) and incubated for three days (Figure 2.9). The plant components were then taken out of solutions, and were suspended individually in methanol and the samples were sonicated for one hour. The methanol extracts were then filtered, and aliquots of the filtrate were subjected to LC-MS analyses. As indicated in Table 2.3, the biosynthesis of chimonanthine may occur in either the leaves or the roots of the plant.

**Table 2.3 Localization of Biosynthesis of Chimonanthine**

Entry	Plant Part	Detection of (118) <i>m/z</i> 383.2042	Detection of (122) <i>m/z</i> 353.2607
1	Leaf	Yes	Yes
2	Stem	No	No
3	Branch	No	No
4	Root	Yes	Yes
5	Control (No plant part)	No	No

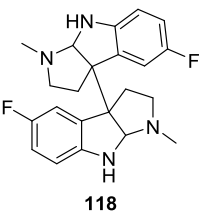
*m/z* of **118**: 383.2042, of **122**: 353.2607

### 2.4.2. Cytoplasmic Protein Extraction from Leaf

The initial attempts to extract the proteins involved in this transformation were performed using commercially available plant protein extraction kits in combination with mechanical extraction methods. For our experiments, we opted to use the P-PER™ Plant Protein Extraction Kit, which has the advantage of being fast and providing pure protein that can be used directly for enzymatic reactions. Specifically, this kit is designed for the protein extraction up to 80 mg of plant sample but can only extract cytoplasmic proteins.

Following the extraction protocol on leaves as described by the manufacturer, the extracted sample was incubated with *N*<sub>6</sub>-methyltryptamine derivatives **112** and **113** overnight under several conditions. Table 2.4 summarizes the experimental data. The samples were then filtered through Amicon® 3K centrifuge tubes and aliquots from each sample were subjected to LC-MS analyses. Unfortunately, the products having desired *m/z* were not detected in any of the samples. The lack of success from these experiments may be due to the use of an inappropriate buffer during the *in vitro* enzymatic reaction or protein extraction.

**Table 2.4 In vitro assay with protein extracts by P-PER™ Plant Protein Extraction Kit**

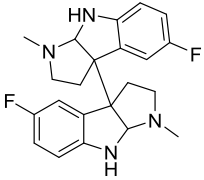
Entry	Precursor	Buffer	Cofactor	pH	Temperature (°C)	
						 <p>118</p>
1	5-F- <i>N<sub>b</sub></i> -methyltryptamine	A	N/A	7.4	rt	No
2	5-F- <i>N<sub>b</sub></i> -methyltryptamine	A	N/A	7.4	4	No
3	5-F- <i>N<sub>b</sub></i> -methyltryptamine	A	N/A	7.4	30	No
4	5-F- <i>N<sub>b</sub></i> -methyltryptamine	A	N/A	4	rt	No
5	5-F- <i>N<sub>b</sub></i> -methyltryptamine	A	N/A	9	rt	No
6	5-F- <i>N<sub>b</sub></i> -methyltryptamine	A	Vitamin C	7.4	rt	No
7	5-F- <i>N<sub>b</sub></i> -methyltryptamine	A	Mg	7.4	rt	No
8	5-F- <i>N<sub>b</sub></i> -methyltryptamine	A	FeCl <sub>3</sub>	7.4	rt	No
9	5-F- <i>N<sub>b</sub></i> -methyltryptamine	A	NADH	7.4	rt	No
10	5-F- <i>N<sub>b</sub></i> -methyltryptamine	A	FAD	7.4	rt	No
11	5-F- <i>N<sub>b</sub></i> -methyltryptamine	A	NAD	7.4	rt	No
12	5-F- <i>N<sub>b</sub></i> -methyltryptamine	B	N/A	7.8	rt	No
13	5-F- <i>N<sub>b</sub></i> -methyltryptamine	B	N/A	7.8	4	No
14	5-F- <i>N<sub>b</sub></i> -methyltryptamine	B	N/A	7.8	30	No
15	5-F- <i>N<sub>b</sub></i> -methyltryptamine	B	MgBr <sub>2</sub>	7.8	rt	No
16	5-F- <i>N<sub>b</sub></i> -methyltryptamine	B	FeCl <sub>3</sub>	7.8	rt	No
17	5-F- <i>N<sub>b</sub></i> -methyltryptamine	B	FeSO <sub>4</sub>	7.8	rt	No
18	5-F- <i>N<sub>b</sub></i> -methyltryptamine	B	NADH	7.8	rt	No
19	5-F- <i>N<sub>b</sub></i> -methyltryptamine	B	FAD	7.8	rt	No
20	5-F- <i>N<sub>b</sub></i> -methyltryptamine	B	NAD	7.8	rt	No
	Precursor	Buffer	Cofactor	pH	Temperature (°C)	Detection of <i>m/z</i> of 353.2607
21	5-F- <i>N<sub>b</sub></i> -methyltryptamine	A	N/A	4	rt	No
22	5-F- <i>N<sub>b</sub></i> -methyltryptamine	A	N/A	7.4	rt	No
23	5-F- <i>N<sub>b</sub></i> -methyltryptamine	A	N/A	9	rt	No
24	5-F- <i>N<sub>b</sub></i> -methyltryptamine	A	N/A	7.4	4	No
25	5-F- <i>N<sub>b</sub></i> -methyltryptamine	A	N/A	7.4	30	No
26	5-F- <i>N<sub>b</sub></i> -methyltryptamine	A	Vitamin C	7.4	rt	No
27	5-F- <i>N<sub>b</sub></i> -methyltryptamine	A	MgBr <sub>2</sub>	7.4	rt	No
28	5-F- <i>N<sub>b</sub></i> -methyltryptamine	A	FeCl <sub>3</sub>	7.4	rt	No

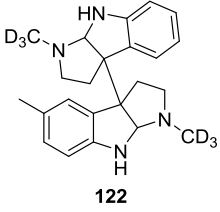
29	5-F- <i>N<sub>b</sub></i> -methyltryptamine	A	NADH	7.4	rt	No
30	5-F- <i>N<sub>b</sub></i> -methyltryptamine	A	FAD	7.4	rt	No
31	5-F- <i>N<sub>b</sub></i> -methyltryptamine	A	NAD	7.4	rt	No
32	5-F- <i>N<sub>b</sub></i> -methyltryptamine	B	N/A	7.8	rt	No
33	5-F- <i>N<sub>b</sub></i> -methyltryptamine	B	N/A	7.8	4	No
34	5-F- <i>N<sub>b</sub></i> -methyltryptamine	B	N/A	7.8	30	No
35	5-F- <i>N<sub>b</sub></i> -methyltryptamine	B	MgBr <sub>2</sub>	7.8	rt	No
36	5-F- <i>N<sub>b</sub></i> -methyltryptamine	B	FeCl <sub>3</sub>	7.8	rt	No
37	5-F- <i>N<sub>b</sub></i> -methyltryptamine	B	FeSO <sub>4</sub>	7.8	rt	No
38	5-F- <i>N<sub>b</sub></i> -methyltryptamine	B	NADH	7.8	rt	No
39	5-F- <i>N<sub>b</sub></i> -methyltryptamine	B	Vitamin C	7.8	rt	No
40	5-F- <i>N<sub>b</sub></i> -methyltryptamine	B	FAD	7.8	rt	No
41	5-F- <i>N<sub>b</sub></i> -methyltryptamine	B	NAD	7.8	rt	No

**Buffer A:** PBS. **Buffer B:** 0.2M Tris-HCl, pH 7

The second attempt to obtain protein extracts used homogenized extracts of leaves. In a cold room (4 °C), 20 g of freshly removed leaves of *Chimonanthus praecox* were placed in a blender with 150 ml of various cold buffers (Table 2.5). The leaves were homogenized in a blender for 4 × 10 seconds pulses. The plant debris were filtered over cheesecloth and the filtrate was centrifuged at 14,000 rpm for 30 min at 4 °C. The resulting supernatants were collected and concentrated by using Amicon® centrifuge tubes. The protein samples were then incubated with precursor analogues **103** and **104** in various conditions (Table 2.5), but the enzymatic reactions were not conclusive.

**Table 2.5. In vitro assay with protein extracts from homogenized plant leaf samples after blending**

Entry	Precursor	Extraction Buffer	pH	Temperature (°C)	
					 <p style="text-align: center;"><b>118</b></p>
1	5-F- <i>N<sub>b</sub></i> -methyltryptamine	A	7.4	4, rt, 37	No
2	5-F- <i>N<sub>b</sub></i> -methyltryptamine	B	7.8	4, rt, 37	No
3	5-F- <i>N<sub>b</sub></i> -methyltryptamine	C	7.4	rt	No

4	5-F- <i>N<sub>b</sub></i> -methyltryptamine	D	7.1	rt	No
5	5-F- <i>N<sub>b</sub></i> -methyltryptamine	E	7.0	rt	No
6	5-F- <i>N<sub>b</sub></i> -methyltryptamine	F	4.3, 5.3, 6.4, 7.3, 8.3, 9.1,10	rt	No
Entry	Precursor	Extraction Buffer	pH	Temperature (°C)	
					 122
7	D <sub>3</sub> - <i>N<sub>b</sub></i> -methyltryptamine	A	4, 7.4, 9	4, rt, 37	No
8	D <sub>3</sub> - <i>N<sub>b</sub></i> -methyltryptamine	B	7.8	4, rt, 37	No
9	D <sub>3</sub> - <i>N<sub>b</sub></i> -methyltryptamine	C	7.4	rt	No
10	D <sub>3</sub> - <i>N<sub>b</sub></i> -methyltryptamine	D	7.1	rt	No
11	D <sub>3</sub> - <i>N<sub>b</sub></i> -methyltryptamine	E	7.0	rt	No
12	D <sub>3</sub> - <i>N<sub>b</sub></i> -methyltryptamine	F	4.3, 5.3, 6.4, 7.3, 8.3, 9.1,10	4, rt, 37	No

**Buffer A:** PBS. **Buffer B:** 0.2M Tris-HCl pH of 7.8. **Buffer C:** PBS, 1 mM PEG, 5% (w/v) PVPP, 0.01% Triton X-100. **Buffer D:** 25mM HEPES-Na, 0.5 mM EDTA, 8 mM MgCl<sub>2</sub>, 8 mM DTT. **Buffer E:** 0.2M MOPS, 5% w/v PVPP, 1% Triton X-100 (v/v), 10% glycerol, 2 mM DTT. **Buffer F:** 50 mM Tris-HCl, 10 mM DTT, 0.5 M sucrose. **Buffer F:** 0.45 M Mannitol, 50 mM sodium phosphate, 2 mM EDTA  
rt: room temperature

### 2.4.3. Cytoplasmic Protein Extraction from Root

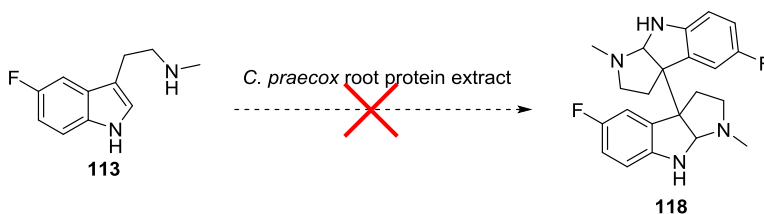
Following the failure to isolate the enzymes responsible for the biosynthetic pathway from the leaves of *C. praecox*, the next target was the root of the plant (Figure 2.10). The roots of *C. praecox* were collected and subjected to the same extraction procedure as that previously described for the leaves, with the notable exception that a pH 4.5 sodium acetate buffer was used because we assumed that in lower pH the

precursors have better solubility in water.<sup>[83]</sup> Further purification and separation of root proteins was performed by ammonium sulfate precipitations at concentrations of 0-20%, 20-40%, 40-60%, 60-80% and 80-95%, and the proteins from each precipitation were collected after dialysis in pH 4.5 sodium acetate buffer.



**Figure 2.10.** Image of roots of *Chimonanthus praecox* washed with distilled water.

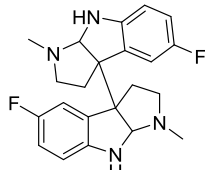
The crude protein samples were concentrated by Amicon® centrifugation tubes followed by ammonium sulfate precipitation. The crude root protein samples were incubated with D<sub>3</sub>-N<sub>b</sub>-methyltryptamine (**112**) or 5-fluoro-N<sub>b</sub>-methyltryptamine (**113**) (Scheme 2.2).



**Scheme 2.2.** Expected incorporation of **113** to **118** *in vitro* assay with root protein extract

Unfortunately, these experiments were unsuccessful (Table 2.6). In light of the failures encountered in the protein extract-based experiments, we suspended further investigation into isolating the key enzyme from the roots, primarily due to the detrimental effects on the plant as a result of removing its roots for our studies.

**Table 2.6. In vitro assay with 118 and protein extracts from homogenized plant root samples after blending and ammonium sulfate precipitation**

Entry	Cofactor (s)	Ammonium sulfate (%)	 118
1	N/A	crude	No
2	FAD	crude	No
3	NADP <sup>+</sup> , NADPH	crude	No
4	NADP <sup>+</sup> , NADPH, FeCl <sub>3</sub> , FeSO <sub>4</sub>	crude	No
5	N/A	0-20	No
6	FAD	0-20	No
7	NADP <sup>+</sup> , NADPH	0-20	No
8	NADP <sup>+</sup> , NADPH, FeCl <sub>3</sub> , FeSO <sub>4</sub>	0-20	No
9	N/A	20-40	No
10	FAD	20-40	No
11	NADP <sup>+</sup> , NADPH	20-40	No
12	NADP <sup>+</sup> , NADPH, FeCl <sub>3</sub> , FeSO <sub>4</sub>	20-40	No
13	N/A	40-60	No
14	FAD	40-60	No
15	NADP <sup>+</sup> , NADPH	40-60	No
16	NADP <sup>+</sup> , NADPH, FeCl <sub>3</sub> , FeSO <sub>4</sub>	40-60	No
17	N/A	60-80	No
18	FAD	60-80	No
19	NADP <sup>+</sup> , NADPH	60-80	No
20	NADP <sup>+</sup> , NADPH, FeCl <sub>3</sub> , FeSO <sub>4</sub>	60-80	No
21	N/A	80-95	No
22	FAD	80-95	No
23	NADP <sup>+</sup> , NADPH	80-95	No
24	NADP <sup>+</sup> , NADPH, FeCl <sub>3</sub> , FeSO <sub>4</sub>	80-95	No

Buffer: 50 mM sodium acetate, pH 4.5, reaction at room temperature overnight.  $m/z$  of difluorinated chimonanthine is 383.2042

#### 2.4.4. *In vitro* Assay with Protoplast

The cell wall that surrounds the plasma membrane is a distinct cellular component of plant cells. Our lack of success in the preceding experiments led us to believe that the cell wall may hinder the homogenization of plant protein samples during blending. Thus, we next removed the cell wall to obtain the protoplasts, which are plant cells without a cell wall. The protoplast preparation was adapted from Sheen's methods<sup>[84]</sup> (for detailed procedures, see the experimental section 2.7.11). The cell wall was digested enzymatically by incubation of leaves of *Chimonanthus praecox* with two enzymes: cellulase and pectinase (Figure 2.11). After preparation of protoplasts, 5-fluorotryptamine (**108**) was added to the protoplast samples and incubated overnight at room temperature. The samples were filtered through Amicon® ultra centrifugal tubes. Unfortunately, these experiments did not produce the desired difluorochimonanthine.

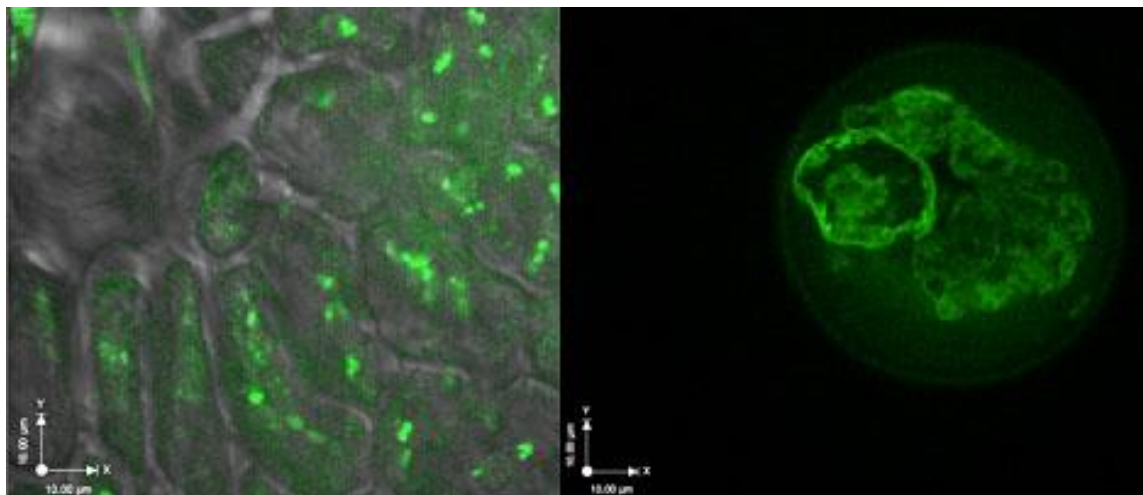


**Figure 2.11. Fluorescent microscopy images of plant cells. Native plant cells (left) and a protoplast after enzymatic digestion (Right).**

The images were taken with WaveFX spinning disc confocal microscopy with 40x objective and Hamamatsu 9100 EMCCD camera. The native plant cells (left) are in shape in the presence of cell wall, but the protoplast (right) after enzymatic digestion of cell wall in native cells becomes rounded. The scale bars indicate 10 μm



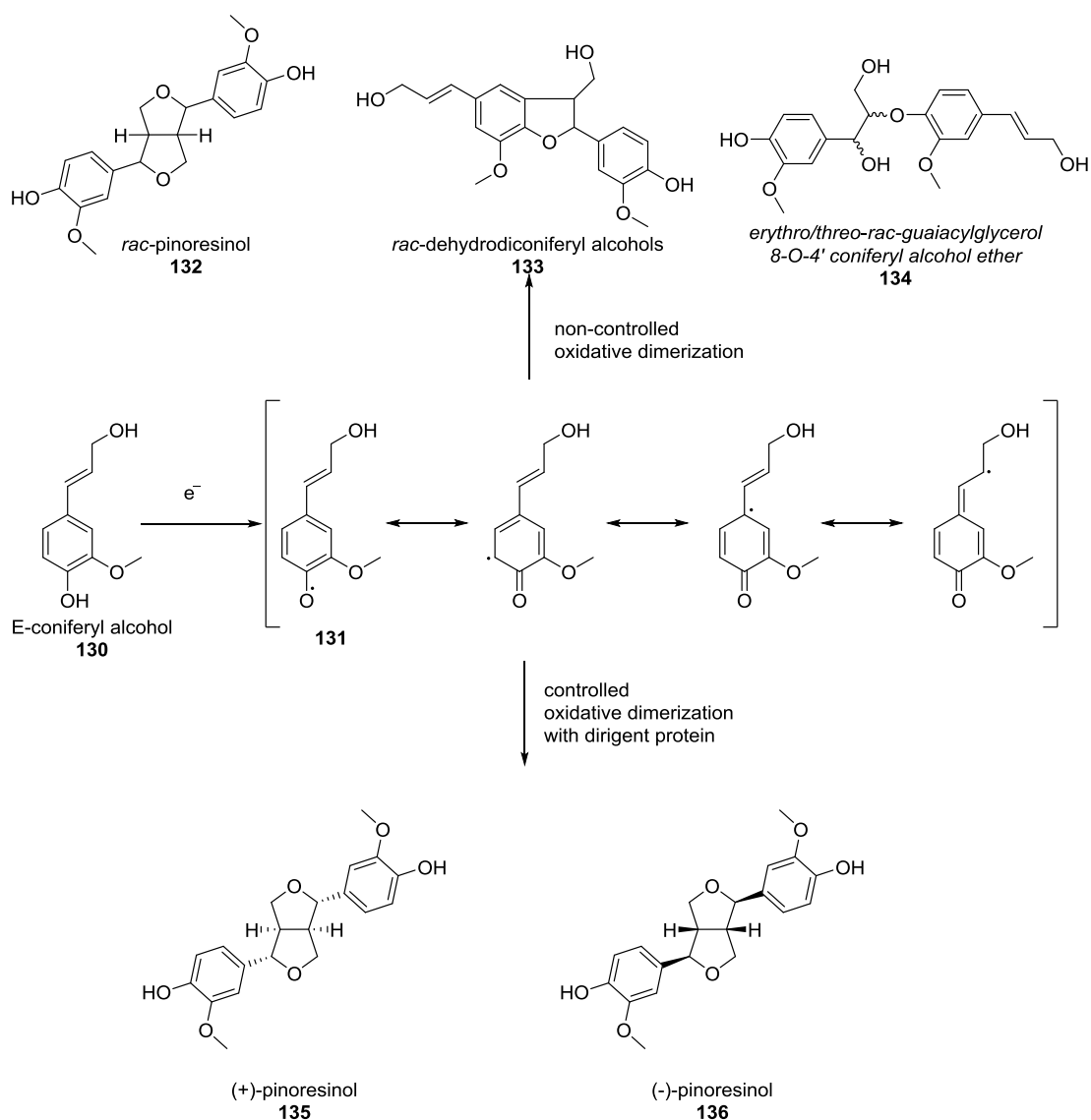
## 2.4.5. Proteins from Cell Walls

The cell wall was then considered as a possible site for this elusive enzymatic reaction, since no chimonanthine analogues were produced during our cytoplasmic protein extracts and protoplasts feeding experiments. The plant cell wall is known to protect cells from insects, and provide rigidity to maintain the shape of the cell as well as to help it endure internal osmotic pressure. Also, it is mainly composed of carbohydrates including cellulose, hemicellulose, and pectin. Other compositions of cell walls are lignin, suberin, waxes and proteins. However, the protein and enzyme content of cell walls is not well known.<sup>[85–87]</sup>

In 1997, however, the Lewis group at Washington State University reported a new kind of protein involved in the synthesis of (+)-pinoresinol called 'dirigent protein' found in the cell wall of *Forsythia suspensa*.<sup>[88–93]</sup> The meaning of dirigent is 'to align', and the main function of the dirigent protein is to provide only the desired stereoselective product by avoiding undesired C-C bond formation by aligning two substrates with specific orientation. The enzyme was also proposed to stabilize one of the radical intermediates involved in the reaction. Their study examined the biosynthesis of (+)-pinoresinol (**135**, Scheme 2.3), which is a dimer of (*E*)-coniferyl alcohol (**130**). Lewis and coworkers postulated that an enzyme is responsible for coupling two (*E*)-coniferyl (**130**) alcohols selectively to form (+)-pinoresinol. They reported that pure (*E*)-coniferyl alcohol (**130**) spontaneously led to several different isomers (**132-134**). However, the 'dirigent protein' offered region-and stereospecific control in the production of (+)-pinoresinol in the presence of an oxidant. Several years later, another dirigent protein which afforded (-)-pinoresinol (**136**) from (*E*)-coniferyl alcohol (**130**) was discovered in 2010 (Scheme 2.3).<sup>[94,95]</sup>

The evidence for dirigent proteins in the cell wall of *F. suspensa* provided an important precedent for the investigation of enzymes embedded in the cell wall. With this in mind, we decided to investigate the cell wall of *C. praecox* to determine if it contained the elusive dimerase we were seeking. Several important biosynthetic similarities exist in regards to the formation of the downstream metabolites present in *F. suspensa* and *Chimonanthus praecox*. For example, the dimeric nature of pinoresinol is similar to that observed in chimonanthine, albeit synthesized from different monomers. Furthermore,

the biosynthesis of pinoresinol occurs via an oxidative dimerization reaction, which is also postulated to occur during the biosynthesis of chimonanthine. Based on these topical similarities, we set out to isolate the cell wall proteins from *C. praecox* with the rationale being that the enzyme involved in the formation of chimonanthine might be present in this cellular component.



**Scheme 2.3. Comparison between uncontrolled and controlled oxidative dimerization to afford natural product**

The procedure used for the cell wall preparation was that described by Lewis (see experimental section 2.7.13 for details) (Figure 2.12). Following the preparation of cell wall material, 0 mg, 100 mg, 200 mg, 300 mg and 400 mg of this cell wall preparation was incubated with an aqueous solution of 1 mL of 50 mM potassium phosphate buffer (pH 7), 5 mM 5-fluoro-*N*<sub>6</sub>-methyltryptamine (**113**), and 2.5 μM ammonium persulfate overnight at 30 °C. The samples were then filtered through 3K Amicon® centrifugal tubes, to remove proteins and insoluble materials, and then submitted for analyses by LC-MS.

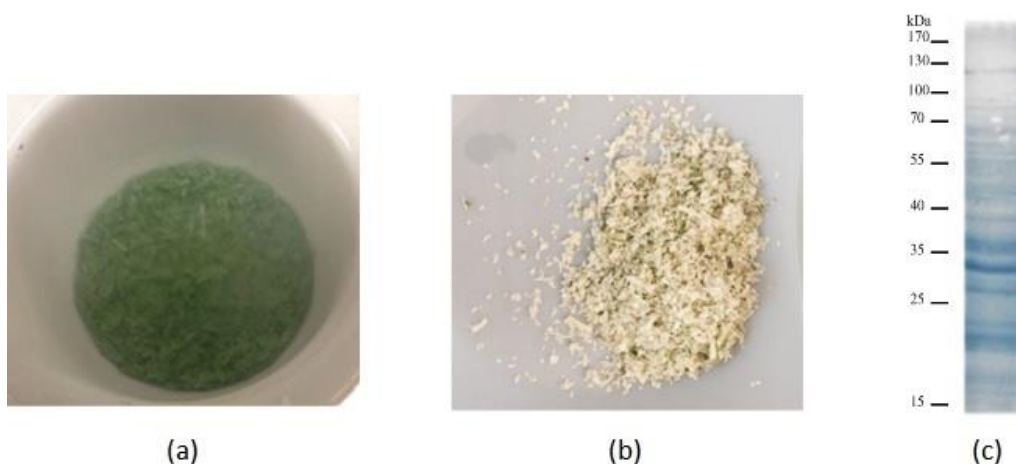


**Figure 2.12. Images of ground leaves in liquid nitrogen in a mortar (a), cell wall powders after removing cellular components (b) and cell wall proteins on SDS-PAGE (c)**

A green power was obtained after grinding leaves of *C. praecox* in liquid nitrogen using a mortar and pestle (a). Mild detergent and acetone works to remove cytoplasmic components by opening up the cell membrane to afford pale-yellow cell wall materials (b). Proteins were then extracted from the crude cell wall materials and separated by SDS-PAGE (c).

We were delighted to find that the crude cell wall preparation appeared to promote the dimerization of our fluorinated precursors as demonstrated by the presence of *m/z* signal of  $383.2042 \pm 0.002$  corresponding to difluorinated chimonanthine analogue (**128**) (Figure 2.13). This observation provides good evidence for the presence of the dimerase within the cell walls of *Chimonanthus praecox*.

Figure 2.13 displays the EIC for the *m/z* signal of  $383.2042 \pm 0.002$ . Notably the intensity of the signals at a retention time of 4.7 min becomes stronger as the amount of cell wall materials used in the assays is increased. This data indicates that more product

was formed in the reaction mixture containing the cell wall components. One reservation, however, is that the retention time observed is not the same as that observed for the isolated difluorochimonanthines. Furthermore, we did not perform a control experiment in which no precursor was added to test for the presence of molecules having the expected mass within the cell wall fraction. Nevertheless, this preliminary observation provided some impetus to investigate further these cell wall materials as a potential source of the putative dimerase.

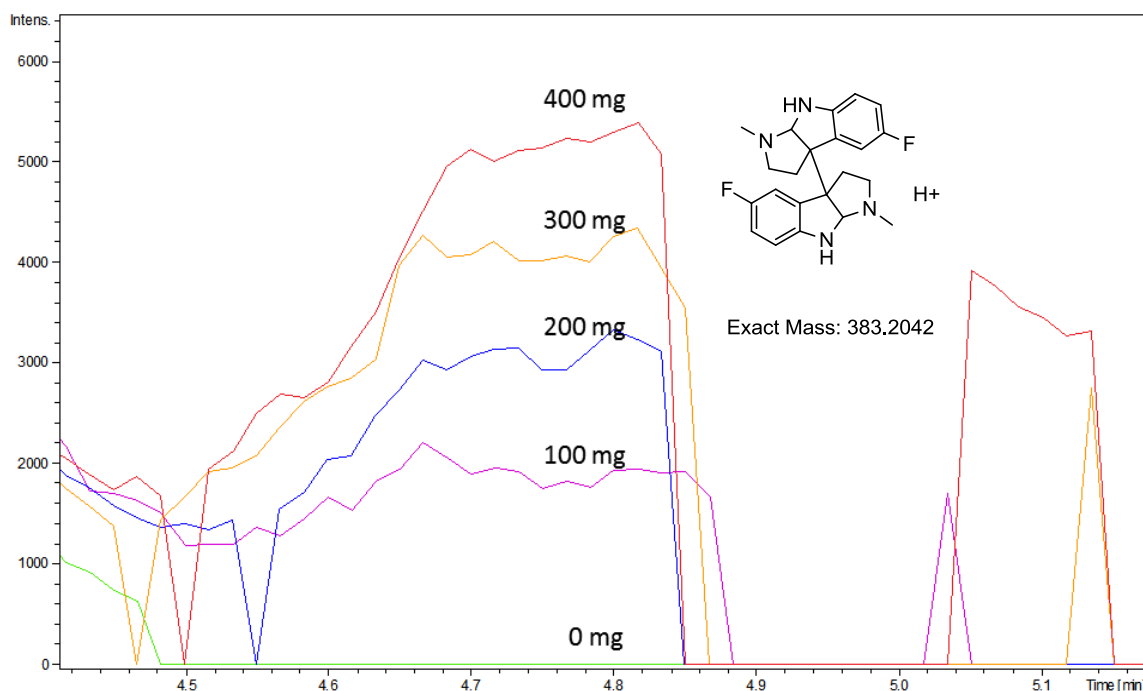


**Figure 2.13.** Extracted ion chromatograms of  $m/z$  of  $383.2042 \pm 0.002$  in the time interval of 4.4 min to 5.2 min after incubation of precursor with different amount of cell walls

To further test for the presence of the putative dimerase enzyme in cell walls, the cell wall proteins were extracted with 1M NaCl from the pale yellow crude cell walls (Figure 2.12. (b)). After concentrating the extracted protein samples by 3K Amicon® centrifugal tubes, 200  $\mu$ L of the resulting crude protein sample was obtained having a protein concentration of 1.8 mg/mL as determined by using DC Protein Assay (Bio-Rad). Incubation of the resulting extracted proteins (0  $\mu$ L, 15  $\mu$ L, 30  $\mu$ L, 45  $\mu$ L and 60  $\mu$ L of 1.8  $\mu$ g/ $\mu$ L protein solution) were added to the same reaction buffer that was previously developed (ammonium persulfate in potassium phosphate buffer) and the 5-fluoro- $N_b$ -

methyltryptamine precursor was added. The mixtures were incubated overnight at 30 °C and the samples were then filtered through 3k Amicon ® centrifugal tubes. As shown in Figure 2.14a, EIC analysis indicated the presence of a compound having an  $m/z$  of  $383.2042 \pm 0.002$ , which corresponds to the predicted  $m/z$  for **128** ( $m/z = 383.2042$ ). We were able to further confirm the identity of this species as 5,5'-difluorochimonanthine by overlaying the chromatograms of (-)-5,5'-difluorochimonanthine (Figure 2.14.(b)) and *meso*-5,5'-difluorochimonanthine (Figure 2.14.c) with that obtained from our incubation experiments. In the case of (-)-5,5'-difluorochimonanthine (**128**,  $t_R = 1.4$ -1.5 min) and *meso*-5,5'-difluorochimonanthine (**129**,  $t_R = 4.2$ -4.4 min), the peak area and peak height also increased with larger amounts of the extracted cell wall proteins. These results provide good support for our hypothesis that an enzyme associated with the cell wall is responsible for the dimerization of 5-fluoro-*N*<sub>b</sub>-methyltryptamine (**113**).

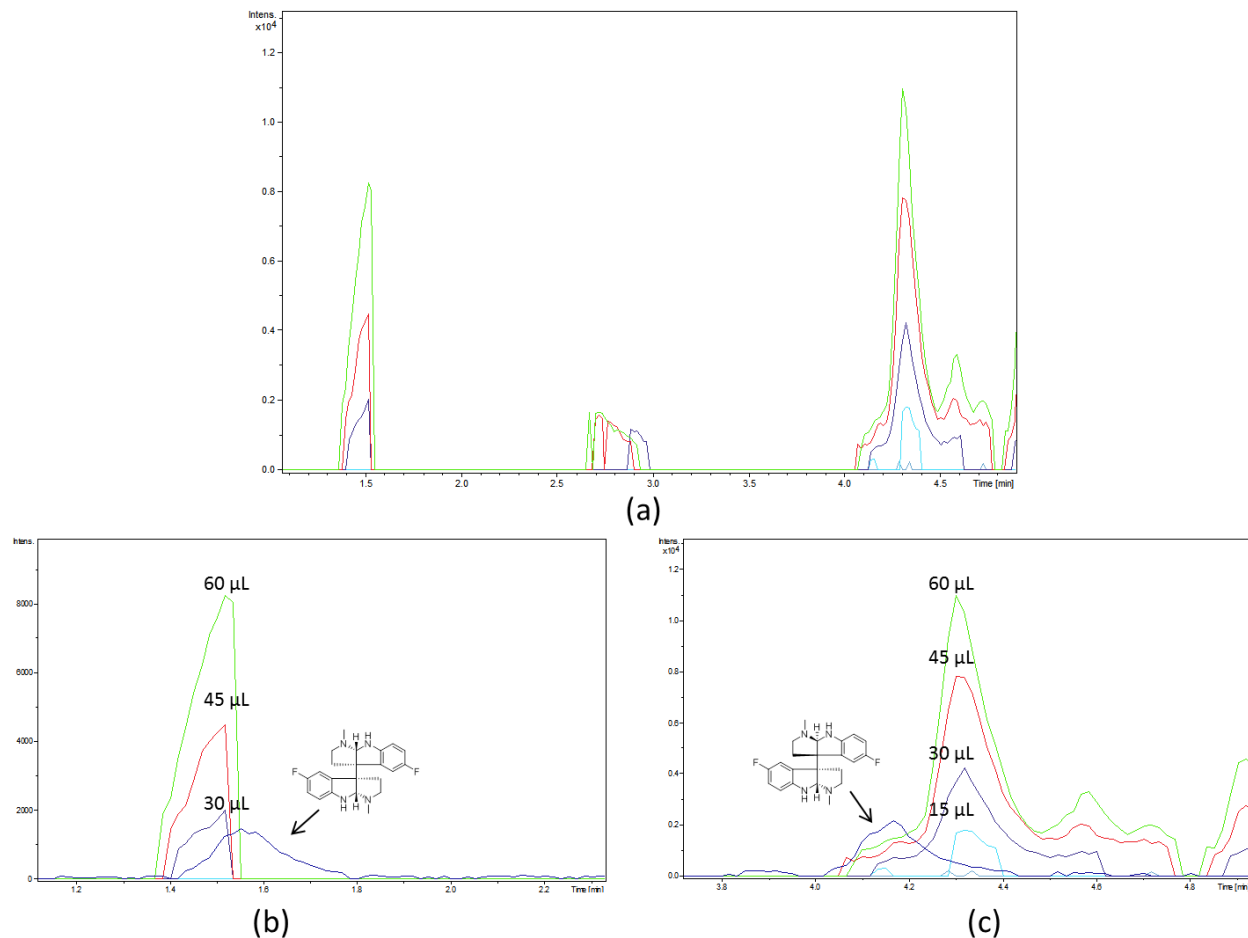


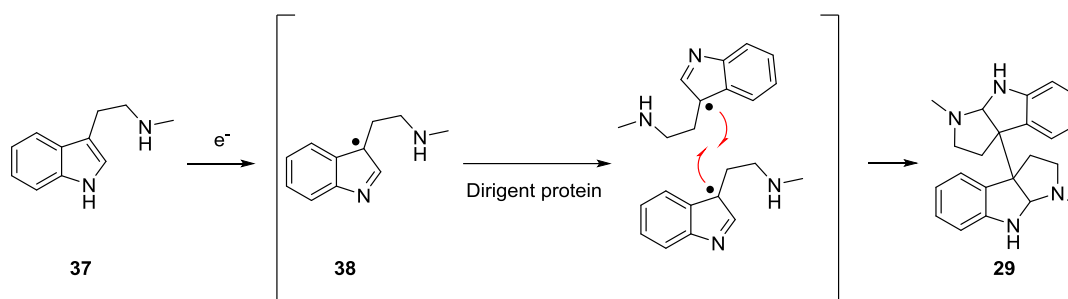
**Figure 2.14. LC-MS EIC chromatograms.**

(a) EIC of  $m/z$  383.204  $\pm$  0.002 in the region of 1.1 min to 4.8 min. (b) EIC overlays with difluorochimonanthine isolated from *Chimonanthus praecox* (time interval: 1.2 min to 2.2 min) (c) EIC overlays with difluorochimonanthine isolated from *Chimonanthus praecox* (time interval: 3.8 min to 4.6 min).

Notably, these signals did not appear in the absence of an oxidant or cell wall preparation. This observation suggests that both an oxidant and cell wall proteins are required for the biosynthesis of chimonanthine.

## 2.5. Summary

Although the identification and characterization of the unknown chimonanthine dimerase has not yet been achieved, the experiments described in this thesis provide an advanced starting point for solving this problem. First, we identified that *Chimonanthus praecox* is able to use several precursor analogues for the biosynthesis of the corresponding unnatural chimonanthines. Also, feeding experiments followed by LC-MS analyses indicated that larger substituents on the C5 and C6 position of tryptamine hindered the incorporation of precursor analogues into the active site during the biosynthesis of unnatural chimonanthines. Then, through incubating different plant parts with a suitable precursor analogue (5-fluoro-*N*<sub>6</sub>-methyltryptamine), we identified that the biosynthesis of chimonanthine should take place either in the leaves or the roots of *Chimonanthus praecox*. During our attempts to purify proteins from different components of plant cells, we were delighted to find good data supporting the presence of protein(s) in the cell wall that catalyze the biosynthesis of chimonanthine in the presence of an oxidant such as ammonium persulfate.



**Scheme 2.4. Possible route of dirigent protein mediated biosynthesis of chimonanthine**

We propose that the biosynthesis of chimonanthine in *C. praecox* involves a dirigent protein. This may occur by the oxidation of starting compound **37** to radical species **38**, upon which an unknown dirigent protein stabilizes the radical on C3, and aligns two *N*<sub>6</sub>-methyltryptamine together to afford (-)-chimonanthine, but not (+)-chimonanthine. There exist, however, alternative possible mechanisms that may be addressed through detailed studied of the enzyme once purified.

## 2.6. Future Direction

The short-term goal of future work should be the investigation of the cell wall fractions in more detail in order to isolate and characterize the putative dimerase. Even though we were able to demonstrate the production of unnatural products through incubation with cell wall protein extracts, we encountered difficulties in subsequent reproduction of the experiments. An improvement of the extraction or reaction protocols through buffer screening would represent the next logical step. After the development of a robust protocol, our next objective would require fractionating the extracts by separation techniques including ion exchange, size exclusion or precursor attached-affinity chromatography,<sup>[96–99]</sup> native gel running,<sup>[100–102]</sup> ammonium sulfate precipitation<sup>[103]</sup> or Rotofor, a preparatory isoelectric focusing apparatus<sup>[104,105]</sup> to search a fraction where the target protein is present. We expect to be able to purify and isolate the target protein through well-established protein separation techniques. Finally, we propose using tryptic digestion of the protein in tandem with MS to help identify protein sequence.<sup>[106–108]</sup>

Another possible approach is via mutasynthesis,<sup>[70,71,75]</sup> which would first involve a viable leaf cell culture of *Chimonanthus praecox*<sup>[109]</sup> followed by silencing tryptamine biosynthesis in the cell.<sup>[110]</sup> Through such a method, the producing organism cannot use tryptamine as a feedstock for chimonanthine biosynthesis, which means unnatural chimonanthine analogues would be the major product as only unnatural precursors would be available to the plant cells. The advantage of this technique is that the separation of unnatural products and chimonanthine analogues would be more facile in the absence of large quantities of the natural product, chimonanthine. This technique has previously been successfully implemented by O'Connor in producing fluorinated unnatural products (**138-141**) from *Catharanthus roseus* hairy root culture (Figure 2.15) In this study, she successfully silenced the tryptophan decarboxylase in hairy root of *C. roseus* which resulted in the absence of tryptamine biosynthesis and the production of unnatural products.<sup>[110]</sup>



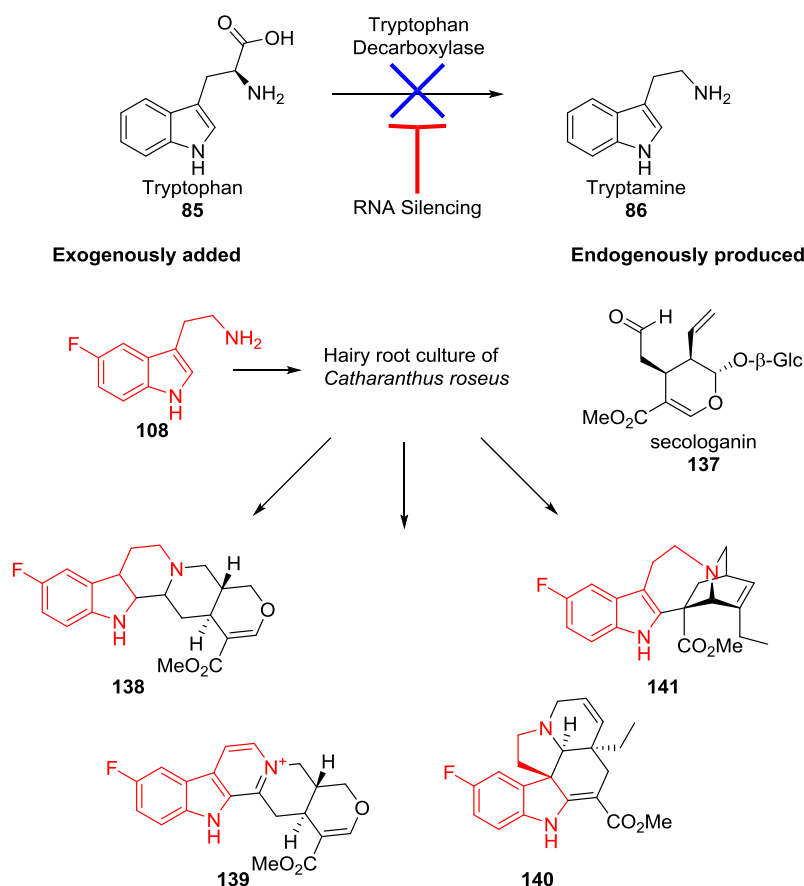


**Figure 2.15. O'Connor's mutasynthesis in *Catharanthus roseus*.**

The administration of unnatural precursor, 5-fluorotryptamine, into the hairy root of *C. roseus* causes production of fluorinated alkaloids, fluorinated-ajmalicine (138), fluorinated-serpentine (139), fluorinated-catharanthine (140), and fluorinated-tabersonine (141) in hairy root culture

The long-term goal of this project will be the recombinant expression of the dimerase enzyme *in vitro*. Specifically, the identification of complete protein sequence of the key enzyme would allow for the direct synthesis of the corresponding mRNA.<sup>[111]</sup> More likely, some protein sequence would allow identification of the gene by genome sequencing or through traditional cloning methods. The resulting gene sequence would be used to recombinantly express the target protein in microbiological systems or convenient plant systems to facilitate scale-up production of the enzyme.<sup>[112–114]</sup> Once enough enzyme is obtained, chemoenzymatic reactions could be performed to prepare various chimonanthine analogues in one step from *N*<sub>b</sub>-methyltryptamine and other alkaloid precursors. Additionally, the chemoenzymatic activity tolerance will be tested in reactions designed to generate quaternary carbon centre(s) in the final downstream

products, which would potentially allow rapid access to structurally complex and diverse natural products.

## 2.7. Experimental

### 2.7.1. General Considerations

All reactions described were performed under an atmosphere of dry nitrogen using oven dried glassware unless otherwise specified. Flash chromatography was carried out with 230-400 mesh silica gel (SiliCycle, SiliaFlash® P60). Concentration and removal of trace solvents was done via a Büchi rotary evaporator using dry ice/acetone condenser, and vacuum applied from an aspirator or Büchi V-500 pump.

All reagents and starting materials were purchased from Sigma Aldrich, Alfa Aesar, TCI America, and/or Strem, and were used without further purification. All solvents were purchased from Sigma Aldrich, AK Scientific, EMD, Anachemia, Caledon, Fisher, or ACP and used without further purification, unless otherwise specified. Diisopropylamine (DIPA) and  $\text{CH}_2\text{Cl}_2$  were freshly distilled over calcium hydride. Tetrahydrofuran (THF) was freshly distilled over Na metal/benzophenone.

Cold temperatures were maintained by use of the following conditions: 5 °C, fridge (True Manufacturing, TS-49G); 0 °C, ice-water bath; -40 °C, acetonitrile-dry ice bath; -78 °C, acetone-dry ice bath; temperatures between -78 °C and 0 °C required for longer reaction times were maintained with a Neslab Cryocool Immersion Cooler (CC-100 II) in a EtOH/2-propanol bath.

Nuclear magnetic resonance (NMR) spectra were recorded using chloroform- $\text{d}_3$  ( $\text{CDCl}_3$ ) or methanol- $\text{d}_4$  ( $\text{CD}_3\text{OD}$ ) or dimethyl sulfoxide- $\text{d}_6$  ( $\text{CD}_3\text{SOCD}_3$ ) as solvents. Signal positions ( $\delta$ ) are given in parts per million from tetramethylsilane ( $\delta$  0) and were measured relative to the signal of the solvent ( $^1\text{H}$  NMR:  $\text{CDCl}_3$ :  $\delta$  7.26,  $\text{CD}_3\text{OD}$ :  $\delta$  3.31,  $\text{CD}_3\text{SOCD}_3$ :  $\delta$  2.50;  $^{13}\text{C}$  NMR:  $\text{CDCl}_3$ :  $\delta$  77.16,  $\text{CD}_3\text{OD}$ :  $\delta$  49.15,  $\text{CD}_3\text{SOCD}_3$ :  $\delta$  39.51).

Coupling constants (J values) are given in Hertz (Hz) and are reported to the nearest 0.1 Hz. <sup>1</sup>H NMR spectral data are tabulated in the following order: multiplicity (s, singlet; d, doublet; t, triplet; q, quartet; quint, quintet; m, multiplet), coupling constants, experimental integration providing the number of protons. NMR spectra were recorded on a Bruker Avance 600 equipped with a QNP or TCI cryoprobe (600 MHz), Bruker 500 (500 MHz), or Bruker 400 (400 MHz). Assignments of <sup>1</sup>H and <sup>13</sup>C NMR spectra are based on analysis of 1H- 1H COSY, HSQC, HMBC spectra, where applicable.

Optical rotations were measured using a PerkinElmer 341 polarimeter at a wavelength of 589 nm.

High resolution mass spectra were performed using a Bruker MaXis Impact TOF LC/MS. The HRMS was calibrated with internal standard sodium formate.

High performance liquid chromatography (HPLC) was performed using an Agilent 1200 Series equipped with a variable wavelength UV-Vis detector ( $\lambda = 254$  nm) and XBridge™ PREP C18 5 $\mu$ m 10x150mm column.

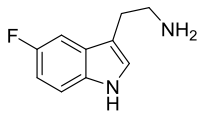
The plant, *Chimonanthus praecox*, was purchased from Flora Excotica, QC, Canada, and then was cultivated in SFU greenhouse facility all the time. They have been watered twice a week to maintain the plant.

*In planta* feeding experiments were performed in a temperature-controlled greenhouse (SFU greenhouse facility). Plant protein samples were concentrated by using 10 kDa Amicon® centrifugation tubes (15 mL, 0.5 mL). They were centrifuged at 4,000 g (15 mL) or 14,000 g (0.5 mL) for 60-minute at 4 °C. The filtrates are discarded and the concentrated samples are all collected, and repeat this procedure again to prepare concentrated protein sample.

Fluorescence microscopy was performed using a WaveFX spinning disc confocal system equipped with a Yagogawa CSU-10 confocal head, lasers with  $\lambda = 441, 491, 561, 647$  nm, and a Hammamatsu 9100 EMCCD camera. An objective lens of 40x magnification was used.

## 2.7.2. Experimental Information for Tryptamine Analogues

### Preparation of 5-fluorotryptamine (**108**)



**108**

To a heterogeneous mixture of 5-fluoroindole (**100**, 1.5g, 11.1 mmol) and 1-dimethylamino-2-nitroethylene (1.4 g, 12.2 mmol) was added trifluoroacetic acid (20 ml, 0.55 M) and the reaction mixture was stirred for two hours. After this time, the reaction mixture turned black and was then diluted with EtOAc (50 mL) and 10 % aqueous Na<sub>2</sub>CO<sub>3</sub> (150 mL). The phases were separated and the aqueous phase was washed with EtOAc (4 x 50 mL). The combined organic phases were then washed with brine (150 mL), dried over MgSO<sub>4</sub> and the solvent was removed *in vacuo*. The crude mixture was then suspended in hot Et<sub>2</sub>O, filtered through Celite® and the solvent was removed *in vacuo* to give the crude product (2.1 g) as a yellow solid.

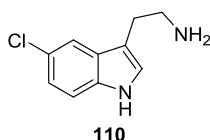
To a stirred flask containing THF (75 mL) at 0 °C was added sodium borohydride (1.26 g, 33.4 mmol). BF<sub>3</sub>•OEt<sub>2</sub> (6.3 g, 44.5 mmol, 4 equiv) was then added slowly to the reaction mixture and stirred for 15 minutes at room temperature. The crude product from the first step was then added dropwise as a solution in THF (20 mL). The reaction mixture was heated at reflux for two hours, then cooled to room temperature and acidified to pH 1 by the addition of 1N HCl solution (~25 mL). The reaction mixture was refluxed for an additional two hours, then cooled to room temperature and washed with Et<sub>2</sub>O (100 ml x 4). The combined organic phases were dried over MgSO<sub>4</sub> and filtered, then the solvent was removed *in vacuo*. Purification of the crude material by flash chromatography (10% ammonia solution (7N in MeOH), 90% CH<sub>2</sub>Cl<sub>2</sub>) to afford 5-fluorotryptamine (**108**, 1.05 g, 51 %) as a brown solid.

<sup>1</sup>H NMR (400 MHz, CD<sub>3</sub>OD) δ: 7.28 (dd, *J* = 4.4, 8.6 Hz, 1H), 7.20 (dd, *J* = 2.5, 10.0 Hz, 1H), 7.14 (s, 1H), 6.85 (dt, *J* = 2.5, 9.1 Hz, 1H), 2.93 (dt, *J* = 2.4, 6.6 Hz, 2H), 2.85 (dt, *J* = 2.4, 6.6 Hz, 2H)

$^{13}\text{C}$  NMR (100 MHz,  $\text{CD}_3\text{OD}$ )  $\delta$ : 158.9 (d,  $J = 231.9$  Hz), 134.81, 129.01 (d,  $J = 9.6$  Hz), 125.6, 113.5 (d,  $J = 4.7$  Hz), 113.0 (d,  $J = 9.7$  Hz), 110.4 (d,  $J = 26.5$  Hz), 103.8 (d,  $J = 23.4$  Hz), 42.9, 29.15

HRMS:  $m/z$  calculated for  $\text{C}_{10}\text{H}_{11}\text{FN}_2$ : 179.0979 (M+H); Found: 179.0975 (M+H)

### Preparation of 5-chlorotryptamine (110)



To a heterogeneous mixture of 5-chloroindole (500 mg, 3.397 mmol) and 1-dimethylamino-2-nitroethylene (435 mg, 3.74 mmol) was added trifluoroacetic acid (7 ml, 0.48 M), and the reaction mixture was stirred for two hours. After this time, the reaction mixture turned black and was then diluted with EtOAc (50 mL) and 10 % aqueous  $\text{Na}_2\text{CO}_3$  (150 mL). The phases were separated and the aqueous phase was washed with EtOAc (4 x 50 mL). The combined organic phases were then washed with brine (150 mL), dried over  $\text{MgSO}_4$  and the solvent was removed *in vacuo*. The crude mixture was then suspended in hot  $\text{Et}_2\text{O}$ , filtered through Celite® and the solvent was removed *in vacuo* to give the crude product (0.7 g) as an orange solid.

To a stirred flask containing THF (55 mL) at 0 °C was added sodium borohydride (400 mg, 10.5 mmol).  $\text{BF}_3 \cdot \text{OEt}_2$  (1.9 g, 13.6 mmol) was then added slowly to the reaction mixture and stirred for 15 minutes at room temperature. The crude product from the first step was then added dropwise as a solution in THF (10 mL). The reaction mixture was heated at reflux for two hours, then cooled to room temperature and acidified to pH 1 by the addition of 1N HCl solution (~15 mL). The reaction mixture was refluxed for an additional two hours, then cooled to room temperature and washed with  $\text{Et}_2\text{O}$  (100 ml x 4). The combined organic phases were dried over  $\text{MgSO}_4$  and filtered, then the solvent was removed *in vacuo*. Purification of the crude material by flash

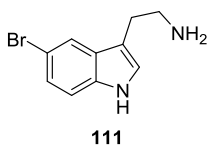
chromatography (10% ammonia solution (7N in MeOH), 90% CH<sub>2</sub>Cl<sub>2</sub>) to afford 5-chlorotryptamine (**110**, 0.21 g, 32 %) as a brown solid.

<sup>1</sup>H NMR (600 MHz, CD<sub>3</sub>OD) δ: 7.52 (dd, *J* = 0.5, 2.0 Hz, 1H), 7.30 (dd, *J* = 0.5, 8.6 Hz, 1H), 7.12 (s, 1H), 7.05 (dd, *J* = 2.0, 8.6 Hz, 1H), 2.92 (dt, *J* = 1.6, 7.1 Hz, 2H), 2.85 (dt, *J* = 1.6, 7.1 Hz, 2H)

<sup>13</sup>C NMR (150 MHz, CD<sub>3</sub>OD) δ: 136.6, 129.8, 125.4, 125.3, 122.5, 118.7, 113.5, 113.2, 42.9, 29.0

HRMS: *m/z* calculated for C<sub>10</sub>H<sub>11</sub>ClN<sub>2</sub>: 195.0684 (M+H); Found: 195.0682 (M+H)

### Preparation of 5-bromotryptamine (**111**)



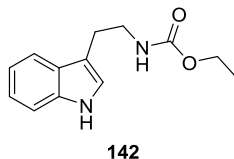
5-bromotryptamine hydrochloride salt (1.0 g, 3.6 mmol) was dissolved in water (30 mL) and basified with 15% NaOH in water (7 mL). The aqueous phase was extracted with dichloromethane (20 ml x 3). The combined organic phases were dried over MgSO<sub>4</sub> and filtered, then the solvent was removed *in vacuo* to afford 5-bromotryptamine (**111**) as a brown solid (0.77 g, 3.2 mmol, 89 %)

<sup>1</sup>H NMR (600 MHz, CD<sub>3</sub>OD) δ: 7.68 (dd, *J* = 1.7 Hz, 1H), 7.25 (dd, *J* = 8.6 Hz, 1H), 7.17 (dd, *J* = 1.8, 8.6 Hz, 1H), 7.10 (s, 1H), 2.91 (t, *J* = 6.6 Hz, 2H), 2.85 (t, *J* = 6.6 Hz, 2H)

<sup>13</sup>C NMR (150 MHz, CD<sub>3</sub>OD) δ: 136.8, 130.6, 125.1, 125.0, 121.9, 113.9, 113.2, 112.8, 43.0, 29.2

HRMS: *m/z* calculated for C<sub>10</sub>H<sub>11</sub>BrN<sub>2</sub>: 239.0178, 241.0158 (M+H); Found: 239.0182, 241.0163 (M+H)

## Preparation of carbamate **142**



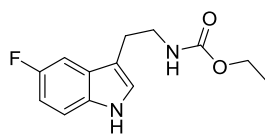
To a stirred solution of tryptamine (**88**, 1.0 g, 6.2 mmol) in  $\text{CH}_2\text{Cl}_2$  (16 mL) was added triethylamine (0.87 mL, 12 mmol) then cooled to 0 °C. Ethyl chloroformate (0.62 mL, 6.5 mmol) was then added dropwise then the reaction mixture was warmed to room temperature then diluted with  $\text{H}_2\text{O}$  (25 mL) and the phases were separated. The organic phase was washed with 1N HCl (15 mL), 5% aqueous  $\text{NaHCO}_3$  (15 mL),  $\text{H}_2\text{O}$  (15 mL) and brine (15 mL) then dried ( $\text{MgSO}_4$ ) and filtered and the solvent removed *in vacuo*. Purification of the crude material by flash chromatography (EtOAc-hexanes 30:70) provided carbamate **142**. (1.35 g, 5.8 mmol, 93%) as a yellow oil.

$^1\text{H}$  NMR (400 MHz,  $\text{CD}_3\text{OD}$ )  $\delta$ : 7.56 (d,  $J = 7.9$  Hz, 1H), 7.32 (dt,  $J = 0.8, 8.1$  Hz, 1H), 7.08 (dt,  $J = 1.0, 7.1$  Hz, 1H), 7.04 (s, 1H), 6.99 (dt,  $J = 1.0, 7.1$  Hz, 1H), 4.05 (q,  $J = 7.1$  Hz, 2H), 3.38 (m, 2H), 2.91 (t,  $J = 7.5$  Hz, 2H), 1.21 (t,  $J = 7.1$  Hz, 3H)

$^{13}\text{C}$  NMR (150 MHz,  $\text{CD}_3\text{OD}$ )  $\delta$ : 159.2, 138.1, 128.8, 123.3, 122.2, 119.5, 119.3, 113.3, 112.2, 61.6, 42.8, 26.8, 15.0

HRMS:  $m/z$  calculated for  $\text{C}_{13}\text{H}_{16}\text{N}_2\text{O}_2$ : 255.1104 (M+Na); Found: 255.1103 (M+Na)

## Preparation of 5-fluorocarbamate **103**



103

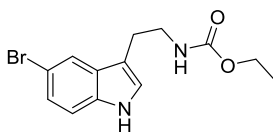
To a stirred solution of 5-fluorotryptamine (**108**, 180 mg, 1.0 mmol) in CH<sub>2</sub>Cl<sub>2</sub> (10 mL) was added triethylamine (0.15 mL, 1.1 mmol) then cooled to 0 °C. Ethyl chloroformate (0.10 mL, 1.1 mmol) was then added dropwise then the reaction mixture was warmed to room temperature then diluted with H<sub>2</sub>O (15 mL) and the phases were separated. The organic phase was washed with 1N HCl (15 mL), 5% aqueous NaHCO<sub>3</sub> (15 mL), H<sub>2</sub>O (15 mL) and brine (15 mL) then dried (MgSO<sub>4</sub>) and filtered and the solvent removed *in vacuo*. Purification of the crude material by flash chromatography (EtOAc-hexanes 30:70) provided 5-fluorocarbamate **103**. (0.24 g, 0.97 mmol, 97%) as a yellow oil.

<sup>1</sup>H NMR (500 MHz, CD<sub>3</sub>OD) δ: 7.56 (d, *J* = 7.9 Hz, 1H), 7.32 (dt, *J* = 0.8, 8.1 Hz, 1H), 7.08 (dt, *J* = 1.0, 7.1 Hz, 1H), 7.04 (s, 1H), 6.99 (dt, *J* = 1.0, 7.1 Hz, 1H), 4.05 (q, *J* = 7.1 Hz, 2H), 3.38 (m, 2H), 2.91 (t, *J* = 7.5 Hz, 2H), 1.21 (t, *J* = 7.1 Hz, 3H)

<sup>13</sup>C NMR (125 MHz, CD<sub>3</sub>OD) δ: 159.3, 158.8 (d, *J* = 231.9 Hz), 134.6, 129.1 (d, *J* = 9.4 Hz), 125.4, 113.6 (d, *J* = 5.0 Hz), 112.9 (d, *J* = 9.7 Hz), 110.3 (d, *J* = 26.5 Hz), 103.9 (d, *J* = 23.4 Hz), 61.6, 42.8, 26.8, 15.0

HRMS: *m/z* calculated for C<sub>13</sub>H<sub>15</sub>N<sub>2</sub>FO<sub>2</sub>: 273.1010 (M+Na); Found: 273.1009 (M+Na)

### Preparation of 5-bromocarbamate 143



143



To a stirred solution of 5-bromotryptamine (**111**, 630 mg, 2.6 mmol) in CH<sub>2</sub>Cl<sub>2</sub> (25 mL) was added triethylamine (0.37 mL, 5.2 mmol) then cooled to 0 °C. Ethyl chloroformate (0.47 mL, 5.2 mmol) was then added dropwise then the reaction mixture was warmed to room temperature then diluted with H<sub>2</sub>O (35 mL) and the phases were separated. The organic phase was washed with 1N HCl (35 mL), 5% aqueous NaHCO<sub>3</sub> (35 mL), H<sub>2</sub>O (35 mL) and brine (35 mL) then dried (MgSO<sub>4</sub>) and filtered and the solvent removed *in vacuo*. Purification of the crude material by flash chromatography (EtOAc-hexanes 30:70) provided 5-bromocarbamate **143**. (0.78 g, 2.5 mmol, 96%) as a brown oil.

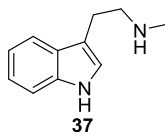
<sup>1</sup>H NMR (400 MHz, CD<sub>3</sub>OD) δ: 7.67 (s, 1H), 7.21 (d, *J* = 8.6 Hz, 1H), 7.13 (d, *J* = 8.6 Hz, 1H), 7.05 (s, 1H), 4.02 (q, *J* = 6.7 Hz, 2H), 3.1 (t, *J* = 7.4 Hz, 2H), 2.84 (t, *J* = 7.4 Hz, 2H), 1.18 (t, *J* = 6.7 Hz, 3H)

<sup>13</sup>C NMR (100 MHz, CD<sub>3</sub>OD) δ: 159.2, 136.7, 130.7, 125.0, 121.9, 113.8, 113.2, 112.8, 61.6, 42.7, 26.6, 15.0

HRMS: *m/z* calculated for C<sub>13</sub>H<sub>15</sub>BrN<sub>2</sub>O<sub>2</sub>: 333.0209, 335.0189 (M+Na); Found: 333.0206, 335.0185(M+Na)

### 2.7.3. Experimental Information for *N*<sub>b</sub>-methyltryptamine analogues

#### Preparation of *N*<sub>b</sub>-methyltryptamine (**37**)



To a cold (0 °C), stirred solution of carbamate **42** (2.52 g, 10.8 mmol) in THF (100 mL) was added LiAlH<sub>4</sub> (1.2 g, 31.6 mmol) and the reaction was heated to reflux for 90 minutes. Following this, the reaction was cooled to 0 °C, diluted with Et<sub>2</sub>O (50 mL) and treated by the dropwise addition of H<sub>2</sub>O (3 mL) followed by 15% aqueous NaOH (3

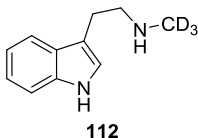
mL) and a further addition of H<sub>2</sub>O (9 mL). MgSO<sub>4</sub> was then added and the reaction mixture was stirred for 15 minutes then filtered and the solvent was removed *in vacuo* to afford *N<sub>b</sub>*-methyltryptamine (**7**) as a yellow solid (1.58 g, 9.1 mmol, 84%)

<sup>1</sup>H NMR (400 MHz, CD<sub>3</sub>OD) δ: 7.53 (td, *J* = 0.9, 8.0 Hz, 1H), 7.32 (td, *J* = 0.5, 8.1 Hz, 1H), 7.08 (ddd, *J* = 1.1, 7.1, 8.1 Hz, 1H), 7.03 (s, 1H), 6.99 (ddd, *J* = 1.1, 7.1, 8.1 Hz, 1H), 2.91 (m, 2H), 2.81 (m, 2H), 2.33 (s, 3H)

<sup>13</sup>C NMR (150 MHz, CD<sub>3</sub>OD) δ: 138.2, 128.6, 123.4, 122.4, 119.6, 119.2, 113.4, 112.3, 53.0, 35.9, 26.0

HRMS: *m/z* calculated for C<sub>11</sub>H<sub>14</sub>N<sub>2</sub>: 175.1230 (M+H); Found: 175.1236 (M+H)

#### Preparation of D<sub>3</sub>-*N<sub>b</sub>*-methyltryptamine (**112**)



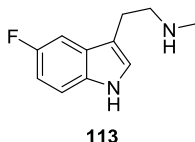
To a cold (0 °C), stirred solution of carbamate **42** (0.65 g, 2.8 mmol) in THF (50 mL) was added LiAlD<sub>4</sub> (0.46 g, 2.8 mmol) and the reaction was heated to reflux for 16 hours. Following this, the reaction was cooled to 0 °C, diluted with Et<sub>2</sub>O (50 mL) and treated by the dropwise addition of H<sub>2</sub>O (0.5 mL) followed by 15% aqueous NaOH (0.5 mL) and a further addition of H<sub>2</sub>O (1.5 mL). MgSO<sub>4</sub> was then added and the reaction mixture was stirred for 15 minutes then filtered and the solvent was removed *in vacuo*. Purification of the crude material by flash chromatography (10% ammonia solution (7N in MeOH), 90% CH<sub>2</sub>Cl<sub>2</sub>) to afford D<sub>3</sub>-*N<sub>b</sub>*-methyltryptamine (**112**) as a yellow solid (0.22 g, 1.2 mmol, 44%).

<sup>1</sup>H NMR (400 MHz, CD<sub>3</sub>OD) δ: 7.55 (td, *J* = 0.9, 8.0 Hz, 1H), 7.33 (td, *J* = 0.5, 8.1 Hz, 1H), 7.09 (ddd, *J* = 1.1, 7.1, 8.1 Hz, 1H), 7.08 (s, 1H), 7.00 (ddd, *J* = 1.1, 7.1, 8.1 Hz, 1H), 2.98 (m, 2H), 2.92 (m, 2H)

$^{13}\text{C}$  NMR (150 MHz,  $\text{CD}_3\text{OD}$ )  $\delta$ : 138.3, 128.6, 123.5, 122.4, 119.7, 119.2, 112.9, 112.3, 52.6, 34.8 (m), 25.6

HRMS:  $m/z$  calculated for  $\text{C}_{11}\text{H}_{11}\text{D}_3\text{N}_2$ : 178.1418 (M+H); Found: 178.1420 (M+H)

### Preparation of 5-fluoro- $N_b$ -methyltryptamine (113)



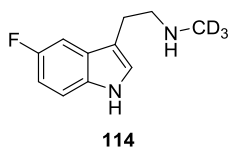
To a cold (0 °C), stirred solution of 5-fluorocarbamate **103** (0.10 g, 0.40 mmol) in THF (10 mL) was added  $\text{LiAlH}_4$  (46 mg, 1.2 mmol) and the reaction was heated to reflux for two hours. Following this, the reaction was cooled to 0 °C, diluted with  $\text{Et}_2\text{O}$  (25 mL) and treated by the dropwise addition of  $\text{H}_2\text{O}$  (50  $\mu\text{L}$ ) followed by 15% aqueous  $\text{NaOH}$  (50  $\mu\text{L}$ ) and a further addition of  $\text{H}_2\text{O}$  (150  $\mu\text{L}$ ).  $\text{MgSO}_4$  was then added and the reaction mixture was stirred for 15 minutes then filtered and the solvent was removed *in vacuo* to afford 5-fluoro- $N_b$ -methyltryptamine (**113**) as a brown oil (81.9 mg, 9.1 mmol, 84%)

$^1\text{H}$  NMR (500 MHz,  $\text{CD}_3\text{OD}$ )  $\delta$ : 7.28 (dd,  $J=4.4, 8.7$  Hz, 1H), 7.21 (dd,  $J=2.4, 9.9$  Hz, 1H), 7.12 (s, 1H), 6.85 (dt,  $J = 2.6, 9.2$  Hz, 1H), 2.90 (m, 2H), 2.85 (m, 2H), 2.4 (s, 3H)

$^{13}\text{C}$  NMR (125 MHz,  $\text{CD}_3\text{OD}$ )  $\delta$ : 158.8 (d,  $J = 231.9$  Hz), 134.8, 128.9 (d,  $J = 9.5$  Hz), 125.5, 113.4 (d,  $J = 4.6$  Hz), 113.0 (d,  $J = 9.6$  Hz), 110.4 (d,  $J = 26.4$  Hz), 103.8 (d,  $J = 23.5$  Hz), 52.7, 35.8, 25.7

HRMS:  $m/z$  calculated for  $\text{C}_{11}\text{H}_{14}\text{FN}_2$ : 193.1136 (M+H); Found: 193.1136 (M+H)

### Preparation of 5-fluoro- $\text{D}_3$ - $N_b$ -methyltryptamine (114)



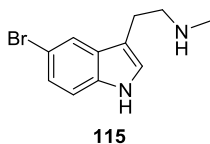
To a cold (0 °C), stirred solution of 5-fluorocarbamate **103** (0.10 g, 0.40 mmol) in THF (10 mL) was added LiAlD<sub>4</sub> (0.10 g, 2.4 mmol) and the reaction was heated to reflux for 16 hours. Following this, the reaction was cooled to 0 °C, diluted with Et<sub>2</sub>O (25 mL) and treated by the dropwise addition of H<sub>2</sub>O (100 μL) followed by 15% aqueous NaOH (100 μL) and a further addition of H<sub>2</sub>O (300 μL). MgSO<sub>4</sub> was then added and the reaction mixture was stirred for 15 minutes then filtered and the solvent was removed *in vacuo*. Purification of the crude material by flash chromatography (10% ammonia solution (7N in MeOH), 90% CH<sub>2</sub>Cl<sub>2</sub>) to afford 5-fluoro-D<sub>3</sub>-N<sub>b</sub>-methyltryptamine (**114**) as a brown solid (0.22 g, 1.2 mmol, 44%).

<sup>1</sup>H NMR (600 MHz, CD<sub>3</sub>OD) δ: 7.28 (dd, *J* = 4.4, 8.7 Hz, 1H), 7.21 (dd, *J* = 2.4, 9.9 Hz, 1H), 7.11 (s, 1H), 6.85 (dt, *J* = 2.5, 9.1 Hz, 1H), 2.90 (m, 2H), 2.83 (m, 2H)

<sup>13</sup>C NMR (150 MHz, CD<sub>3</sub>OD) δ: 158.8 (d, *J* = 231.9 Hz), 134.8, 128.9 (d, *J* = 9.5 Hz), 125.5, 113.5 (d, *J* = 4.7 Hz), 113.0 (d, *J* = 9.6 Hz), 110.4 (d, *J* = 26.5 Hz), 103.8 (d, *J* = 23.4 Hz), 52.7, 35 (hept, *J* = 20.5 Hz), 25.8

HRMS: *m/z* calculated for C<sub>11</sub>H<sub>14</sub>D<sub>3</sub>FN<sub>2</sub>: 196.1324 (M+H); Found: 196.1326 (M+H)

### Preparation of 5-bromo-N<sub>b</sub>-methyltryptamine (115)



To a cold (0 °C), stirred solution of 5-bromocarbamate **143** (0.81 g, 2.6 mmol) in THF (25 mL) was added LiAlH<sub>4</sub> (380 mg, 10 mmol) and the reaction was heated to reflux

for two hours. Following this, the reaction was cooled to 0 °C, diluted with Et<sub>2</sub>O (30 mL) and treated by the dropwise addition of H<sub>2</sub>O (0.4 mL) followed by 15% aqueous NaOH (0.4 mL) and a further addition of H<sub>2</sub>O (1.2 mL). MgSO<sub>4</sub> was then added and the reaction mixture was stirred for 15 minutes then filtered and the solvent was removed *in vacuo* to afford 5-bromo-*N*<sub>b</sub>-methyltryptamine (**115**) as a brown oil (650 mg, 2.5, 99%)

<sup>1</sup>H NMR (400 MHz, CD<sub>3</sub>OD) δ: 7.68 (d, *J* = 1.7 Hz, 1H), 7.25 (d, *J* = 8.6 Hz, 1H), 7.16 (dd, *J* = 1.7, 8.6 Hz, 1H), 7.09 (s, 1H), 2.90 (m, 2H), 2.83 (m, 2H), 2.34 (s, 3H)

<sup>13</sup>C NMR (100 MHz, CD<sub>3</sub>OD) δ: 136.8, 130.5, 125.1, 125.0, 121.8, 113.9, 113.2, 112.8, 52.9, 35.9, 25.7

HRMS: *m/z* calculated for C<sub>11</sub>H<sub>14</sub>BrN<sub>2</sub>: 253.0335, 255.0315 (M+H); Found: 253.0338, 255.0318 (M+H)

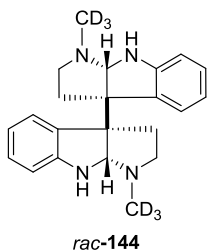
## 2.7.4. Synthetic Standards of D<sub>6</sub>-chimonanthines

### Preparation of D<sub>6</sub>-chimonanthine 144 and 145

This procedure was adapted from Takayama's chimonanthine synthesis.

To a cold (-30 °C), stirred solution of carbamate **142** (1.5 g, 6.35 mmol) in trifluoroethanol (8 mL) was added [bis(trifluoroacetoxy)iodo]benzene (1.8 g, 4.1 mmol) was added over 3 hours by the addition of 0.3 g portions every 30 minutes, and the reaction was stirred at -30 °C for two hours. Following this, the reaction was warmed to room temperature, and the solvent was removed *in vacuo*. The crude mixture was dissolved in freshly distilled THF (60 mL), and the reaction mixture was cooled to 0 °C. To a cold (0 °C), stirred solution was added LiAlD<sub>4</sub> (0.80 g, 19 mmol) and the reaction was heated to reflux for 16 hours. Following this the reaction was cooled to 0 °C, diluted with Et<sub>2</sub>O (100 mL) and treated by the dropwise addition of H<sub>2</sub>O (0.8 mL) followed by 15% aqueous NaOH (0.8 mL) and a further addition of H<sub>2</sub>O (2.4 mL). MgSO<sub>4</sub> was then added and the reaction mixture was stirred for 15 minutes then filtered and the solvent was removed *in vacuo*. Purification of the crude material by flash chromatography (10%

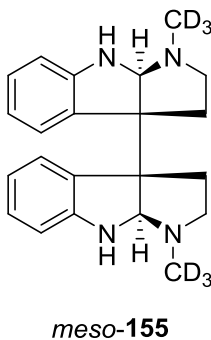
ammonia solution (7N in MeOH), 90% CH<sub>2</sub>Cl<sub>2</sub>) to afford D<sub>6</sub>-*rac*-**144** (5 mg, 1%) and D<sub>6</sub>-*meso*-**155** (trace)



<sup>1</sup>H NMR (600 MHz, CD<sub>3</sub>OD) δ: 7.23 (broad s, 2H), 6.98 (broad s, 2H), 6.63 (broad s, 2H), 6.54 (broad s, 2H), 2.70-2.09 (m, 10H)

<sup>2</sup>H NMR (600 MHz, CH<sub>2</sub>Cl<sub>2</sub>) δ: 2.39 (s)

HRMS: *m/z* calculated for C<sub>22</sub>H<sub>20</sub>D<sub>6</sub>N<sub>4</sub>: 353.2607 (M+H); Found: 353.2606 (M+H)



<sup>1</sup>H NMR (600 MHz, CD<sub>3</sub>Cl) δ: 7.04 (m, 4H), 6.49 (d, *J* = 7.9 Hz, 4H), 6.63 (broad s, 2H), 2.60-2.35 (m, 6H), 2.06 (m, 2H)

HRMS: *m/z* calculated for C<sub>22</sub>H<sub>20</sub>D<sub>6</sub>N<sub>4</sub>: 353.2607 (M+H); Found: 353.2604 (M+H)

### 2.7.5. Feeding Precursors *in planta* and Screening Precursors by LC-MS

Fresh stems with several leaves were collected from *Chimonanthus praecox*, then the tips of stems were placed to the solutions of each synthetic precursor or two-precursor mixed (**106-115**, 5 mM, H<sub>2</sub>O-DMSO 90:10, 10 mL, pH 4-5, see Table 2.1) and incubated in greenhouse overnight. Then, a leaf from each solution were collected, and the leaf was cut into small pieces individually. The small pieces were placed in MeOH (0.5 mL) in 1.5 mL Eppendorf® tubes, then, the samples were sonicated for one hour. The green methanol solutions was filtered and submitted to LC-MS.

LC-MS was run over 10 minutes with the eluent system (Table 2.7). MS was calibrated with internal standard, sodium formate. Then, the LC-MS chromatograms performed EIC analysis at *m/z* of target unnatural products.

**Table 2.7. LC methods on LC-MS analysis**

Time (min)	Solvent: A (%)	Solvent: B (%)
0	90	10
1	90	10
8	40	60
9	0	100
10	0	100
10.1	90	10
12	90	10

Solvent A: H<sub>2</sub>O with 0.1 % formic acid. Solvent B: acetonitrile with 0.1 % formic acid. Column temperature: 30 °C. Initial flow rate: 0.3 mL/min, ramp to 0.5 mL/min in 8min and Hold till 12 min. Total run time: 12 min

### 2.7.6. Isolation of Fluorinated Unnatural Products

The scale-up experiments commenced with the feeding of 50 mg of 5-fluorotryptamine (**109**) to 20 g of fresh leaves of *Chimonanthus praecox* over 5 days. After 5 days, the leaves were collected and cut into small pieces. The small pieces of leaves were suspended in MeOH (250 mL) and stirred overnight to extract alkaloids, then filtered. The solvent was removed *in vacuo*, and the plant extracts were dissolved in chloroform (75 mL). The mixture was acidified with 1M HCl (75 mL), and the phases were separated. The organic phase was washed with 15% NaOH (75 mL), then the

phases were separated again. The combined organic phases were then washed with brine (100 mL), dried over MgSO<sub>4</sub> and the solvent was removed *in vacuo* to afford brown plant extracts (40 mg).

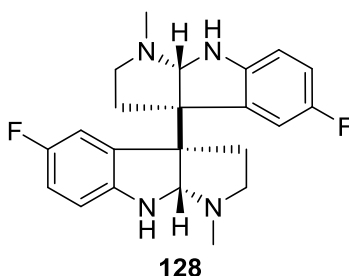
The plant extracts were dissolved in methanol (1 mL) and placed in fridge overnight, then filtered to remove solid impurities. The filtered sample was submitted to HPLC to purify the alkaloids. After HPLC isolation, each fraction was submitted to LC-MS to monitor if the desired *m/z* of 383.2042 was present or not. The fractions that contained the desired *m/z* of 383.2042 were collected and concentrated under vacuum to afford **128** (~0.7 mg) and **129** (~0.05 mg).

**Table 2.8. HPLC eluent system to isolate difluorochimonanthines**

Time (min)	Solvent: A (%)	Solvent: B (%)
0	70	30
6	15	85
8	15	85
8.5	70	30
10	70	30

Solvent A: H<sub>2</sub>O with 0.1 % formic acid, Solvent B: methanol with 0.1 % formic acid. Injection volume 200  $\mu$ L.

### Characterization of isolated alkaloid (-)-128



<sup>1</sup>H NMR (600 MHz, CD<sub>3</sub>Cl)  $\delta$ : 6.86 (broad s, 2H), 6.66 (broad s, 2H), 6.33 (broad s, 2H), 2.64-2.44 (m, 8H), 2.34 (s, 6H), 2.07 (broad s, 2H)

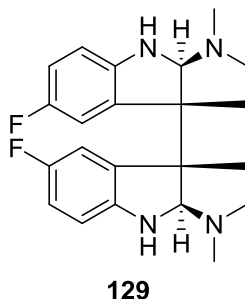
<sup>13</sup>C NMR (150 MHz, CD<sub>3</sub>Cl)  $\delta$ : 157.1 (d, *J* = 239.7 Hz), 146.7, 135.1 (d, *J* = 7.2 Hz), 129.9, 114.5 (d, *J* = 22 Hz), 110.0, 86.1, 53.6, 52.6, 37.3, 35.8



HRMS:  $m/z$  calculated for  $C_{22}H_{24}F_2N_4$ : 383.2042 (M+H); Found: 383.2049 (M+H)

$[\alpha]_D^{20}$ : -35 (c: 0.06,  $CHCl_3$ )

### Characterization of isolated alkaloid *meso*-129



$^1H$  NMR (600 MHz,  $(CD_3)_2SO$ )  $\delta$ : 6.70 (m, 2H), 6.34 (d,  $J = 0.5, 8.5$  Hz, 2H), 6.33 (d,  $J = 8.5$  Hz, 2H), 2.28 (m, 10H), 2.11 (s, 6H)

HRMS:  $m/z$  calculated for  $C_{22}H_{24}F_2N_4$ : 383.2042 (M+H); Found: 383.2038 (M+H)

#### 2.7.7. Plant Protein Extraction with P-PER™ Plant Protein Extraction Kit and *in vitro* Assay

A small leaf (~80 mg) was collected from *Chimonanthus praecox*, and protein extraction procedures were followed as described in P-PER™ Plant Protein Extraction Kit. 100  $\mu$ L of protein samples were used in the *in vitro* assay in combination with precursor analogues in the following reaction buffer system (1mL, 1 mM precursor, 0.1 mM cofactor as indicated in Table 2.4).

Reaction Buffer

Buffer A: PBS

Buffer B: 0.2 M Tris-HCl

After overnight incubation at the specified temperatures, the samples were filtered in 3K Amicon® centrifugation tube, and the filtrate was submitted for LC-MS analysis.

### 2.7.8. Plant Protein Extraction from Leaves Using Blender and *in vitro* Assay

Fresh leaves (~20-50 g) were collected from *Chimonanthus praecox*. These leaves were frozen and then ground into a powder using a mortar and pestle cooled in liquid nitrogen. The powdered leaves were then placed in a blender (Oster®) and cold (4 °C) extraction buffer (200 mL) and protease inhibitor (Roche® cOmplete, Mini, one tablet) were added in a cold (4 °C) room. The blender was run for 15 seconds and this blending was repeated five times. After the blending, the homogenized samples were filtered through 4-layers of cheese cloth, then centrifuged at 14,000 rpm for 30 minutes at 4 °C to remove cellular debris and large cellular components. The supernatant was concentrated by using Amicon® centrifugal tubes as described above and the concentrated supernatant sample was then transferred into pre-cooled 2 mL Eppendorf tubes.

The collected protein samples were then added into the reaction buffers specified below and precursor analogues **112** or **113** (1 mM). After overnight incubation at the specified temperatures, the samples were filtered through 3K Amicon® centrifugal tubes, and finally subjected to LC-MS analysis.

**Table 2.9. Extraction buffers and reaction buffers used in *in vitro* assay**

Entry	Extraction Buffer	Reaction Buffer
1	PBS	PBS
2	0.2 M Tris-HCl	0.2 M Tris-HCl
3	PBS, 1 mM PEG, 5% (w/v) PVPP, 0.01% Triton X-100	PBS
4	25 mM Hepes-Na, 0.5 mM EDTA, DTT, 8 mM MgCl <sub>2</sub>	25 mM Hepes-Na, 8 mM MgCl <sub>2</sub>
5	50 mM Tris-HCl, 10 mM DTT, 0.5 M sucrose.	50 mM Tris-HCl, 0.5 M sucrose.
6	0.45 M Mannitol, 50 mM sodium phosphate, 2 mM EDTA	1 M Mannitol, 0.2 M sodium phosphate

### **2.7.9. Plant Protein Extraction From Roots Using Blender and *in vitro* Assay** <sup>[83]</sup>

Fresh roots (~100 g) were collected from *Chimonanthus praecox*. The roots were washed thoroughly with distilled water (1 L X 5) to remove any residual soil. These roots were ground to provide a powder using a mortar and pestle cooled with liquid nitrogen. The powdered roots were placed in a blender (Oster®) and cooled (4 °C) extraction buffer (500m L) and protease inhibitor (Roche® cOmplete, Mini, 1 tablet) were added to the sample in a cold (4 °C) room. The blender was run for 15 seconds intervals and repeated 5 times. After blending, the homogenized samples were filtered through 4-layers of cheesecloth, then centrifuged at 14,000 rpm for 30 minutes at 4 °C to remove cellular debris and large cellular components. The supernatants were then collected and subjected to ammonium sulfate precipitation to separate and concentrate protein samples.

### **2.7.10. Root protein separation by Ammonium Sulfate Precipitation**

To a beaker of plant protein supernatant sample, in a cold (4 °C) room, was slowly added ammonium sulfate to obtain a 20% solution, which was then stirred for 12 hours. After this time the sample was centrifuged at 14,000 rpm for one hour at 4 °C and the solids were collected. More ammonium sulfate was then added to the filtrate to increase the concentration to 40% and the resulting mixture was stirred for a further 12 hours and then centrifuged at 14,000 rpm for one hour at 4 °C and the solids were collected. This procedure was repeated with ammonium sulfate concentrations of 60%, 80%, and 95% to afford the ammonium sulfate plant protein fractions.

Each solid fraction was later dissolved in sodium acetate buffer (10 mL, 50 mM, pH 4.5), and the ammonium sulfate was removed by dialysis against this same buffer over 16 hours. The protein solution was then centrifuged at 15,000 for 30 minutes to remove residual solids and afford a solution of the protein extracts.

### 2.7.11. Preparation of Protoplasts <sup>[84]</sup>

Fresh leaves (~3-5 g) were collected from *Chimonanthus praecox*, and they were cut into 0.5-1 mm strips using a razor blade. The short strips were placed in digestive enzyme solution (20 mM MES (pH 5.7) containing 1.5% (w/v) cellulose R10, 0.4 % (wt/vol) macrozyme R10, 0.4 M mannitol and 20 mM KCl) in a 50 mL Erlenmeyer flask. The solution was kept in the dark by wrapping the flask with aluminium foil and the solution was gently shaken (100 rpm) for 4 hours at room temperature. The solution was then transferred into a 15 mL Falcon® centrifuge tube and centrifuged at 2,000 g. The solids were collected and washed with washing buffer (0.5 M mannitol, 4 mM MES-KOH, pH 5.5, 20 mM KCl, and 3 x 20 mL). The washed protoplasts were directly used for assays and microscopy.

### 2.7.12. In Vitro Assay with Protoplasts

The collected protoplasts (~0.5 g) were suspended in PBS (1.5 mL) in a 2 mL Eppendorf® tube. Then 5-fluorotryptamine (**108**, 20 µL, 0.2 M) was added and the mixture was incubated at 30 °C overnight. MeOH (0.5 mL) was added after which the sample was sonicated for one hour. The sample was filtered using a 3K Amicon® centrifugal tube and then subjected to analysis by LC-MS.

### 2.7.13. Preparation of Cell Wall<sup>[88]</sup>

Leaves of *Chimonanthus praecox* were collected (15 g), frozen in liquid nitrogen and ground into powder using a cooled mortar and pestle. The resulting green powder was transferred into a 500 mL-beaker containing potassium phosphate buffer (250 mL, 50 mM, and pH 7.0) with 1 % (v/v) of Triton X-100 and stirred for 4 hours at 4 °C. The mixture was then filtered through one layer of cheesecloth, the insoluble materials were then washed with cold distilled water (1 L) and squeezed in the cheesecloth to remove any residual water. The insoluble materials were washed overnight with 0.5 M of NaCl (250 mL) and filtered through one layer of cheesecloth. The insoluble materials were washed with cold distilled water (1 L) and squeezed in cheesecloth to remove residual water. 4 g of the cell wall materials were collected in this manner.

#### 2.7.14. Preparation of Cell Wall proteins<sup>[89]</sup>

25 g of leaves were collected and frozen in liquid nitrogen. They were then ground using a cooled mortar and pestle into a fine green powder. The green powder was homogenized in 0.1 M potassium phosphate buffer (pH 7.0, 300 mL) containing 5 mM DTT and then filtered through four-layers of cheese cloth. The insoluble materials were collected, and shaken sequentially with pre-chilled (-20 °C) acetone (3 x 300 mL, 30 min each), solution A (0.1 M potassium phosphate buffer (pH 6.5) with 0.1 % beta-mercaptoethanol, 4 °C 300 mL, 30 min), solution A containing 1% (v/v) Triton X-100 (4 °C, 300 mL, 4 hours), and finally with solution A to remove remaining detergent (4 °C, 300 mL, 16 hours). Between each procedure, the homogenate was filtered through 4 layers of cheesecloth and the insoluble materials were collected.

The collected insoluble materials (pale yellow) were placed into a cooled (4 °C) solution of 200 mL of 1 M NaCl solution (4 hours) and stirred with a magnetic stir bar to extract the proteins from the insoluble residues. The homogenate was decanted and filtered through 4-layers of cheesecloth and the yellow solution (protein sample) was concentrated using 15 mL 10K Amicon® centrifugation tubes (4000 g, 45 mins) and then concentrated again using 0.5 mL 10K Amicon® centrifugation tubes (14,000 g, 45 mins). The protein concentration of the resulting samples was determined by Bradford assay (BioRad), using BSA as a protein standard, to afford 200 µL of yellow protein sample (1.8 mg / mL).

The protein extracts (0, 15, 30, 45, and 60 µL) were assayed in a solution of 0.1 M potassium phosphate (pH 7) containing 5 mM of 5-fluoro-*N*<sub>b</sub>-methyltryptamine and 2.5 µL of ammonium persulfate in 250 µL overnight at 30 °C. After the incubation the samples were filtered through 3K Amicon® centrifugation tubes and the filtrates were submitted for analysis by LC-MS.

## References

- [1] B. Jones, R. J. Kazlauskas, *Nat. Chem.* **2014**, 7, 11–12.
- [2] C. E. Hornsby, R. S. Paton, *Nat. Chem.* **2014**, 6, 88–9.
- [3] J. M. Winter, Y. Tang, *Curr. Opin. Biotechnol.* **2012**, 23, 736–743.
- [4] N. Tibrewal, Y. Tang, *Annu. Rev. Chem. Biomol. Eng.* **2014**, 5, 347–66.
- [5] B. Shen, *Curr. Opin. Chem. Biol.* **2003**, 7, 285–295.
- [6] J. Staunton, K. J. Weissman, *Nat. Prod. Rep.* **2001**, 18, 380–416.
- [7] L. Katz, S. Donadio, *Annu. Rev. Microbiol.* **1993**, 47, 875–912.
- [8] D. a. Hansen, C. M. Rath, E. B. Eisman, A. R. H. Narayan, J. D. Kittendorf, J. D. Mortison, Y. J. Yoon, D. H. Sherman, *J. Am. Chem. Soc.* **2013**, 135, 11232–11238.
- [9] M. Hesse, *Alkaloids: Nature's Curse or Blessing?*, Wiley-VCH, **2002**.
- [10] R. Schemitz, *Pharm. Hist.* **1985**, 27, 61–74.
- [11] E. J. Dimise, S. D. Bruner, *Nat. Chem. Biol.* **2010**, 6, 251–252.
- [12] J. M. Hagel, P. J. Facchini, *Nat. Chem. Biol.* **2010**, 6, 273–275.
- [13] J. Ziegler, P. J. Facchini, *Annu. Rev. Plant Biol.* **2008**, 59, 735–769.
- [14] H. W. Wiley, *Am. Chem. J.* **1889**, 11, 557.
- [15] R. G. Eccles, *Proceeding Am. Pharm. Assoc.* **1888**, 382.
- [16] H. M. Gordin, *J. Am. Chem. Soc.* **1905**, 27, 144.
- [17] H. M. Gordin, *J. Am. Chem. Soc.* **1909**, 1305.
- [18] E. Späth, W. Stroh, *Berichte Der Dtsch. Chem. Gesellschaft* **1925**, 59, 2131.

- [19] G. Barger, J. Madinaveitia, P. Streuli, *J. Chem. Soc.* **1939**, 510–517.
- [20] R. Woodward, C. Yang, T. Katz, V. Clark, J. Harley-Mason, R. Ingleby, N. Sheppard, *Proc. Chem. Soc.* **1960**, 76–78.
- [21] T. A. Hamor, J. M. Robertson, H. N. Shrivastava, J. V. Silverton, *Proc. Chem. Soc.* **1960**, 78–80.
- [22] G. Barger, A. Jacob, J. Madinaveitia, *Recl. des Trav. Chim. des Pays-Bas* **1938**, *57*, 548–554.
- [23] D. G. O'Donovan, M. F. Keogh, *J. Chem. Soc.* **1966**, 1570–1572.
- [24] T. R. Govindachari, K. Nagarajan, S. Rajappa, *J. Sci. Industrial Res.* **1962**, *21*, 455.
- [25] H. F. Hodson, G. F. Smith, *J. Chem. Soc.* **1957**, 1877–1880.
- [26] G.-L. Ma, G.-X. Yang, J. Xiong, W.-L. Cheng, K.-J. Cheng, J.-F. Hu, *Tetrahedron Lett.* **2015**, *56*, 4071–4075.
- [27] Y. Adjibade, H. Saad, T. Sevenet, B. Kuballa, J. C. Quirion, R. Anton, *Planta Med.* **1990**, *56*, 212–215.
- [28] T. a Amador, L. Verotta, D. S. Nunes, E. Elisabetsky, *Phytomedicine* **2001**, *8*, 202–206.
- [29] E. Elisabetsky, T. a. Arnador, R. R. Albuquerque, D. S. Nunes, a. Do CT Carvalho, *J. Ethnopharmacol.* **1995**, *48*, 77–83.
- [30] V. Jannic, F. Guéritte, O. Laprèvote, L. Serani, M. T. Martin, T. Sévenet, P. Potier, *J. Nat. Prod.* **1999**, *62*, 838–843.
- [31] L. Verotta, T. Pilati, M. Tato, E. Elisabetsky, T. a. Amador, D. S. Nunes, *J. Nat. Prod.* **1998**, *61*, 392–396.
- [32] L. Verotta, F. Peterlongo, E. Elisabetsky, T. a. Amador, D. S. Nunes, *J. Chromatogr. A* **1999**, *841*, 165–176.
- [33] H. Hodson, B. Robinson, G. Smith, *Proc. Chem. Soc.* **1961**, 465–466.
- [34] I. J. Grant, T. A. Hamor, J. M. Robertson, G. . Sim, *Proc. Chem. Soc. Chem. Soc.* **1962**, 148–149.
- [35] T. Tokuyama, J. W. Daly, *Tetrahedron* **1983**, *39*, 41–47.

- [36] Y. Adjibade, B. Weniger, J. Quirion, B. Kuballa, P. Cabalion, R. Anton, *Phytochemistry* **1992**, *31*, 317–319.
- [37] L. Verotta, F. Orsini, M. Sbacchi, M. a. Scheidler, T. a. Amador, E. Elisabetsky, *Bioorganic Med. Chem.* **2002**, *10*, 2133–2142.
- [38] K. Ramabadran, M. Bansinath, H. Turndorf, M. M. Puig, *J. Pharmacol. Methods* **1989**, *21*, 21–31.
- [39] T. Morikawa, Y. Nakanishi, K. Ninomiya, H. Matsuda, S. Nakashima, H. Miki, Y. Miyashita, M. Yoshikawa, T. Hayakawa, O. Muraoka, *J. Nat. Med.* **2014**, *68*, 539–549.
- [40] T. S. Chang, V. C. H. Lin, *Int. J. Mol. Sci.* **2011**, *12*, 8787–8796.
- [41] J. M. Gillbro, M. J. Olsson, *Int. J. Cosmet. Sci.* **2011**, *33*, 210–221.
- [42] J. B. Hendrickson, R. Rees, R. Göschke, *Proc. Chem. Soc.* **1962**, 383–384.
- [43] J. B. Hendrickson, R. Göschke, R. Rees, *Tetrahedron* **1964**, *20*, 565–579.
- [44] A. . Scott, F. McCapra, E. S. Hall, *J. Am. Chem. Soc.* **1964**, *86*, 302–303.
- [45] J. T. Link, L. E. Overman, *J. Am. Chem. Soc.* **1996**, *118*, 8166–8167.
- [46] L. E. Overman, D. V. Paone, B. a. Stearns, *J. Am. Chem. Soc.* **1999**, *121*, 7702–7703.
- [47] L. E. Overman, J. F. Larrow, B. a. Stearns, J. M. Vance, *Angew. Chemie - Int. Ed.* **2000**, *39*, 213–215.
- [48] H. Ishikawa, H. Takayama, N. Aimi, *Tetrahedron Lett.* **2002**, *43*, 5637–5639.
- [49] M. Movassaghi, M. a. Schmidt, *Angew. Chemie - Int. Ed.* **2007**, *46*, 3725–3728.
- [50] H. Mitsunuma, M. Shibasaki, M. Kanai, S. Matsunaga, *Angew. Chemie - Int. Ed.* **2012**, *51*, 5217–5221.
- [51] W. Xie, G. Jiang, H. Liu, J. Hu, X. Pan, H. Zhang, X. Wan, Y. Lai, D. Ma, *Angew. Chemie - Int. Ed.* **2013**, *52*, 12924–12927.
- [52] S. Ghosh, S. Chaudhuri, A. Bisai, *Org. Lett.* **2015**, *17*, 1373–1376.
- [53] K. Liang, X. Deng, X. Tong, D. Li, M. Ding, A. Zhou, C. Xia, *Org. Lett.* **2015**, *17*, 206–209.



- [54] Y.-X. Li, H.-X. Wang, S. Ali, X.-F. Xia, Y.-M. Liang, *Chem. Commun.* **2012**, *48*, 2343.
- [55] S. Tadano, Y. Mukaeda, H. Ishikawa, *Angew. Chemie - Int. Ed.* **2013**, *52*, 7990–7994.
- [56] J. Kim, J. a Ashenhurst, M. Movassaghi, *Science* **2009**, *324*, 238–241.
- [57] J. Kim, M. Movassaghi, *J. Am. Chem. Soc.* **2010**, *132*, 14376–14378.
- [58] Y. Li, W.-H. Wang, S.-D. Yang, B.-J. Li, C. Feng, Z.-J. Shi, *Chem. Commun. (Camb)*. **2010**, *46*, 4553–4555.
- [59] S. Tadano, H. Ishikawa, *Synlett* **2014**, *25*, 0157.
- [60] H. Ishikawa, *Yakugaku Zasshi* **2015**, *135*, 383–390.
- [61] J. a. May, B. Stoltz, *Tetrahedron* **2006**, *62*, 5262–5271.
- [62] G. W. Kirby, S. W. Shah, E. J. Herbert, *J. Chem. Soc. Perkin 1* **1969**, *14*, 1916–1919.
- [63] E. J. Herbert, *Studies in Alkaloids Biosynthesis*, **1964**.
- [64] D. D. Songstad, V. De Luca, N. Brisson, W. G. Kurz, C. L. Nessler, *Plant Physiol.* **1990**, *94*, 1410–1413.
- [65] J. C. Thomas, D. C. Adams, C. Nessler, J. K. Brown, H. J. Bohnert, *Plant Physiol.* **1995**, *7–10*.
- [66] I. Islas, V. M. Loyola-Vargas, M. de Lourdes Miranda-Ham, *Vitr. Cell. Dev. Biol. - Plant* **1994**, *30*, 81–83.
- [67] M. a Thompson, R. M. Weinshilboum, *J. Biol. Chem.* **1998**, *273*, 34502–34510.
- [68] Y. H. Kim, Joo, *Exp. Mol. Med.* **2001**, *33*, 23–28.
- [69] M. a Thompson, E. Moon, U. J. Kim, J. Xu, M. J. Siciliano, R. M. Weinshilboum, *Genomics* **1999**, *61*, 285–297.
- [70] R. Thiericke, J. Rohr, *Nat. Prod. Rep.* **1993**, *10*, 265–289.
- [71] J. Kennedy, *Nat. Prod. Rep.* **2008**, *25*, 25–34.
- [72] B. R. Clark, S. O'Connor, D. Fox, J. Leroy, C. D. Murphy, *Org. Biomol. Chem.* **2011**, *9*, 6306–6311.

- [73] S. Brown, S. E. O'Connor, *ChemBioChem* **2015**, *16*, 2129–2135.
- [74] S. E. O'Connor, T. P. Brutnell, *Curr. Opin. Plant Biol.* **2014**, *19*, iv–v.
- [75] S. Weist, R. D. Süssmuth, *Appl. Microbiol. Biotechnol.* **2005**, *68*, 141–150.
- [76] C. Portmann, C. Prestinari, T. Myers, J. Scharfe, K. Gademann, *ChemBioChem* **2009**, *10*, 889–895.
- [77] P. Espinet, A. C. Albéniz, J. a. Casares, J. M. Martínez-Ilarduya, *Coord. Chem. Rev.* **2008**, *252*, 2180–2208.
- [78] O. Ritzeler, G. Klein, J.-L. Reymond, *Phosphorus. Sulfur. Silicon Relat. Elem.* **1999**, *144*, 243–246.
- [79] S. R. Laplante, P. J. Edwards, L. D. Fader, A. Jakalian, O. Hucke, *ChemMedChem* **2011**, *6*, 505–513.
- [80] G. H. Christie, J. Kenner, *J. Chem. Soc. Trans.* **1922**, *121*, 614–620.
- [81] G. Bringmann, A. J. P. Mortimer, P. a. Keller, M. J. Gresser, J. Garner, M. Breuning, *Angew. Chemie - Int. Ed.* **2005**, *44*, 5384–5427.
- [82] G. Bringmann, T. Gulder, T. a M. Gulder, M. Breuning, *Chem. Rev.* **2011**, *111*, 563–639.
- [83] F. Hiibel, E. Beck, *Plant Physiol.* **1996**, *112*, 1429–1436.
- [84] S.-D. Yoo, Y.-H. Cho, J. Sheen, *Nat. Protoc.* **2007**, *2*, 1565–1572.
- [85] K. H. Caffall, D. Mohnen, *Carbohydr. Res.* **2009**, *344*, 1879–1900.
- [86] D. J. Bradley, P. Kjellbom, C. J. Lamb, *Cell* **1992**, *70*, 21–30.
- [87] J. E. Varner, S. Louis, *Cell* **1989**, *56*, 231–239.
- [88] L. B. Davin, D. L. Bedgar, T. Katayama, N. G. Lewis, *Phytochemistry* **1992**, *31*, 3869–3874.
- [89] L. B. Davin, H. B. Wang, A. L. Crowell, D. L. Bedgar, D. M. Martin, S. Sarkanen, N. G. Lewis, *Science* **1997**, *275*, 362–366.
- [90] L. B. Davin, N. G. Lewis, *Plant Physiol.* **2000**, *123*, 453–462.
- [91] V. Burlat, M. Kwon, L. B. Davin, N. G. Lewis, *Phytochemistry* **2001**, *57*, 883–897.

- [92] L. B. Davin, N. G. Lewis, *Curr. Opin. Biotechnol.* **2005**, *16*, 398–406.
- [93] K. W. Kim, S. G. A. Moinuddin, K. M. Atwell, M. A. Costa, L. B. Davin, N. G. Lewis, *J. Biol. Chem.* **2012**, *287*, 33957–33972.
- [94] B. Pickel, M. A. Constantin, J. Pfannstiel, J. Conrad, U. Beifuss, A. Schaller, *Angew. Chemie - Int. Ed.* **2010**, *49*, 202–204.
- [95] B. Pickel, A. Schaller, *Appl. Microbiol. Biotechnol.* **2013**, *97*, 8427–8438.
- [96] K. S. Ham, S. C. Wu, A. G. Darvill, P. Albersheim, *Plant J.* **1997**, *11*, 169–179.
- [97] G. a Rosenthal, *Proc. Natl. Acad. Sci. U. S. A.* **1992**, *89*, 1780–1784.
- [98] Z. Minic, C. Rihouey, C. T. Do, P. Lerouge, L. Jouanin, *Plant Physiol.* **2004**, *135*, 867–878.
- [99] H. Korthout, P. Van Der Hoeven, M. J. Wagner, E. Van Hunnik, a. H. De Boer, *Plant Physiol.* **1994**, *105*, 1281–1288.
- [100] J. Rivoal, C. R. Smith, T. F. Moraes, D. H. Turpin, W. C. Plaxton, *Anal. Biochem.* **2002**, *300*, 94–99.
- [101] D. H. Lee, C. B. Lee, *Plant Sci.* **2000**, *159*, 75–85.
- [102] D. Wu, F. E. Regnier, *Anal. Chem.* **1993**, *65*, 2029–2035.
- [103] R. R. Burgess, *Protein Precipitation Techniques*, Elsevier Inc., **2009**.
- [104] R. O. Musser, D. F. Cipollini, S. M. Hum-Musser, S. a. Williams, J. K. Brown, G. W. Felton, *Arch. Insect Biochem. Physiol.* **2005**, *58*, 128–137.
- [105] a Ayala, J. Parrado, a Machado, *Appl. Biochem. Biotechnol.* **1998**, *69*, 11–16.
- [106] A. Shevchenko, M. Wilm, O. Vorm, M. Mann, *Anal. Chem.* **1996**, *68*, 850–858.
- [107] B. Domon, R. Aebersold, *Science (80- )*. **2006**, *312*, 212–217.
- [108] a J. Link, J. Eng, D. M. Schieltz, E. Carmack, G. J. Mize, D. R. Morris, B. M. Garvik, J. R. Yates, *Nat. Biotechnol.* **1999**, *17*, 676–682.
- [109] B. Kozomara, B. Vinterhalter, L. Radojević, D. Vinterhalter, *Vitr. Cell. Dev. Biol. - Plant* **2008**, *44*, 142–147.
- [110] W. Runguphan, J. J. Maresh, S. E. O'Connor, *Proc. Natl. Acad. Sci. U. S. A.* **2009**, *106*, 13673–13678.

- [111] a Roach, K. Boylan, S. Horvath, S. B. Prusiner, L. E. Hood, *Cell* **1983**, *34*, 799–806.
- [112] A. Nakagawa, H. Minami, J.-S. Kim, T. Koyanagi, T. Katayama, F. Sato, H. Kumagai, *Nat. Commun.* **2011**, *2*, 326.
- [113] H. Minami, J.-S. Kim, N. Ikezawa, T. Takemura, T. Katayama, H. Kumagai, F. Sato, *Proc. Natl. Acad. Sci. U. S. A.* **2008**, *105*, 7393–7398.
- [114] K. M. Hawkins, C. D. Smolke, *Nat. Chem. Biol.* **2008**, *4*, 564–573.

## Appendix A.

### **Total Synthesis of Ascospiroketal A Through a Ag<sup>I</sup>-Promoted Cyclization Cascade**

Reprinted (adapted) with permission from *Angewandte Chemie International Edition*.  
Copyright 2015 John Wiley and Sons.

Chang, S.; Hur, S.; Britton, R. *Angew. Chem. Int. Ed.* **2015**, *54*, 211

Natural Product Synthesis

# Total Synthesis of Ascospiroketal A Through a Ag<sup>I</sup>-Promoted Cyclization Cascade\*\*

Stanley Chang, Soo Hur, and Robert Britton\*

**Abstract:** The total synthesis of four candidate stereostructures for the marine octaketide ascospiroketal A have been achieved. These concise and highly stereocontrolled syntheses feature a unique Ag<sup>I</sup>-promoted cyclization cascade involving an oxetanyl ketochlorohydrin to access the entire tricyclic core of the natural product in one step. These syntheses also establish the full stereochemistry for the ascospiroketal natural products.

In 2007, König reported the isolation of ascospiroketals A (**1**) and B (**2**) (Figure 1) as single spiroacetal epimers from the marine-derived fungus *Ascochyta salicorniae*.<sup>[1]</sup> Following extensive analysis of 1D and 2D NMR spectra, it was proposed that **1** and **2** possess a rare octaketide tricyclic

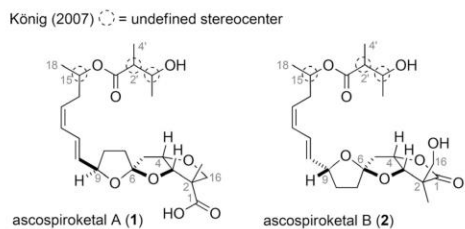
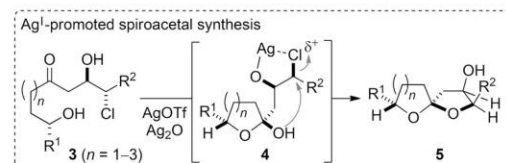


Figure 1. Naturally occurring octaketides ascospiroketals A and B.

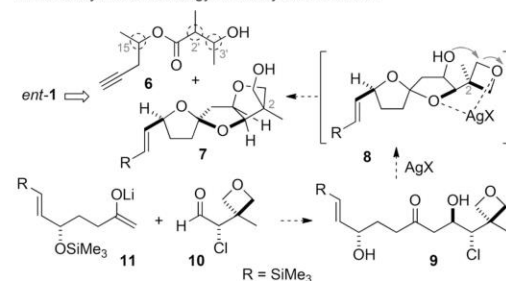
core, in which the terminal ring is cyclized through an ether or ester linkage and includes a quaternary stereogenic center at C2 installed through geminal SAM methylation.<sup>[1]</sup> The relative stereochemistry within the tricyclic core of the ascospiroketals was established from analysis of NOESY experiments and confirmed that these compounds are anomeric spiroacetals. Unfortunately, no information could be obtained regarding their absolute stereochemistry, the configurational relationship between the tricyclic core and side chain, or within the side chain itself. Thus, the relative

stereochemistry of the three remote stereocenters remained undefined. Structurally, these compounds represent the most complex members of a small family of tricyclic 5,5-spiroacetals<sup>[2]</sup> that includes the cephalosporolides,<sup>[3]</sup> penisporolides,<sup>[4]</sup> and opaliferin<sup>[5]</sup> for which several potentially useful biological activities have been ascribed.<sup>[3–5]</sup> Herein we describe the first total synthesis and full stereochemical assignment of ascospiroketal A (**1**)<sup>[6]</sup> through a highly efficient Ag<sup>I</sup>-promoted cyclization cascade that assembles the entire tricyclic core in one step from an acyclic precursor.

We have recently reported that aldol adducts of  $\alpha$ -chloroaldehydes **3** (Scheme 1) undergo Ag<sup>I</sup>-promoted cycli-



Cascade cyclization strategy for the synthesis of *ent*-1



Scheme 1. A silver(I)-promoted spirocyclization strategy to access ascospiroketal A.

zation to afford various spiroacetals **5**,<sup>[7]</sup> including 5,5-spiroacetals such as those embedded in the tricyclic core of the ascospiroketals. This unique spirocyclization strategy involves intramolecular alkylation of a hemiacetal by a Ag<sup>I</sup>-activated chloromethine (e.g., **4**). In contemplating a total synthesis of the ascospiroketals, we envisaged that ultimately the side chain **6** (Scheme 1) would be appended to the fully functionalized core **7** through a Sonogashira coupling.<sup>[8]</sup> Importantly, this late-stage coupling would allow for the rapid production of configurational isomers at the undefined stereocenters C15, C2', and C3'. In turn, a Ag<sup>I</sup>-promoted spirocyclization of the ketochlorohydrin **9** would provide the spiroacetal **8** and the terminal ring would be accessed through

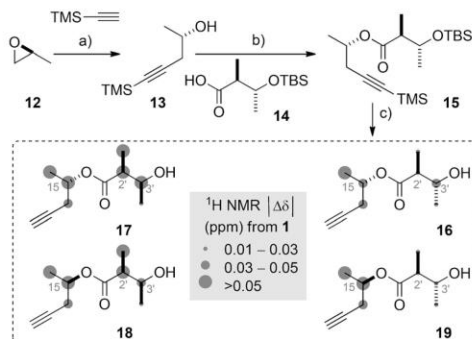
[\*] S. Chang, S. Hur, Prof. R. Britton  
Department of Chemistry, Simon Fraser University  
Burnaby, British Columbia (Canada)  
E-mail: rbritton@sfu.ca

[\*\*] This work was supported by an NSERC Discovery Grant to R.B., a MSFHR Career Investigator Award to R.B., and an NSERC Postgraduate Scholarship for S.C. The authors thank Milan Bergeron-Brlek (SFU) for assistance with X-ray crystallographic analysis.

Supporting information for this article is available on the WWW under <http://dx.doi.org/10.1002/anie.201408905>.

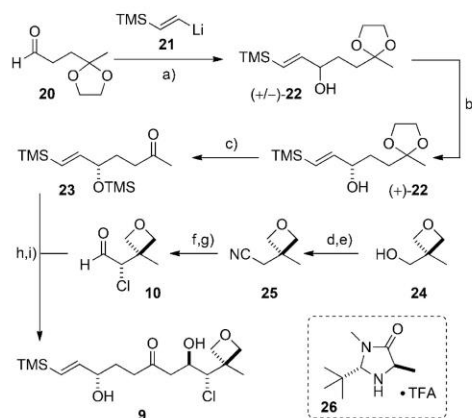
rearrangement of the hydroxy oxetane function (i.e., **8**→**7**).<sup>[9]</sup> Molecular models suggested that Lewis acid activation of the oxetane function in **8** could involve a secondary coordination to the central ring oxygen (Scheme 1). Importantly, this bidentate chelate structure would enforce the desired sense of diastereoselectivity on this critical rearrangement and secure the correct configuration at the all-carbon quaternary center C2. While without precedent, the potential for these two distinct cyclization reactions to be promoted in tandem by a Ag<sup>I</sup> salt was a particularly appealing aspect of this route. Building on our experiences in aldol reactions of  $\alpha$ -chloroaldehydes,<sup>[10]</sup> we expected the ketochlorohydrin **9** to be readily available from the union of suitably functionalized aldol coupling partners **10** and **11**.

In an attempt to address stereochemical uncertainties regarding the ascospiroketal A side chain,<sup>[11]</sup> we first targeted the four potential diastereomeric truncated side chains **16**–**19** (Scheme 2). Thus, readily available TBS-protected (2*S*,3*R*)-3-



**Scheme 2.** Synthesis of diastereomeric ascospiroketal A side chains and comparison of their <sup>1</sup>H NMR spectral data to **1**. a) TMS-acetylene, *n*BuLi, then **12**, BF<sub>3</sub>·OEt<sub>2</sub>, Et<sub>2</sub>O, –78 °C, 69%; b) DIC, DMAP, CH<sub>2</sub>Cl<sub>2</sub>, 20 h, 96%; c) TBAF, THF, 83%. DIC = *N,N'*-diisopropylcarbodiimide, DMAP = 4-(dimethylamino)pyridine, TBAF = tetrabutylammonium fluoride, TBS = *tert*-butyldimethylsilyl, TMS = trimethylsilyl.

hydroxy-2-methylbutyric acid **14**<sup>[11]</sup> was coupled with the homopropargyl alcohol **13** derived from TMS-acetylene addition to (–)-propylene oxide (**12**).<sup>[12]</sup> Deprotection of the resulting silyloxy ester **15** gave the hydroxy ester **16**. Repeating this sequence of reactions separately with (+)-propylene oxide and/or (2*S*,3*S*)-3-hydroxy-2-methylbutyric acid<sup>[13]</sup> (see the Supporting Information (SI) for full details) afforded the corresponding esters **17**–**19**. With these materials in hand, comparison of their <sup>1</sup>H and <sup>13</sup>C NMR spectral data (Scheme 2 and SI) with that reported for the equivalent portion of ascospiroketal A<sup>[1]</sup> suggested that the natural products possess a (2'*S*\*,3'*R*\*) relative configuration as depicted for esters **16** and **19**. Unfortunately, we were not able to confidently assign the relative configuration at C15 using these model compounds. Considering this uncertainty, the complete stereochemical assignment of ascospiroketal A would ultimately require the synthesis of four candidate stereoisomers using the side-chain precursors **16**, **19**, and *ent*-**16**, *ent*-**19**, and

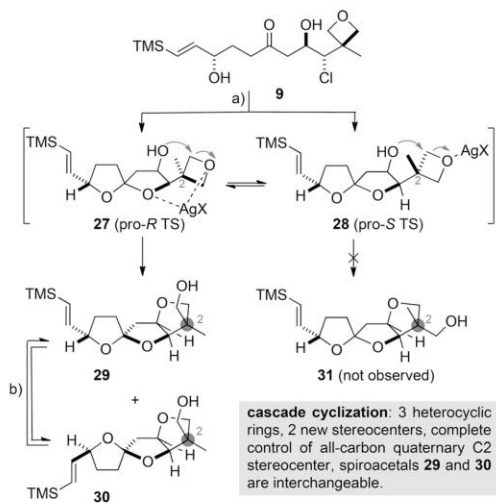


**Scheme 3.** Synthesis of the oxetanyl ketochlorohydrin **9**. a) Et<sub>2</sub>O, –40 °C, 1.5 h, 80%; b) Ti(O*i*Pr)<sub>4</sub>, (–)-DIPT, TBHP, CH<sub>2</sub>Cl<sub>2</sub>, –20 °C, 38 h, 40% (*ee* 98%); c) 1) PTSA, H<sub>2</sub>O/acetone, 65 °C, 2.5 h; 2) Et<sub>3</sub>N, TMSCl, THF, 0 °C to RT, 91% over two steps; d) MsCl, Et<sub>3</sub>N, CH<sub>2</sub>Cl<sub>2</sub>, 0 °C, 1 h; e) KCN, DMF, 80 °C, 16 h, 76% over two steps; f) DIBAL, CH<sub>2</sub>Cl<sub>2</sub>, –5 °C, 1 h; g) NCS, **26** (20 mol%), CH<sub>2</sub>Cl<sub>2</sub>, 5 °C, 24 h, 64% over two steps; h) **23**, LDA, then **10**, THF, –78 °C, 46% (72% based on recovered **23**, d.r. = 12:1); i) PTSA, H<sub>2</sub>O/acetone, 5 min, 83%. (–)-DIPT = (–)-diisopropyl *D*-tartrate, TBHP = *tert*-butyl hydroperoxide, PTSA = *p*-toluenesulfonic acid, TMSCl = chlorotrimethylsilane, DMF = *N,N*-dimethylformamide, DIBAL = diisobutylaluminum hydride, NCS = *N*-chlorosuccinimide, LDA = lithium diisopropylamide.

comparison of their spectral data to that reported for the natural product.

Synthesis of the tricyclic core of ascospiroketal A was initiated with the addition of vinyl lithium reagent **21** to the known aldehyde **20** (Scheme 3).<sup>[14]</sup> Sharpless asymmetric epoxidation<sup>[15]</sup> of **22** afforded the corresponding epoxide (not shown) along with recovered alcohol (+)-**22** in high enantiomeric purity (98% *ee*) at 60% conversion. Removal of the acetal protecting group and protection of the secondary alcohol function in (+)-**22** then yielded the methyl ketone **23**. The preparation of  $\alpha$ -chloroaldehyde **10** involved a one-carbon homologation of commercially available alcohol **24** by displacement of the corresponding mesylate with cyanide and subsequent reduction. The organocatalytic asymmetric  $\alpha$ -chlorination<sup>[10a]</sup> was explored using the conditions reported by MacMillan,<sup>[16]</sup> Jørgensen,<sup>[17]</sup> and Christmann.<sup>[18]</sup> After some experimentation with this unusual substrate, we found that a combination of MacMillan's catalyst **26**<sup>[16]</sup> and NCS<sup>[18]</sup> gave  $\alpha$ -chloroaldehyde **10** in optimal enantiomeric purity (85% *ee*). Finally, coupling of the lithium enolate derived from methyl ketone **23** with the  $\alpha$ -chloroaldehyde **10** provided the aldol adduct **9** in good yield and excellent diastereoselectivity (d.r. = 12:1).<sup>[10f]</sup>

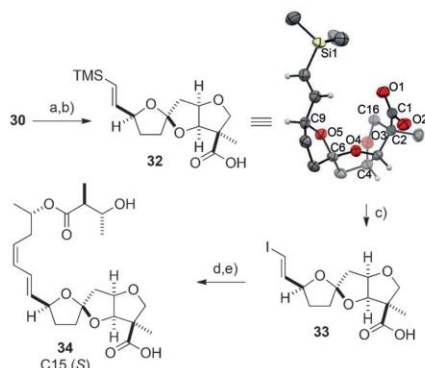
Having established a concise, 6-step synthesis of keto-chlorohydrin **9** we next explored the key spirocyclization reaction. Using our optimized conditions<sup>[7]</sup> for the formation of simple spiroacetals, we were delighted to find that overnight reaction of **9** with AgOTf and Ag<sub>2</sub>O proceeded smoothly to afford the anomeric spiroacetals **27** in good combined yield. Pleasingly, the only by-products produced in



**Scheme 4.** Ag<sup>I</sup>-promoted cascade cyclization of **9**. a) Ag<sub>2</sub>O, AgBF<sub>4</sub>, THF, 20 °C to 50 °C, 82% (**29/30** ~1:1); b) ZnCl<sub>2</sub>, MgO, CH<sub>2</sub>Cl<sub>2</sub>, 6.5 h, **29/30** (2:1).

any appreciable quantity were the tricycles **29** and **30**. Further optimization of the formation of these tricycles involved a brief screen of Ag<sup>I</sup> salts, whereupon a combination of AgBF<sub>4</sub> and Ag<sub>2</sub>O<sup>[7]</sup> was identified as optimal, delivering **29** and **30** in a combined isolated yield of 82%. As highlighted in Scheme 4, the complete diastereoselectivity observed in the opening of the prochiral oxetane may be attributed to chelation of the central ring oxygen and that of the oxetane to the Ag<sup>I</sup> salt (see **27**). This bidentate chelation<sup>[19]</sup> is not possible in the pro-*S* transition structure **28**. It is notable that the Ag<sup>I</sup>-promoted cyclization cascade effects the formation of three heterocyclic rings and a spiroacetal center, and secures the relative stereochemistry at the all-carbon quaternary center required for ascospiroketal A. To improve the overall efficiency of this reaction, the undesired spiroacetal **29** was readily epimerized using Dudley's conditions (ZnCl<sub>2</sub>, MgO)<sup>[3a,20]</sup> to provide a mixture of the anomeric spiroacetals **29** and **30** and a means to recycle the former material.

Completion of the total synthesis of the candidate stereostructures for ascospiroketal A is depicted in Scheme 5. A two-step oxidation<sup>[21,22]</sup> of the primary alcohol function in tricycle **30** provided the carboxylic acid **32** without epimerization of the spiroacetal center. At this point, suitable crystals were obtained for X-ray crystallographic analysis (see ORTEP, Scheme 5), which confirmed our stereochemical assignment of the tricyclic core. Moreover, the spectral data (<sup>1</sup>H and <sup>13</sup>C NMR) derived from **32** were in close agreement with that reported for the same region of ascospiroketal A, supporting the assigned stereochemistry for the natural product. Following silicon to iodine exchange (**32**→**33**),<sup>[23]</sup> Sonogashira coupling<sup>[8]</sup> of the side chain **16** with vinyl iodide **33** provided the full carbon skeleton of ascospiroketal A. Lindlar reduction<sup>[24]</sup> of the resulting enyne completed the total synthesis of candidate stereostructure **34**, which required



**Scheme 5.** Synthesis of candidate stereostructure **34** and ORTEP representation of **32**. a) DMP, NaHCO<sub>3</sub>, CH<sub>2</sub>Cl<sub>2</sub>, 1 h, 79%; b) NaClO<sub>2</sub>, NaH<sub>2</sub>PO<sub>4</sub>·H<sub>2</sub>O, 2-methyl-2-butene, H<sub>2</sub>O:tBuOH, 45 min, 87%; c) NIS, HFIP, 0 °C, 30 min, 67%; d) **16**, PdCl<sub>2</sub>(PPh<sub>3</sub>)<sub>2</sub>, CuI, DIPA, THF, 14 h; e) H<sub>2</sub> (balloon), Lindlar catalyst, quinoline, EtOH, 46% over two steps. DMP = Dess–Martin periodinane, NIS = *N*-iodosuccinimide, HFIP = 1,1,1,3,3,3-hexafluoro-2-propanol, DIPA = diisopropylamine. Ellipsoids are given at 50% probability.

only 12 steps from the readily available aldehyde **20**. Repetition of the final two reactions using the stereochemically unique side chains **19**, *ent*-**16**, and *ent*-**19** gave the candidate stereostructures **35**, **36**, and **37**, respectively (Figure 2). Whereas the <sup>1</sup>H NMR spectra derived from these synthetic materials were similar, the resonances for the diastereotopic protons at C14 proved to be diagnostic for the C15-*S*) and C15-*R*) series. Notably, only the spectra derived from the C15-*S*) diastereomers **34** and **37** contained H14a/H14b resonances characteristic of ascospiroketal A (see truncated spectra, Figure 2).<sup>[25]</sup> Furthermore, whereas the <sup>1</sup>H NMR spectrum of **37** acquired at 500 MHz closely matched that of the natural product, several subtle differences in the chemical shift ( $\Delta\delta > 0.01$  ppm) and/or shape of resonances for H10, H13, H14, and H3' existed between the spectra of **34** and ascospiroketal A.<sup>[25]</sup> Thus, based on the distinct <sup>1</sup>H NMR spectra of the candidate stereostructures **34**–**37**, the relative configuration for ascospiroketal A was confidently assigned as that depicted for **37**. The specific rotation for **37** ( $[\alpha]_D^{20} = +5$  (c 0.20 in MeOH)) was also consistent in sign with that reported for the natural product ( $[\alpha]_D^{20} = +20$  (c 0.45 in MeOH)),<sup>[1]</sup> confirming the absolute stereochemistry of ascospiroketal A as shown for **37**. Interestingly, the structurally related octaketide cephalosporolide H,<sup>[26]</sup> also isolated from a marine-derived fungus, possesses the same absolute stereochemistry within its tricyclic spiroacetal core.

In summary, exploiting a Ag<sup>I</sup>-promoted cyclization cascade, concise (14-step) syntheses of four candidate stereostructures of the naturally occurring polyketide ascospiroketal A were realized. Comparison of their spectral data with that reported for **1** allowed for the confident assignment of the relative and absolute stereochemistry for the natural product as (2*R*, 3*R*, 4*R*, 6*R*, 9*S*, 15*S*, 2'*R*, 3'*S*). Considering the similarities in structure between the ascospiroketals A (**1**) and



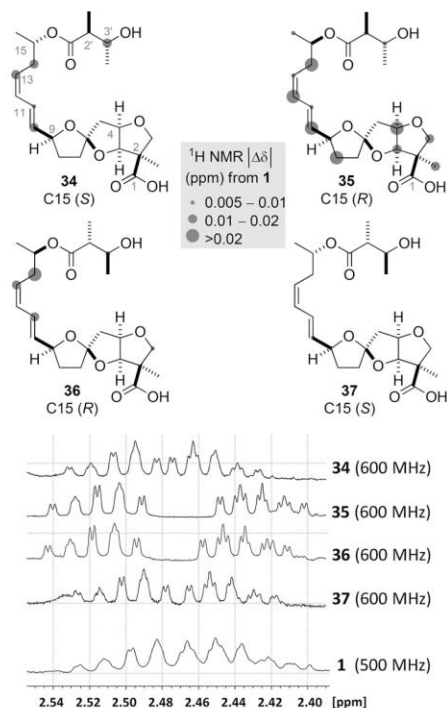


**Figure 2.** Comparison of the  $^1\text{H}$  NMR spectra ( $[\text{D}_6]$ acetone) of candidate stereostructures **34–37** to **1** and enlargement of the H14 resonances from the  $^1\text{H}$  NMR spectra of **1**<sup>[23]</sup> and **34–37**.

**B (2)**, the relative and absolute stereochemistry of ascospiroketal **B** should also be revised accordingly.

Received: September 8, 2014  
Published online: November 6, 2014

**Keywords:** natural products · polyketides · stereochemical assignment · tandem cyclization · total synthesis

- [1] S. F. Seibert, A. Krick, E. Eguereva, S. Kehraus, G. M. König, *Org. Lett.* **2007**, *9*, 239–242.
- [2] a) M. J. Ackland, J. R. Hanson, P. B. Hitchcock, *J. Chem. Soc. Perkin Trans. 1* **1985**, 843–847; b) V. Rukachaisirikul, S. Pramjit, C. Pakawatchai, M. Isaka, S. Supothina, *J. Nat. Prod.* **2004**, *67*, 1953–1955; c) X. Li, Y. Yao, Y. Zheng, I. Sattler, W. Lin, *Arch. Pharmacol. Res.* **2007**, *30*, 812–815.
- [3] For recent cephalosporolide syntheses, see: a) S. F. Tlais, G. B. Dudley, *Org. Lett.* **2010**, *12*, 4698–4701; b) M. A. Brimble, O. C. Finch, A. M. Heapy, J. D. Fraser, D. P. Furkert, P. D. O'Connor, *Tetrahedron* **2011**, *67*, 995–1001; c) S. F. Tlais, G. B. Dudley, *Beilstein J. Org. Chem.* **2011**, *7*, 570–577; d) S. F. Tlais, G. B. Dudley, *Beilstein J. Org. Chem.* **2012**, *8*, 1287–1292; e) L. Song, Y. Liu, R. Tong, *Org. Lett.* **2013**, *15*, 5850–5853; f) R. A. Fernandes, M. B. Halle, *Asian J. Org. Chem.* **2013**, *2*, 593–599; g) C. N. Kona, C. V. Ramana, *Tetrahedron* **2014**, *70*, 3653–3656.
- [4] X. Li, I. Sattler, W. Lin, *J. Antibiot.* **2007**, *60*, 191–195.
- [5] A. Grudniewska, S. Hayashi, M. Shimizu, M. Kato, M. Suenaga, H. Imagawa, T. Ito, Y. Asakawa, S. Ban, T. Kumada, T. Hashimoto, A. Umeyama, *Org. Lett.* **2014**, *16*, 4695–4697.
- [6] For a synthetic approach to ascospiroketal **B**, see: J. W. Kim, H. W. Lee, D.-H. Lee, *Bull. Korean Chem. Soc.* **2011**, *32*, 2877–2878.
- [7] S. Chang, R. Britton, *Org. Lett.* **2012**, *14*, 5844–5847.
- [8] K. Sonogashira, Y. Tohda, N. Hagihara, *Tetrahedron Lett.* **1975**, *16*, 4467–4470.
- [9] R. N. Loy, E. N. Jacobsen, *J. Am. Chem. Soc.* **2009**, *131*, 2786–2787.
- [10] a) B. Kang, J. Mowat, T. Pinter, R. Britton, *Org. Lett.* **2009**, *11*, 1717–1720; b) B. Kang, S. Chang, S. Dekker, R. Britton, *Org. Lett.* **2010**, *12*, 1716–1719; c) J. Draper, R. Britton, *Org. Lett.* **2010**, *12*, 4034–4037; d) S. Halperin, B. Kang, R. Britton, *Synthesis* **2011**, *12*, 1946–1953; e) M. T. Holmes, R. Britton, *Chem. Eur. J.* **2013**, *19*, 12649–12652; f) R. Britton, B. Kang, *Nat. Prod. Rep.* **2013**, *30*, 227–236.
- [11] C. E. O'Connell, K. A. Salvato, Z. Meng, B. A. Littlefield, C. E. Schwartz, *Bioorg. Med. Chem. Lett.* **1999**, *9*, 1541–1546.
- [12] J. D. White, T. C. Somers, G. N. Reddy, *J. Org. Chem.* **1992**, *57*, 4991–4998.
- [13] P. Renaud, D. Seebach, *Helv. Chim. Acta* **1986**, *69*, 1704–1710.
- [14] A. P. Ramirez, A. M. Thomas, K. A. Woerpel, *Org. Lett.* **2009**, *11*, 507–510.
- [15] a) T. Katsuki, K. B. Sharpless, *J. Am. Chem. Soc.* **1980**, *102*, 5974–5976; b) V. S. Martin, S. S. Woodard, T. Katsuki, Y. Yamada, M. Ikeda, K. B. Sharpless, *J. Am. Chem. Soc.* **1981**, *103*, 6237–6240.
- [16] M. Amatore, T. D. Beeson, S. P. Brown, D. W. C. MacMillan, *Angew. Chem. Int. Ed.* **2009**, *48*, 5121–5124; *Angew. Chem.* **2009**, *121*, 5223–5226.
- [17] N. Halland, A. Braunton, S. Bachmann, M. Marigo, K. A. Jørgensen, *J. Am. Chem. Soc.* **2004**, *126*, 4790–4791.
- [18] P. Winter, J. Swatschek, M. Willot, L. Radtke, T. Olbrisch, A. Schäfer, M. Christmann, *Chem. Commun.* **2011**, *47*, 12200–12202.
- [19] a) A. Yanagisawa, Y. Matsumoto, K. Asakawa, H. Yamamoto, *Tetrahedron* **2002**, *58*, 8331–8339; b) A. M. Szpilman, E. M. Carreira in *Silver in Organic Chemistry* (Ed.: M. Harmata), Wiley, New Jersey, **2010**, pp. 46–73.
- [20] Treating compound **29** or a structurally related model system with the following Lewis or Brønsted acids also resulted in the production of ~1:1 mixtures of spiroacetals: pyridinium *p*-toluenesulfonate,  $\text{BF}_3\cdot\text{OEt}_2$ , camphorsulfonic acid,  $\text{Sc}(\text{OTf})_3$ ,  $\text{InCl}_3$ .
- [21] D. B. Dess, J. C. Martin, *J. Org. Chem.* **1983**, *48*, 4155–4156.
- [22] B. S. Bal, W. E. Childers, Jr., H. W. Pinnick, *Tetrahedron* **1981**, *37*, 2091–2096.
- [23] a) D. P. Stamos, A. G. Taylor, Y. Kishi, *Tetrahedron Lett.* **1996**, *37*, 8647–8650; b) E. A. Iardi, C. E. Stivala, A. Zakarian, *Org. Lett.* **2008**, *10*, 1727–1730.
- [24] For Lindlar reduction of 1,3-enynes, see: a) K. C. Nicolaou, S. E. Webber, *J. Am. Chem. Soc.* **1984**, *106*, 5734–5736; b) G. A. Molander, F. Dehmel, *J. Am. Chem. Soc.* **2004**, *126*, 10313–10318; c) M. Bock, R. Dehn, A. Kirschning, *Angew. Chem. Int. Ed.* **2008**, *47*, 9134–9137; *Angew. Chem.* **2008**, *120*, 9274–9277.
- [25] The authors thank Professor Gabrielle König for providing a data file of the 500 MHz  $^1\text{H}$  NMR spectrum of ascospiroketal **A** (500 MHz,  $[\text{D}_6]$ acetone).